№3, 2022 ISSN 2706-977X

MATERIAL AND MECHANICAL ENGINEERING TECHNOLOGY

Material and Mechanical Engineering Technology | MMET.KZ

Editorial board of the journal

Content

DOI 10.52209/2706-977X_2022_3_3 **IRSTI 55.03.31** **UDC 621.791.927**

Analysis of the Spline Shafts Reliability by Machine-Building enterprises

Buzauova T. M.*, Tlekbayeva D. K., Smailova B.K., Mateshov A.K.
Abylkas Saginov Karaganda Technical University, Karaganda, Kazakhstan
*corresponding author

Abstract. The aim of the study is to ensure the optimal reliability of splined shafts of manufacturers. This article examines the patterns of occurrence of spline shaft failures, using the «Statistica» program, methods for calculating reliability and predicting failures are developed using the analysis of statistical data characterizing reliability. The analysis of the reliability and quality of the object's functioning is reduced to the analysis of time intervals (operating time) during which the object is in a state of operability and random time intervals during which it is idle (restored, repaired). This software product provides a choice of a wide range of methods for reliability analysis and predicting equipment failures. These methods can be used in processing the results of observations of spline shafts, the uptime of which is subordinated to one or another distribution - exponential, Weibull, logarithmically normal, etc. Using a software product, it is possible to assess reliability assurance without involving the mathematical apparatus of the classical theory of reliability.

Key words: splined joint, distribution function, risk analysis, probability density, survival analysis, reliability assessment, statistical data.

Introduction

To improve the quality of the machines, reduce the cost of their maintenance, it is necessary to ensure optimal reliability of machine parts and assemblies. The reliability of a machine is determined by the reliability of its aggregates, assemblies and parts, so the developer should pay close attention to this criterion of each part [1].

In machine designs, splined joints are among the most important. They largely determine the reliability, cost and, consequently, the competitiveness of aggregates and machines as a whole.

Spline shafts are designed to transmit torque, are widely used in almost all areas of industry, as well as mechanical engineering, mining.

Splined joints are distinguished by the profile of the teeth – straight, involute, triangular. This article discusses straight-line spline shafts [2].

Spline joints are operated in difficult conditions under oscillatory and shock loads, as well as when high positioning accuracy, efficiency, and improved stroke quality are required, all of these operating conditions lead to frequent failure of the spline shaft. A significant number of spline shaft failures occur due to non-compliance with the manufacturing process and unsatisfactory operation [3].

1. The theory of the research

The theory of the question. The main issues studied by the theory of reliability are failures of components and parts; criteria and quantitative characteristics of reliability (failures, wear and tear); manufacturing and operation. Thus, in order to obtain the necessary information on ensuring the optimal reliability of parts at the enterprises of the Karaganda region (2018-2020), the pattern of occurrence of spline shaft failures are analyzed. Using the statistical data of “Maker KLMZ” LLP, “Karadel Mechanics” LLP and “Karaganda Metalware Plant” LLP, we identify failures (Fig. 1, 2), wear and tear (Fig. 3).

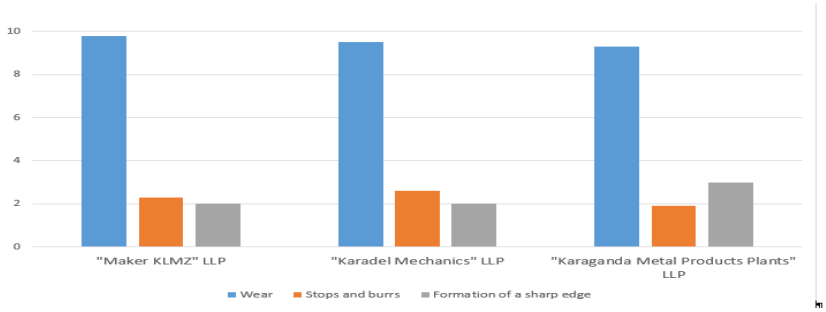

Fig. 1. – Spline shaft failures

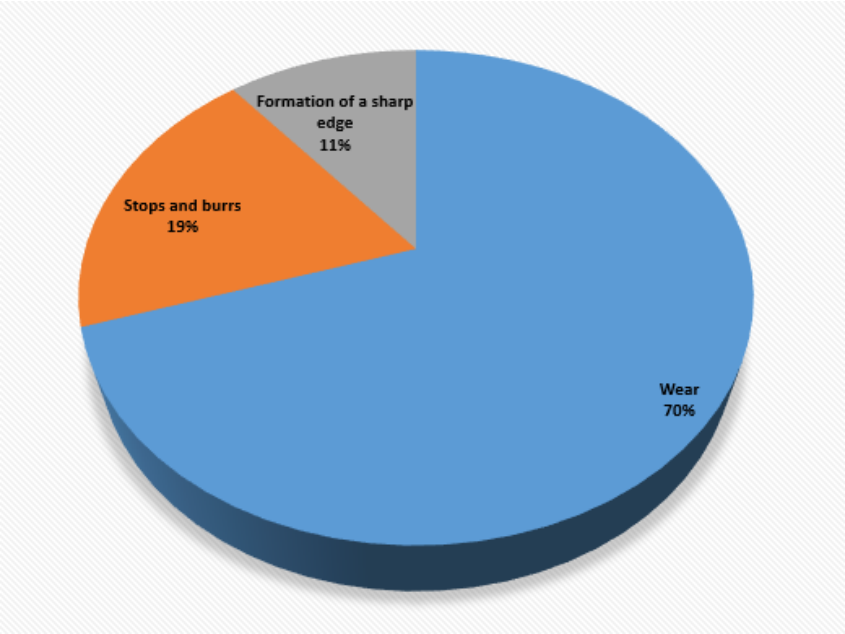

Fig. 2. - Types of wear in percentage terms

Fig.3. – Wear of spline shafts

The revealed wear of the spline shafts disrupt the interaction of parts and assemblies, can cause significant additional loads, shocks in the joints and vibrations, and cause sudden destruction. Therefore, ensuring optimal reliability of spline shafts in the manufacture of machine-building enterprises of the Karaganda region is an urgent task [4, 5].

The reliability calculation in the “Statistica” program is based on statistical data, in accordance with GOST, expressed as probabilistic characteristics.

2. Materials and methods

The provision of optimal reliability of splined shafts produced by “Maker KLMZ” LLP, “Karadel Mechanics” LLP and "Karaganda Metal Products Plant" LLP using the “Statistica” program is evaluated.

To do this, at the beginning of the program, the following initial data are entered into the table (Fig.4):

1. release date of the spline shaft;
2. condition of the spline shaft (fit/not fit);
3. operating time to failure, operating time of the spline shaft from the start of operation to the occurrence of the first failure, these data were removed from the defect log of the relevant organizations;
4. spline shaft type according to the ESCD classifier, class 72;
5. centering on the inner diameter d, mm;
6. centering on the outer diameter D, mm;
7. centering on the side teeth b, mm;
8. manufacturer of the spline shaft.

Data: Spreadsheet1* (10v by 10c)

	1 Start	2 End	3 Condition of the spline shaft	4 Type	5 Centering on inner diameter "d"	6 Centering on te outer diameter "D"	7 Centering on the side surfaces of the teeth "b"	8 Manufacturer
1	06.01.2016	05.12.2018	Fit	721114	23	26	6	"Maker KLMZ" LLP
2	02.05.2016	15.01.2018	Fit	721115	26	30	6	"Maker KLMZ" LLP
3	31.08.2016	30.07.2019	Unfit	721116	28	32	7	"Maker KLMZ" LLP
4	05.10.2016	09.09.2019	Unfit	721124	21	25	5	"Karadel Mechanics" LLP
5	15.02.2017	23.05.2018	Fit	721125	23	28	6	"Karadel Mechanics" LLP
6	16.07.2017	16.02.2020	Unfit	721126	26	32	6	"Karadel Mechanics" LLP
7	14.07.2017	18.03.2020	Fit	721212	28	34	7	"Maker KLMZ" LLP
8	16.01.2018	21.08.2019	Unfit	721213	13	16	3,5	"Karaganda Metal Products Plan
9	13.04.2018	30.05.2020	Fit	721214	16	20	4	"Karaganda Metal Products Plan
10	03.09.2018	16.11.2020	Fit	721215	18	22	5	"Karaganda Metal Products Plan

Fig.4. - Initial data

To establish reliability indicators, in the "Analysis" tab, select "In-depth methods", then "Tables from the life cycle" (Fig. 5).

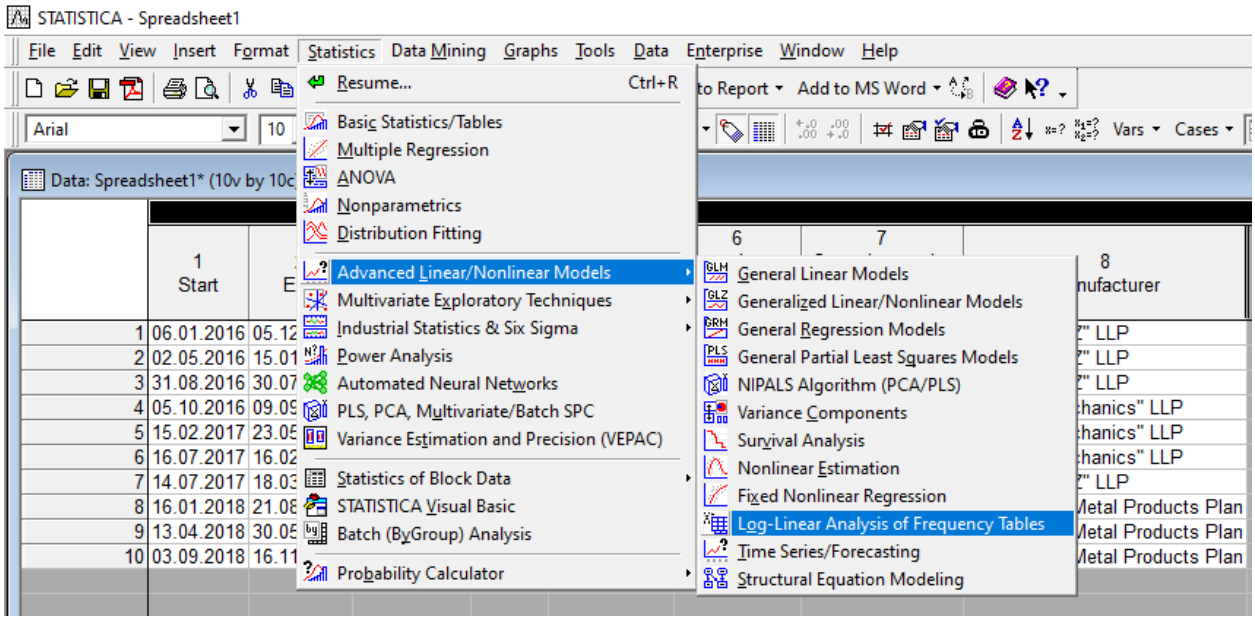

Fig.5. - Fragment of the "Table from the life cycle"

For a natural description of the reliability function methods , it is necessary to build Tables from the product life cycle (Fig. 6). The number of observations with the same value variants are called frequency, i.e. if the value x1 was observed m_1 times, x_2 was observed m_2 times, ..., xk – mk times, then m1,m2, ...,mk - frequencies. For an interval series, the frequency of the i-th interval is equal to the number of mi values observed in the i-th interval. The sum of the frequencies is equal to the sample size [6]:

$$\sum_{i=1}^{k} m_i = \sum_{j=1}^{r} m_j = n \quad (1)$$

where k is the number of options;
r is the number of intervals;
n is the sample size.

The ratio of frequency to sample size is called frequency (relative frequency): $\hat{p}_i = \frac{m_i}{n}$.

Options (a list of intervals for the interval series) and their corresponding frequencies (frequencies) form a statistical series of the sample (Fig. 6).

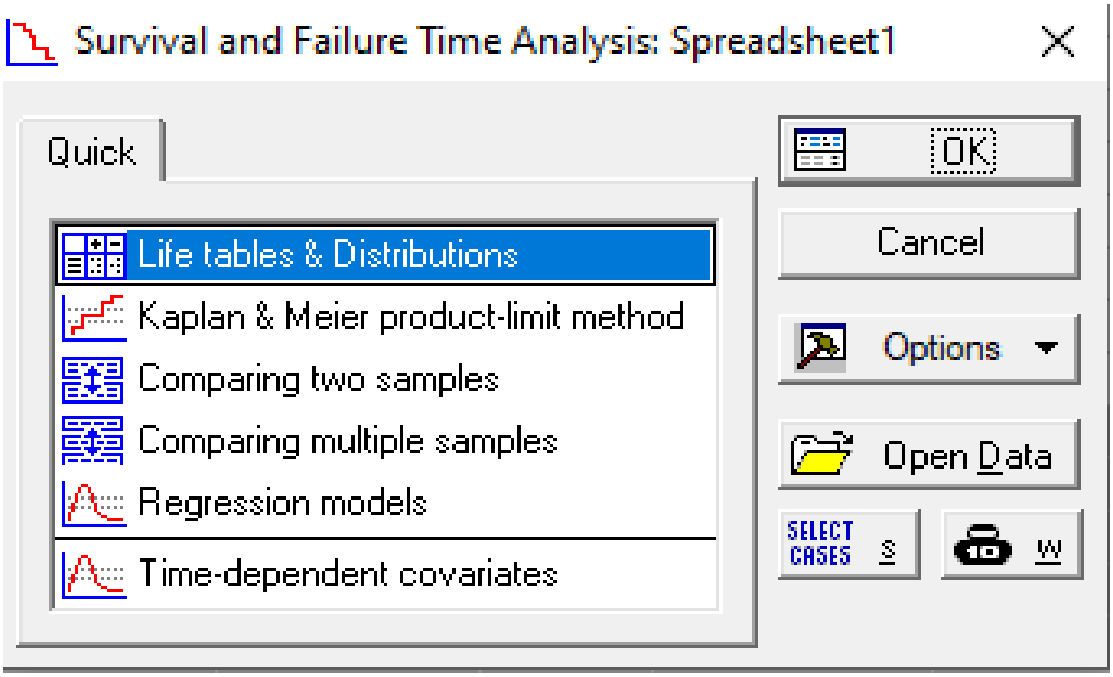

Fig. 6. – The "Survival Analysis" dialog box

After such preparation, various statistical characteristics (statistics) can be obtained. Next, the range of possible times is calculated, respectively, for each interval, the number and proportion of objects that worked at the beginning of the considered interval are calculated.As well as the number and proportion of objects that were rejected in this interval, and the number and proportion of objects that were withdrawn in each interval (Fig.7).

e Table (Spreadsheet1)

Life Table (Spreadsheet1)
Log-Likelihood for data: -16,4589

Interval	Interval Start	Mid Point	Interval Width	Number Entering	Number Withdrwn	Number Exposed	Number Dying	Proportn Dead	Proportn Survivng	Cum.Prop Survivng	Problty Density	**Hazard Rate**	St Cum
Intno.1	0,000	48,591	97,18182	10	0	10,00000	0	0,050000	0,950000	1,000000	0,000514	0,000528	0,
Intno.2	97,182	145,773	97,18182	10	0	10,00000	0	0,050000	0,950000	0,950000	0,000489	0,000528	0,
Intno.3	194,364	242,955	97,18182	10	0	10,00000	0	0,050000	0,950000	0,902500	0,000464	0,000528	0,
Intno.4	291,545	340,136	97,18182	10	0	10,00000	0	0,050000	0,950000	0,857375	0,000441	0,000528	0,
Intno.5	388,727	437,318	97,18182	10	0	10,00000	1	0,100000	0,900000	0,814506	0,000838	0,001083	0,
Intno.6	485,909	534,500	97,18182	9	1	8,50000	0	0,058824	0,941176	0,733056	0,000444	0,000624	0,
Intno.7	583,091	631,682	97,18182	8	0	8,00000	1	0,125000	0,875000	0,689935	0,000887	0,001372	0,
Intno.8	680,273	728,864	97,18182	7	0	7,00000	0	0,071429	0,928571	0,603693	0,000444	0,000762	0,
Intno.9	777,455	826,045	97,18182	7	0	7,00000	2	0,285714	0,714286	0,560572	0,001648	0,003430	0,
Intno.10	874,636	923,227	97,18182	5	1	4,50000	0	0,111111	0,888889	0,400409	0,000458	0,001211	0,
Intno.11	971,818	1020,409	97,18182	4	1	3,50000	2	0,571429	0,428571	0,355919	0,002093	0,008232	0,
Intno.12	1069,000			1	1	0,50000	0	1,000000	0,000000	0,152537			0,

Life Table (Spreadsheet1)

Fig.7 .– Table of lifetimes

The key aspect is the Weibull distribution, named after the Swedish researcher Waloddi Weibull, who used this distribution to describe failure times of various types in reliability theory.

The Weibull distribution is a two-parameter distribution. The Weibull law satisfactorily describes the distribution of the time to failure of shafts and bearings; it is used to assess the reliability of machine parts and assemblies, in particular automobiles, as well as to assess the reliability of machines in the process of their running-in.

The wide application of the Weibull law is explained by the fact that this law is universal, since it can describe processes with distributions: normal, logarithmically normal and exponential [6].

The distribution is given by two parameters (Fig. 8), shape parameters; and scale.

Estimatn Method	Parameter Estimates, Model: Weibull (Spreadsheet1) Note: Weights: 1=1., 2=1./V, 3=N(I)*H(I) Lambda	Variance Lambda	Std.Err. Lambda	Gamma	Variance Gamma	Std.Err. Gamma	Covarnce Gam-Lamd	Log-Likelhd.	Chi-Sqr.	df	p
Weight 1	0,000016	0,000000	0,000048	1,621975	0,203136	0,450707	-0,000021	-20,3118	7,705907	9	0,564042
Weight 2	0,000002	0,000000	0,000005	1,994860	0,173206	0,416181	-0,000002	-21,2453	9,572839	9	0,386192
Weight 3	0,000031	0,000000	0,000101	1,502401	0,226031	0,475427	-0,000048	-20,2989	7,680036	9	0,566693

Fig. 8. – Estimates of Weibull parameters

When choosing parameters, we focus on the log likelihood value and the significance level. In our case, we select the last row of the table, since the log likelihood value is the maximum. Next, we evaluate the reliability functions and the risk of failure.

Reliability function – the probability that the failure occurred after the moment t. The reliability function is determined by the following formula [6]:

$$R(t) = 1 - F(t), t > 0 \quad (2)$$

where F(t) is the distribution function.

3. Discussion of the results

Using the statistical data (Fig. 4), we evaluate the function of non-failure operation (survival) (Fig. 9).

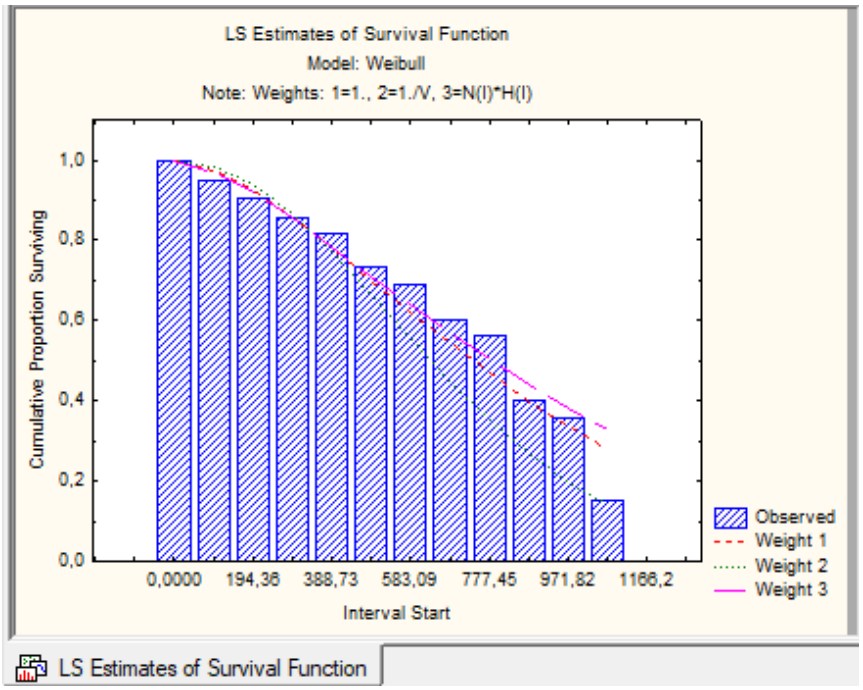

Fig. 9 – Histogram of the reliability (survival) function

This histogram (Fig.9) is called a histogram of specific repeatability. Its area of specific repeatability is equal to the sum of all specific repeatability, i.e. unit.

When analyzing the reliability of spline shafts, it is natural to consider the probability of failure within a short time interval, provided that there was no failure at the beginning of the interval.

Analyzing the histogram of the reliability function (Fig. 9), we conclude that for a splined shaft, the intensity function has the shape of a U-shaped curve. Next, in the program, we will consider estimates of the risk function at various time intervals (Fig. 10) according to the initial data shown in Fig. 4. Then we plot the dependence of the failure risk on the interval (Fig. 11).

Interval	Estimates of Survival Function; Model: Weibu Note: Weights: 1=1., 2=1./V, 3=N(I)*H(I) **Interval Start**	Weight 1	Weight 2	Weight 3
Intno.1	0,000	1,000000	1,000000	1,000000
Intno.2	97,182	0,974259	0,983740	0,970095
Intno.3	194,364	0,922868	0,936749	0,917578
Intno.4	291,545	0,856467	0,863545	0,853698
Intno.5	388,727	0,781090	0,770720	0,783723
Intno.6	485,909	0,701306	0,666006	0,711228
Intno.7	583,091	0,620705	0,557246	0,638815
Intno.8	680,273	0,542066	0,451456	0,568400
Intno.9	777,455	0,467453	0,354156	0,501358
Intno.10	874,636	0,398304	0,269027	0,438635
Intno.11	971,818	0,335514	0,197891	0,380820
Intno.12	1069,000	0,279523	0,140958	0,328224

Fig. 10 - Estimates of the risk function

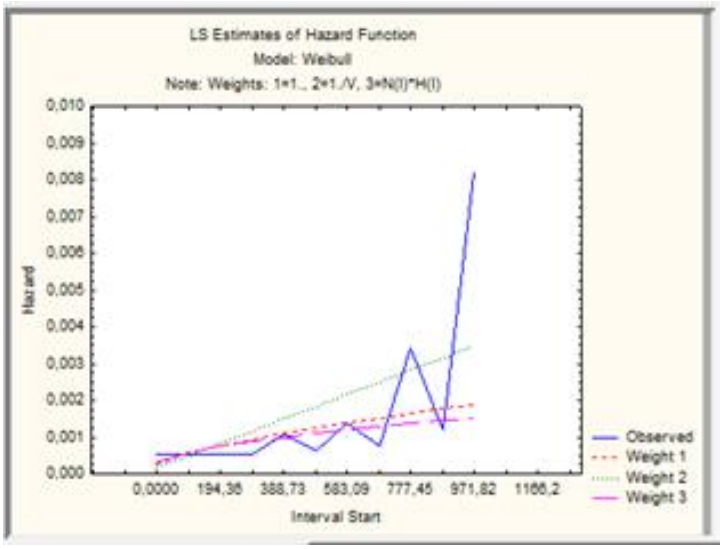

Fig.11. – Dependence of the failure risk on the interval

Investigating the obtained dependence, we conclude that at the beginning of the spline shaft operation, the risk of failure is in the minimum zone and the proportion of the risk volume is 0.1-0.3. Then the proportion of the failure risk volume is 0.4-0.7 and the risk of failure increases. After 4 years of operation, the risk of failure returns again – this is due to the wear of the spline shaft.

In order to assess the provision of optimal reliability of manufacturers LLP "Maker KLMZ", LLP "Karadel Mechanics", LLP "Karaganda Metalware Plant" we carry out a comparison (Fig. 12).

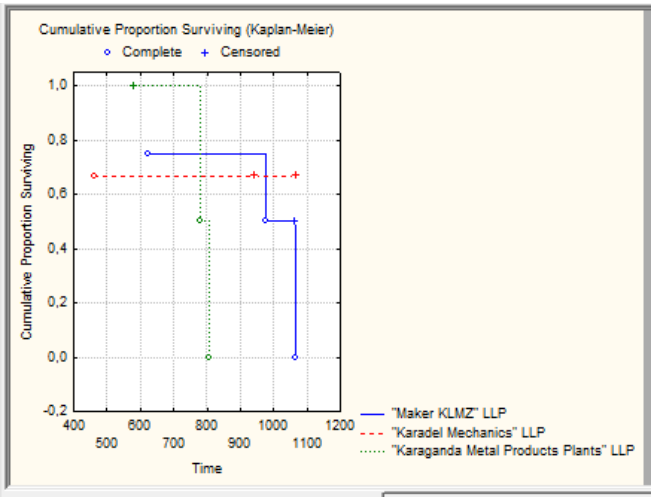

Fig.12. - Evaluation of ensuring optimal reliability of spline shafts

According to the graph (Fig. 12), we conclude that at the beginning of operation, the spline shafts are provided with optimal reliability. After a certain time, the spline shafts produced by the “Karaganda Metal Products Plant” LLP begin to lose reliability in relation to the other two enterprises. If we evaluate the manufacturers of "Maker KLMZ" LLP and "Karadel Mechanics" LLP among themselves, then it is impossible to make a definite conclusion, since a certain number of intersections of reliability function estimates are monitored at different time intervals.

Based on the conducted research, recommendations have been developed for monitoring taking into account the operating time intervals. This method allows you to significantly reduce operating costs by ensuring timely preventive maintenance, thereby avoiding equipment downtime during the working cycle. The developed method of ensuring the reliability of spline shafts is being tested in the conditions of enterprises operating these shafts.

Conclusions

Using computational and statistical methods for assessing reliability, models of spline shaft failures have been developed.

During the study of statistical data, the reliability of the spline shaft was assessed, a graph of the dependence of the risk of failure on the operating interval was constructed.

According to the work carried out, it was found that the spline shafts produced by "Maker KLMZ" LLP and "Karadel Mechanics" LLP are provided with optimal reliability.

Based on the conducted research, a method has been developed to ensure the reliability of spline shafts during operation.

References

[1] Truhanov V.M. Nadezhnost' izdelij mashinostroenija. M.: Spektr, 2013. – 335 p.

[2] GOST 1139-80. Osnovnye normy vzaimozamenjaemosti. Soedinenija shlicevye prjamobochnye. Razmery i dopuski. - M.: 1980. - 12 p.

[3] Buzauova T.M., Tlekbaeva D.K. Issledovanie fiziko-mehanicheskih svojstv legirovannyh stalej dlja shlicevyh valov / Trudy Mezhdunarodnoj nauchno-prakticheskoj online konferencii «Integracija nauki, obrazovanija i proizvodstva – osnova realizacii Plana nacii» (Saginovskie chtenija № 13), 2021 - Karaganda: Izd-vo KarTU. – P. 1504.

[4] Sivachenko L.A. Intensifikacija tehnologicheskih processov v apparatah adaptivnogo dejstvija. pod red. L.A. Sivachenk. - Baranovichi, BarSU, 2020. - 359 p.

[5] Kravchenko E.G., Shirtladze A.G. Nadezhnost' tehnicheskih sistem v mashinostroenii. Staryj Oskol: TNT, 2017. – 152 p.

[6] Shirshikov A.S., Ljandenburskij V.V. Belokovyl'skij A.M., Ocenka nadezhnosti tehnicheskih sistem. Penza: PGUAS, 2015. – 240 p.

Information of the authors

Buzauova Toty Meyerbekova, candidate of technical science, associate professor of the department "Technological equipment, mechanical engineering and standardization" of Abylkas Saginov Karaganda Technical University

E-mail: toty_77@mail.ru

Tlekbayeva Diana Kairatovna, master student of the department "Technological equipment, mechanical engineering, standardization" of Abylkas Saginov Karaganda Technical University
E-mail: tlekbayeva_d@mail.ru

Smailova Baglan Kabdulaevna, master, senior lecturer of the department "Technological equipment, mechanical engineering, standardization" of Abylkas Saginov Karaganda Technical University
E-mail: b.smailova.82@mail.ru

Mateshov Arman Karievich, master, senior lecturer of the department "Technological equipment, mechanical engineering, standardization" of Abylkas Saginov Karaganda Technical University
E-mail: makashka_m@mail.ru

DOI 10.52209/2706-977X_2022_3_11 **IRSTI 81.09.03** **UDC 621.762(075.8)**

Powder Particle Mixture Influence on The Injection Molding of Metal Powder

Khairur Rijal Jamaludin*
University of Technology Malaysia, Kuala Lumpur, Malaysia
*corresponding author

Abstract. Mixture of powder particles will influence the injection molding capability of the feedstock. The rheological behavior of the feedstock will provide initial information for predicting the success of the injection molding of the feedstock. The monomodal and bimodal powder particles feedstocks with powder loading 64 vol. % and 65 vol. %. was investigated and discussed to show its molding capability. Results demonstrates significant fluidity behavior by its rheological properties as samples were successfully injection molded. Fine powder particles at 64 vol. % demonstrated higher temperature sensitivity than the coarse powder feedstock. However, the coarse powder feedstock shows its sensitivity to the injection pressure. The monomodal feedstock exhibits higher viscosity over the bimodal feedstock. Binder separation is also likely to occur in the monomodal feedstock prepared with coarse powder especially at a high injection temperature. The investigation found that the injection temperature has its influence to the final quality of the compact. Injection temperature of 140 ºC was found to be the optimum. However, the investigation does not find any significant on the injection temperature to the debinding rate. The flow behavior index decreases when the temperature increases. The investigation also shows that the feedstock flow sensitivity depends on the fine powder distributions in the feedstock. Since all the feedstock demonstrates a good pseudo plastic behavior, it therefore is suitable to be injection molded.

Keywords: metal injection molding, feedstock, particle size, bimodal, moldability, rheology

Introduction

Metal injection molding (MIM) has emerged as a viable method of producing complex shaped parts at a competitive cost [1,2]. The MIM process uses a combination of powder metallurgy and injection molding technologies to produce net-shape parts and is comprised of five main sub processes: raw materials selection (powder/binder), feedstock preparation, injection molding, debinding, and sintering. One of the advantages of MIM is its ability to produce parts with complex geometry without machining. However, to stay within the ever-tighter tolerances demanded by component manufacturers' customers, MIM parts must be produced with a high degree of dimensional control to minimize the dimensional variability of critical dimensions [3, 4].

Shape of powder particles is among the important parameter that effect the density of the final products. However, the most popular powder particles which is a spherical shape powder is expensive. Fine spherical shape powder will result better shape retention and densification after sintering. On the other hand, fine non spherical shape powder usually those are produced by water atomized method, although less cost but it is difficult for injection molding. This is due to the high friction between powder particles. Thus, Zauner et al. [5] investigates the effects of powder type and powder size on dimensional variability. Their study is to show the effect of powder size, powder shape, powder size distribution, and surface area focusing on dimensional variation and its dependence on powder type, particle shape, and particle size. Arakida and Miura [6] also studied the effect of fine (20 μm), coarse (150 μm) gas- and water-atomized powders, and their effect on packing density and fluidity. Their work showed that fine gas-atomized powder exhibits higher density, which in turn produces improved mechanical properties. Dihora et al. [7] found that the instability index for feedstocks increases with particle size. Almost all the studies that dealt with powder characteristics focused on rheometry rather than dimensional variation. This is by the fact that during injection, the rheological behavior of feedstocks is controlled by multiple variables including powder characterization [8], binder feedstock properties [9] and injection parameters [10]. This has been further elaborated by Langlais et al. [11] in their study to correlate feedstock moldability performance with melt viscosity and dry powder rheology.

Powder loading is another aspect for minimizing shrinkage of the final products. The study by Yimin et al. [12] have investigated the effect of powder loading (60, 64, 68 and 72 vol. %) on MIM. The investigation proved that 68 vol. % powders loading was the optimum for injection molded gas atomized spherical 17-4 PH stainless steel powder and the binder of 65 % PW + 30 % EVA + 5 % SA. The 68 vol. % powder loading can be injection molded with a comparatively low viscosity on a relatively wide temperature range, and it is best to get quick powder re-packing and binder molecule orientation during injection molding. From the standpoint of compact shape retention and dimension tolerance control, the optimal powder loading of 68 vol. % was also the best. Furthermore, the compact of 68 vol. % powder loading is easy to get sinter densification and has superior mechanical properties and microstructures. While Pandey et al. [13] has studied the melt flow properties of metal powder at various powder loading at different properties with elevated temperature to

find the applicability of the composite in MIM and rapid prototyping. The study indicates that the melt flow properties reveal that formed composite can attain high flowability at elevated temperatures.

While, in another work, Hwang et al. [14] investigated the debinding rate of solvent debinding for compacts prepared with different particle sizes. The investigation concluded that the debinding rate is determined by the cross-section thickness, particle size does not affect the tortuosity for spherical powders, and thus not the debinding rate. Further, on the investigation to higher powder loading compacts, the debinding rate was slightly slower. With a higher powder loading, the debinding rate decreases because the total porosity and flux area for the soluble binder component to diffuse through decreases.

The requirement for small particle dimensions has led to some concerns regarding the potential cost of the process, making MIM a relatively expensive route to produce larger components. Therefore, a primary motivation for adding coarser particles to fine powders as composite mixture of metal powder is to lower the manufacturing costs of MIM. However, there are some disadvantages that may lead to the non-homogeneity in the sintered structure. Thus, avoidance of component defects requires a quantitative understanding of the effects of process parameters on the rheological and injection behavior of the feedstock. This will be discussed further with the present work how the fluidity of the composite mixture of metal powder will enhance the injection molding of feedstock.

1. Experimental Procedures

1.1 Materials

The metal powder used in this study is the ANVAL 316L stainless steel gas atomized powder with the pycnometer density of 7.93 g/cm^3. A binder system based on polyethylene glycol (PEG) was prepared. The minor component is polymethyl methacrylate (PMMA) and stearic acid (SA) was added as the surface-active agent. The binder composition is 73 % PEG + 25 % PMMA + 2 % SA based on the weight fraction. The powder loadings are for the monomodal powders were 64 and 65 vol. % while for the bimodal was 64 vol. %.

The distribution of particle size as shown in Table 1 was measured using Mastersizer, Malvern Instrument. This method was used to measure the size percentage of the powder.

Table 1. Particle size distribution

	D_{10}	D_{50}	D_{90}	S_W
Coarse	9.563	19.606	40.058	4.159
Fine	5.780	11.225	19.840	4.873

1.2 Experiment procedure

The feedstock classification for the bimodal is as shown in Table 2. Prior investigation, stainless steel powder was mixed with binders in the sigma blade mixer for 95 minutes at 70 °C. After mixing, the paste was removed from the mixer and will be fed into the strong crusher for granulation.

Table 2. Feedstock classification for the bimodal powder at powder loading 64 % vol.

Feedstock Abbreviation	Description
A1_64	Bimodal: 70% mass of coarse powder
B1_64	Bimodal: 30% mass of fine powder

The rheological characteristic of the feedstocks was investigated using Shimadzu 500-D capillary rheometer and the MIMA tensile specimen was injection molded with the Battenfeld BA 250 CDC injection-molding machine. To evaluate the temperature influence, injection pressure was remains at 350 bars while the injection temperature was varied from 120, 130,140 and 150 °C.

3. Results and Discussion

3.1 Rheological properties

In MIM process, the feedstock rheological properties are key features which influences the steady flow and the uniform filling into the mold. The evaluation of the feedstock rheological properties is based on the viscosity and its shear

sensitivity and temperature sensitivity [8]. Fig. 1 shows the pseudo plastic behavior of both feedstocks at injection temperature of 120, 130 and 140 ºC. Generally, the viscosity was decreasing when shear rate was increased.

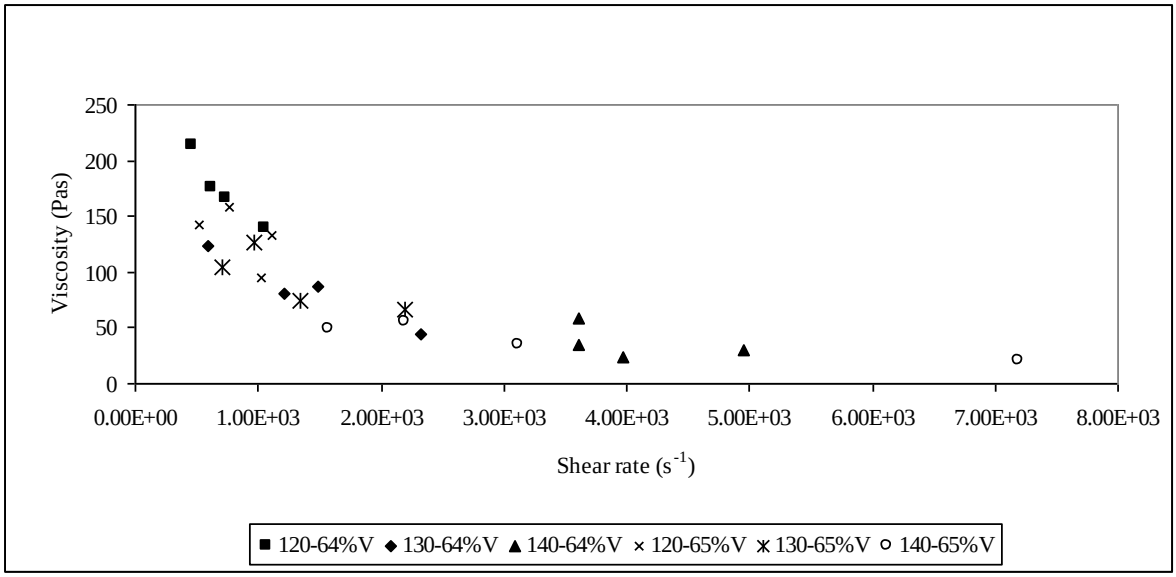

a) fine powder

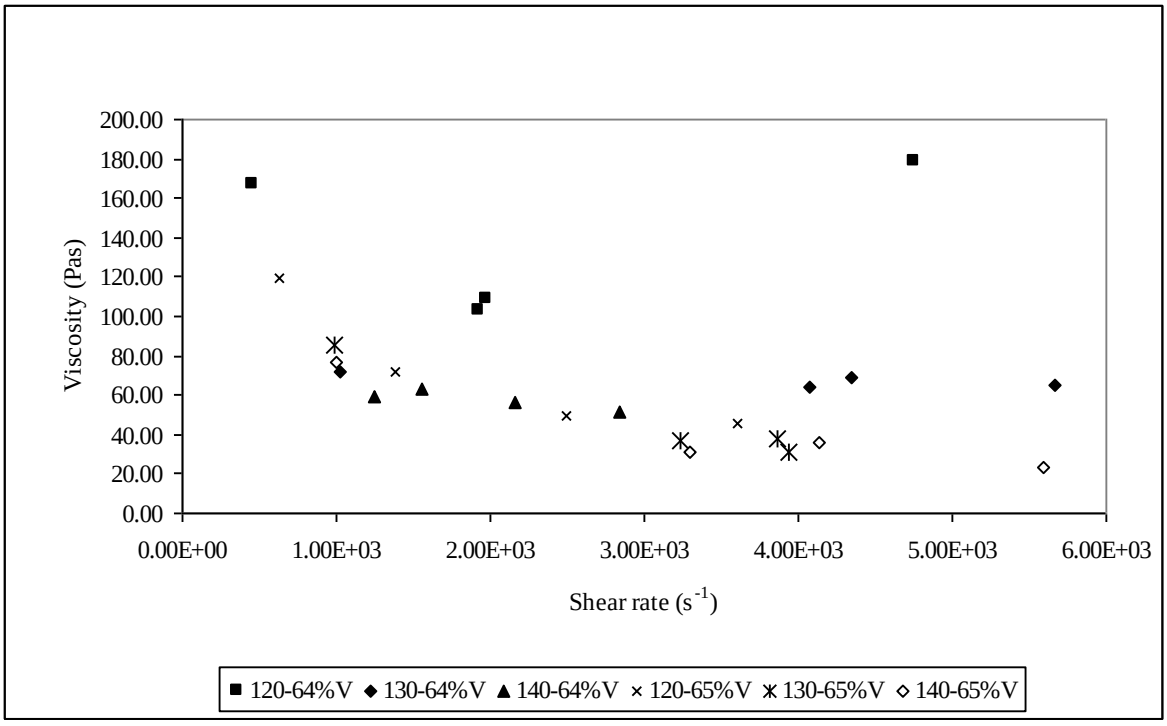

b) coarse powder

Fig. 1. - Feedstock pseudo plastic behavior

Fig. 1 (a) shows the fine powder feedstock was more viscous than that shown in Fig. 1 (b). This is due the fine powder contains smaller interstitial spaces than the coarse powder thus it increases its interparticle friction. Beside that, fine powder has larger particle surface contact area between powder particles [3].

An MIM feedstock is generally considered pseudo plastic fluid [14]. For pseudo plastic fluid, there is

$$\tau = k(\dot{\gamma})^n \quad (1)$$

where τ is the shear stress;

$\dot{\gamma}$ is the shear stress;

k is the constant;

n is the flow behavior index (<1).

The value of n indicates the degree of shear sensitivity. The lower the value of n, the more quickly the viscosity of feedstock changes with shear rate. Injection molding of MIM feedstock is conducted under pressure and temperature. It is desirable that the viscosity of the feedstock should decrease quickly with increasing shear rate during molding. This high shear rate sensitivity is especially important in producing complex and delicate parts.

Table 3. Activation energy, E and flow behavior index, n

Abbreviation	E (kJ/mol)	Temp (°C)	n
16_64 (fine)	79.54	120	0.49
		130	0.23
		140	-0.22
16_65 (fine)	33.67	120	0.67
		130	0.49
		140	0.36
31_64 (coarse)	49.33	120	0.98
		130	0.95
		140	0.81
31_65 (coarse)	9.8	120	0.43
		130	0.33
		140	0.35

Moreover, the feedstock viscosity depends exponentially on absolute temperature T as follows [9]:

$$\eta = \eta_o exp\left(\frac{E}{RT}\right) \quad (2)$$

where η_o is the reference viscosity,

E is the flow activation energy,

R is the gas constant;

T is the absolute temperature.

The value of E expresses the effect of temperature on the viscosity of the feedstock. If the value of E is low, the viscosity is not so sensitive to temperature variation. Therefore, any small fluctuation of temperature during molding will not result in sudden viscosity change. A sudden viscosity change could cause under stress concentrations in molded parts, resulting in cracking and distortion [9-10].

Table 3 shows the activation energy at shear rate 1000 s^{-1} and flow behavior index of the feedstock. Fine powder feedstock exhibits higher sensitivity than the coarse feedstock. This can be seen that the fine feedstock has high activation energy than the coarse feedstock. However, Table 3 shows that the sensitivity was reducing when the powder loading is increases.

Further, the flow behavior indexes (<1) demonstrate a shear thinning of the feedstock when applied to shear stress. The flow behavior indexes of each feedstock are reducing when the injection temperature arises. Lower the flow behavior index, higher the sensitivity. As 16_64 has negative flow behavior index at 140 °C, then it shows that this feedstock is very much sensitive to the change of temperature and shear rate during injection. The melt will possibly freeze inside the mold cavity when drastic temperature change occurs in the mold cavity.

Therefore, any small fluctuation of temperature during molding results in a sudden viscosity change. This could cause defects in the molded parts, such as cracking and distortion due to the undue stress concentration appeared [14]. In addition, feedstock with high sensitivity to temperature is also sensitive to pressure [2].

However, for the bimodal powder particles as shown in Fig. 2, 3 and 4 show the correlation of viscosity and shear rate at injection temperatures of 120 °C, 130 °C, and 140 °C.

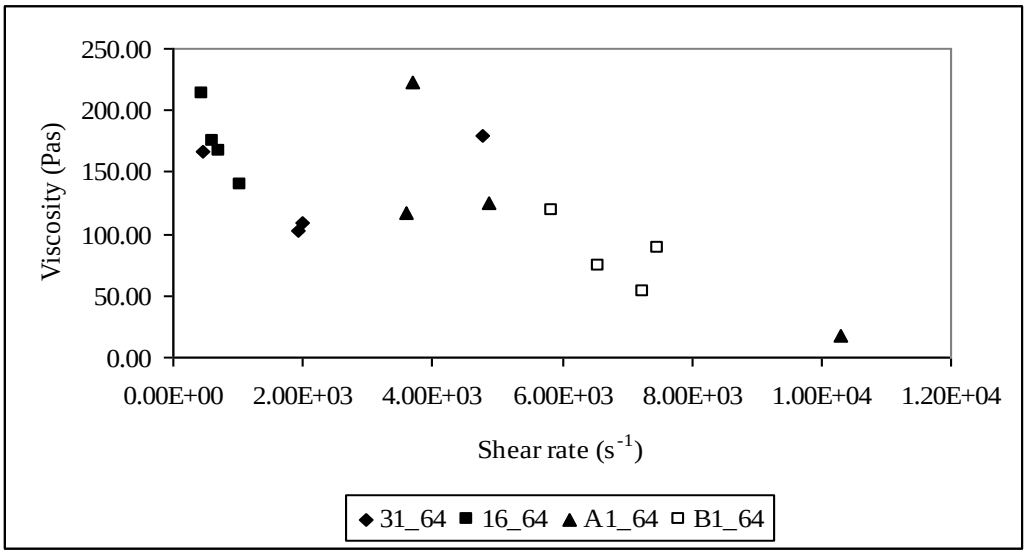

Fig. 2. - Correlation of viscosity and shear rate at 120 °C

The bimodal feedstock, A1_64 as shown in Fig. 2 exhibits the highest viscosity while B1_64 is at the lowest at this injection temperature. Powder-binder separation occurs at a high shear rate on the monomodal feedstocks, 31_64 and B1_64. However, when the temperature was increased to 130 °C (Fig. 3) the viscosity of A1_64 is reduced. Furthermore, the feedstock became inhomogeneous due to powder and binder separation [15]. Thus, Maetzig et al. [16] suggested maintaining the injection molding at relatively low flow rate to prevent separation of powder and binder.

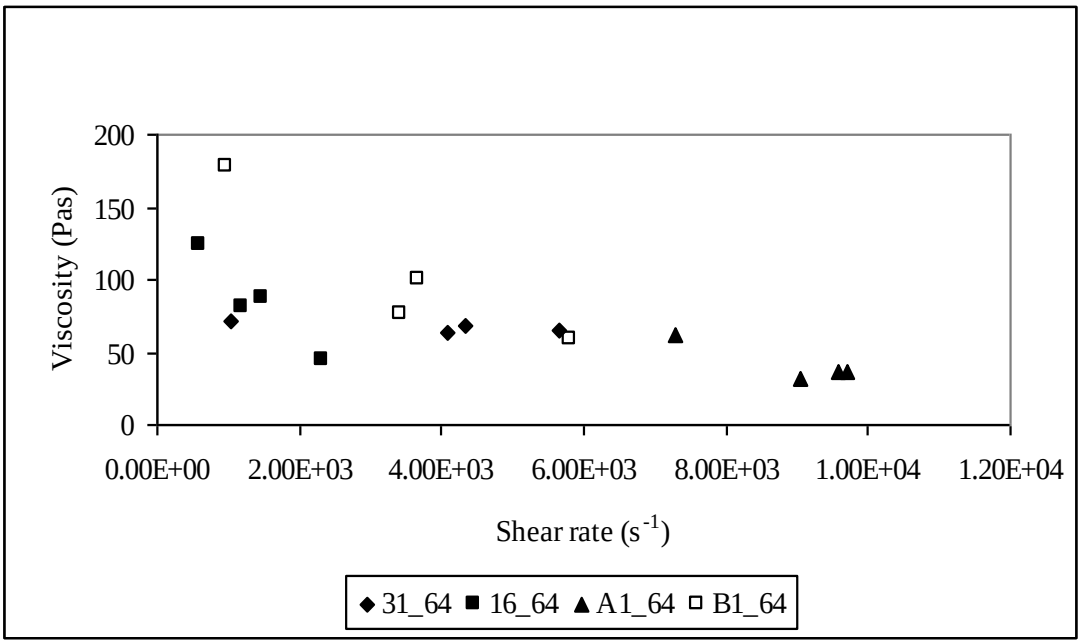

Fig. 3. - Correlation of viscosity and shear rate at 130 °C

When the injection temperature was increased to 130 °C, the bimodal feedstock, B1_64 exhibited a higher viscosity at a shear rate less than 2000 s^{-1} as compared to the monomodal feedstocks. However, when the shear rate is lower than 8000 s^{-1}, A1_64 is more viscous as compared to the B1_64. However, the viscosity is almost the same at the high shear rate.

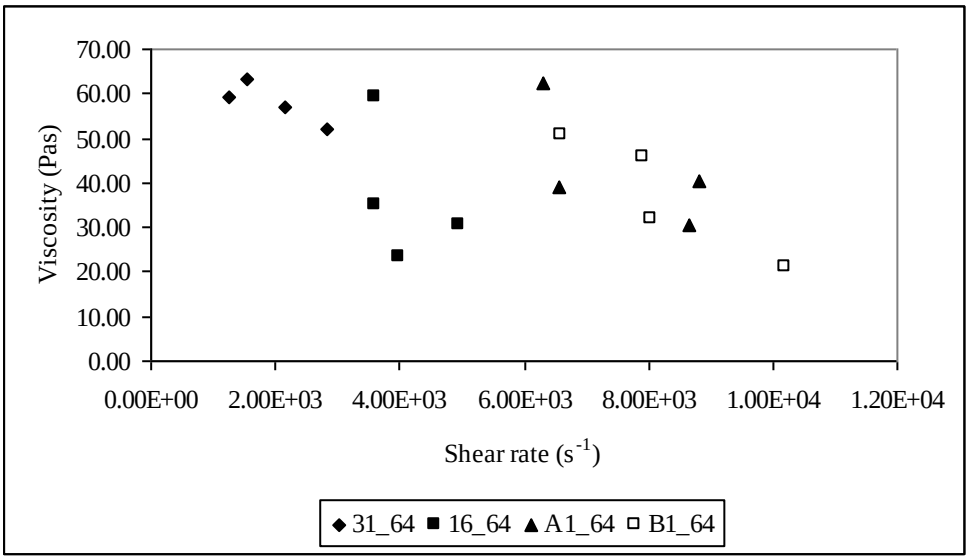

Fig. 4. - Correlation of viscosity and shear rate at 140 °C

Moreover, when the temperature was increased to the maximum (Fig. 3), the monomodal feedstock, 31_64 became more viscous than 16_64. This is possibly due to the binder separation of the coarse powder. Fine powders prevent the feedstock from powder-binder separation during injection molding, as this effect is more likely to be introduced through large particles, especially when a low viscosity binder and metal powders of high density are used by literature [17]. At the same time, the bimodal feedstock A1_64 is more viscous than B1_64. However, the bimodal feedstocks are still dominant in terms of viscosity as compared to the monomodal feedstocks in every injection temperature. The bimodal particle distributions do affect the feedstock viscosity as seen in Fig. 2, 3 and 4 that the viscosity of A1_64 and B1_64 is among the lowest.

Conversely, literature [18] discovers that using carbonyl iron powder that particle distribution does not affect viscosity for powder fraction of 60 % volume as the monomodal and bimodal distributions present the same viscosity because the shear rate was varied. As the powder fraction was increased from 60 % to 65 % volume in a bimodal distribution, the viscosity was less affected than when the powder fraction was increased from 55 % to 60 % volume in a monomodal distribution. Finally, he concludes that the bimodal distribution for carbonyl iron powder is to be recommended only for very high powder loading.

Particle size ratio in the bimodal powder distribution system has its significance. A large particle size ratio can also provide higher packing density, better stability in debinding, good moldability, and lower shrinkage in sintering. However, there are a number of problems associated with such blends and these include larger clearances needed between the screw and barrel in the molding machine, and the potential for non-homogeneity in the sintered structure, which can adversely affect the part's physical and mechanical properties [19].

Fig. 2, 3 and 4 also indicate that the coarse powder (31_64) exhibits lower viscosity than the fine powder (16_64). This is due to coarse particles in a system diffuse to a lesser extent than the fine powder and less energy is dissipated in the flow. Therefore, the relative viscosity decreases with the increase of the particle size. Consequently, by adding coarse powder to the fine powder, a feedstock with lower relative viscosity at the same solid loading content can be obtained [19].

A binder separation phenomenon is likely to occur in the 31_64 at all temperatures. Nevertheless, Fig. 2, 3 and 4 do not indicate any occurrence of binder separation phenomenon in 16_64. Modelling the binder separation phenomenon as flow through porous medium enables identification of the parameters influencing the separation that occurs during the tests. The following equations (Kozeny-Carman and the Blake Kozeny equation respectively) describe the permeability constant of a porous medium, k

$$k = \frac{\varphi^3}{5S^2(1-\varphi)^2} \tag{3}$$

$$k = \frac{D^2\varphi^3}{150(1-\varphi)^2} \tag{4}$$

where φ is medium porosity;
S is specific pore surface (pore surface exposed to the fluid per unit volume of a porous material);

D is particle diameter.

These two relations shows that the permeability constant is low when the particle size is small, and the pore surface area is large. Binder separation is less likely to occur when the flow through the porous medium is low, which is equivalent to a lower permeability value. Therefore, the tendency for binder separation would be less if fine powder and irregular shape are used.

3.2 Temperature influence

Feedstock viscosity dependence to the melt temperature is shown by Fig. 5 and 6. The error bars indicate the maximum and minimum viscosities. As shown in Fig. 5, A1_64 has a broad viscosity range from temperatures of 120 and 125 °C, when it was extruded at 29 bars from the rheology test barrel. Besides, Fig. 6, B1_64 shows a wide viscosity range at 130 °C when pressures at bars 29 and 59 were applied.

As shown in Fig. 5, viscosity decreases when the extrusion pressure and the test temperature is increased, regardless, in Fig. 6 the viscosity fluctuates with the increase of temperature. This is possibly due to the occurrence of binder separation as the feedstock in Fig. 6 has broader coarse powder distribution as compared to A1_64.

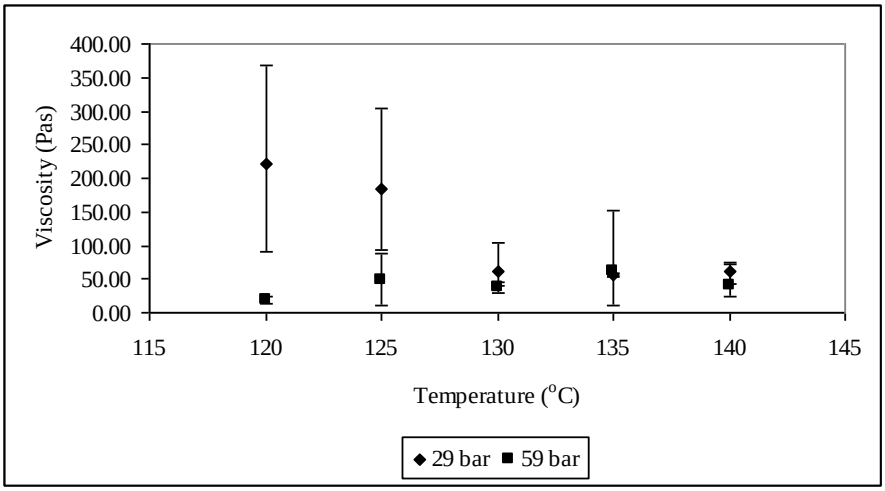

Fig. 5. - Temperature influence on the viscosity for A1_64

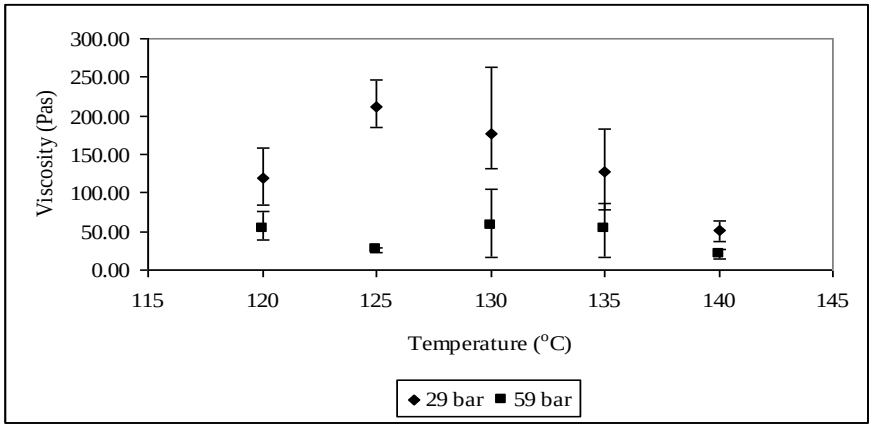

Fig. 6. - Temperature influence on the viscosity for B1_64

Some molding defects such as jetting are associated with small n, i.e., higher shear sensitivity [21]. During the injection molding process, pseudo plastic behavior is desirable and, therefore, a decrease in viscosity with an increase in the shear rate is suitable. This dependent behavior of the viscosity against the shear rate is especially important when producing complex and delicate parts, which are vital products in the MIM industry [22]. The comparison of the feedstock rheological properties of the bimodal powder is shown in Table 4.

Generally, the feedstocks in Table 4 demonstrate pseudo plasticity as the index is smaller than one, thus it indicates shear thinning occurs in the feedstock when applied to a shear stress. The flow behavior index of 16_64 is smaller than 31_64. This indicates that at shear rate 16_64 the viscosity of the feedstock changes more quickly. The coarse

powder is likely to become dilatant at a low temperature, as the flow behavior index for 31_64 seems inversely proportional to the temperature and is expected that the value becomes higher than unity.

Table 4. Rheological properties of the feedstock

Feedstock	Temp	Flow behavior index, n	Activation Energy, E	Apparent Viscosity, η	Moldability index, α_{STV}
31_64	120	0.98	49.33	137.06	24.60
	130	0.95	49.33	71.62	117.68
	140	0.81	49.33	64.67	487.40
16_64	120	0.49	79.54	141.77	376.03
	130	0.23	79.54	94.44	852.24
	140	-0.22	79.54	35.76	3571.93
A1_64	120	-1.12	24.43	2544.20	284.15
	130	-1.00	24.43	2924.30	233.23
	140	-0.16	24.43	323.89	1222.24
B1_64	120	-0.95	36.54	2850.56	155.66
	130	0.41	36.54	177.69	755.55
	140	-1.06	36.54	2735.65	171.35

Furthermore, B1_64 exhibits high sensitivity than A1_64. However, the sensitivity of B1_64 reduces with the increase of temperature. The sensitivity of A1_64 is high due to the high fine powder composition in the bimodal system as compared to B1_64. B1_64 which shows inconsistency of the flow behavior index when the temperature increases.

In addition, the controllability of viscosity within an injection molding barrel by controlling the temperature of barrel, nozzle and mold, the temperature dependence of viscosity may influence the response of the material to the sudden non-uniform cooling within a cavity. For example, during the molding stage, the feedstock is forced into the mold where it immediately begins to cool. If the cooling is accompanied by a rapid increase in the viscosity, the result may be incomplete filling of the mold and induces cracking or porosity in the molded parts. Therefore, low temperature dependence is desired to minimize problems arising from fluctuating molding temperatures, thereby minimizing stress concentration, cracks, and shape distortions [23]. The activation energies and the viscosities at shear rate 1000 s^{-1} in Table 4 can cast some lights on the nature of the feedstocks.

The monomodal feedstock, 16_64 has low activation energy than 31_64 while the activation energy of the bimodal feedstock, A1_64 is lower than the B1_64. Nevertheless, the bimodal feedstock has low activation energies compared to the monomodal feedstock. Thus, it indicates that the bimodal feedstock is less sensitive to any temperature fluctuation during the injection molding process. This feedstock can therefore be injection molded in a relatively wide temperature range. High activation energy of feedstock 31_64 indicates a drastic viscosity increase upon cooling, and thus feedstock 31_64 requires a more accurate temperature control during injection molding. Otherwise, mold temperature distribution will cause non-uniform flow, which induces internal stresses.

To establish a general molding index, the model Weir proposes for polymers to be used including the main parameters as regards to flow [22].

$$\alpha_{STV} = \frac{1}{\eta_o} \frac{\left|\frac{\partial log\eta}{\partial log\dot{\gamma}}\right|}{\eta_o \frac{\partial log\eta}{\partial 1/T}} \tag{5}$$

where η is the viscosity;

η_0 is a reference viscosity;

T is the temperature; $\dot{\gamma}$ is the shear rate;

α_{STV} is the rheological index or moldability index [14].

Simplifying the equation:

$$\alpha_{STV} = \frac{1}{\eta_o}\frac{|n-1|}{E/R} \quad (6)$$

The higher the value of α_{STV}, the better the rheological properties. In Table 4, 16_64 has better rheological properties at 140 °C while 31_64 has poor rheological property at 120 °C. In general, the rheological properties are proportional to the temperatures.

3.3 As molded compact part

After the green compact has been ejected from the mold cavity, then the green strength of each compact produced were tested with the three-point bend test using INSTRON 5567 according to the MPIF Standard 15. The density was measured with Archimedes water immersion method according to the MPIF Standard 42. The result is as shown in Fig. 7.

Fig. 7 shows that in overall the as-molded strength were increasing when the injection temperature was increased. The plot shown that 16_65 was stronger than 16_64 at 120 and 130 °C but was vice versa at 140 °C and 150 °C. At most of injection temperatures, 31_65 was the strongest except at 120 °C. This is because at high powder loading feedstock has ability to increase the as-molded strength because powder particles interlocked each other's [2].

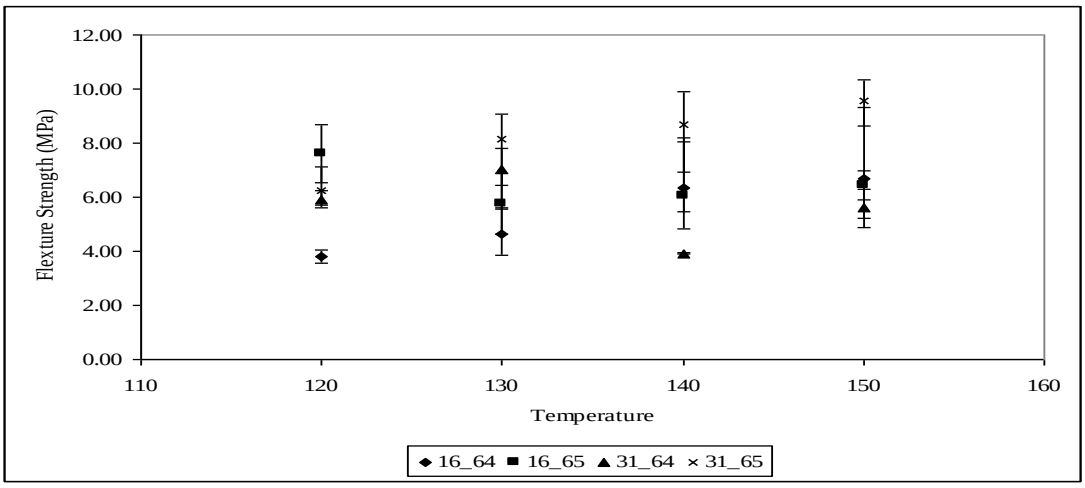

Fig. 7. - As-molded strength

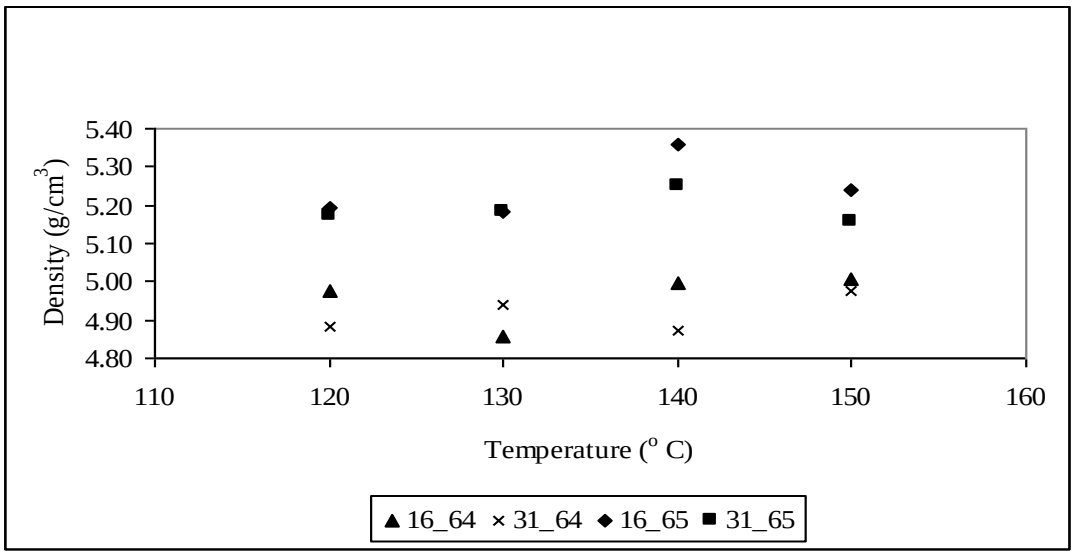

Fig. 8. - As-molded density

Fig. 8 shows the as-molded density at various injection temperatures. 16_65 has higher as-molded density than the others do at all injection temperatures followed by 31_65. In general, the result shows that the fine powder feedstock produces higher green compact density than the coarse powder as the fine powder has small interstitial spaces [2]. The result shows that 16_64, 16_65 and 31_65 were best injection molded at 140 ºC. This is due to the density shown in Fig. 8 were at peak when it was molded at 140 ºC. However, the peak for 31_64 was at 150 ºC.

However, most of the compacts that were injection molded with powder loading 65 vol. % appear many defects such as incomplete filling, compact breaking during mold opening etc. This is due to high melt viscosity during injection molding at 350 bars. Thus, higher injection temperature and pressure is required, but flashing was discovered on the compact if the injection pressure goes beyond 350 bars. However, bimodal powder distributions could be a solution to this molding difficulties [2].

Due to high sensitivity of the fine powder feedstocks (Table 2), many of the compacts produced with 16_64 appears weld line at the down stream. This is possibly due to the melt was freeze before it reached the end. However, coarse powder feedstock exhibits better results. This indicates that the rheological property of the feedstock has great significant in predicting the final parts quality.

3.4 As leached compact part

This section presents the debinding results of the fine and coarse powder feedstocks at powder loading 64 vol. %. Three-point bend test result shown in Fig. 9 is the as-leached strength of the compact. Result shows that the fine powder gives higher as-leached strength compared to the coarse powder and, the strongest was when it was injection molded at 140 ºC. However, the coarse powder flexure as-leached strength was improved when injection molded at 150 ºC. This may be possibly due to the polymer backbone network that properly formed when injection molded at higher temperature. However, since the coarse powder has less surface contact area compared to the fine powder, the coarse powder particles has less ability to interlocked each other causing its weaker as-leached strength.

The as-leached density shown in Fig. 10 exhibits that the compact produced with fine powder feedstock is denser than the coarse powder when injection molded at 140 and 150 ºC, especially at 140 ºC. However, at lower injection temperatures, the coarse powder compact is denser. This is possibly due to the powder was separates from the binder matrix during molten feedstock extrusion in the barrel and finally more binders was injection molded and the remaining powders was left behind inside the barrel.

Further, as shown in Fig. 9 and 10, the compact as-leached strength and density were proportional to the injection temperatures but 140 ºC is shown to be the best injection temperature because it enables to produce stronger and denser as-leached parts. This has its significant because high density compact will minimize sintered part shrinkage.

The relation between PEG loss and immersion time in water is shown in Fig. 11. During water debinding, water diffuses into the binder to react with and dissolve the PEG. PEG molecules become hydrated before they separate from the unhydrated mass to dissolve into water. The hydrated molecules of PEG then must diffuse out of the compacts through a network of pores formed by the PMMA and stainless-steel particles. As the molecular weight of the water is significantly lower than the molecular weight of PEG, water can diffuse into compacts faster than the PEG diffuses out of the compacts. Consequently, the rate limiting process is the diffusion of the hydrated PEG molecules rather than their dissolution or inward diffusion of the much smaller water molecules [21].

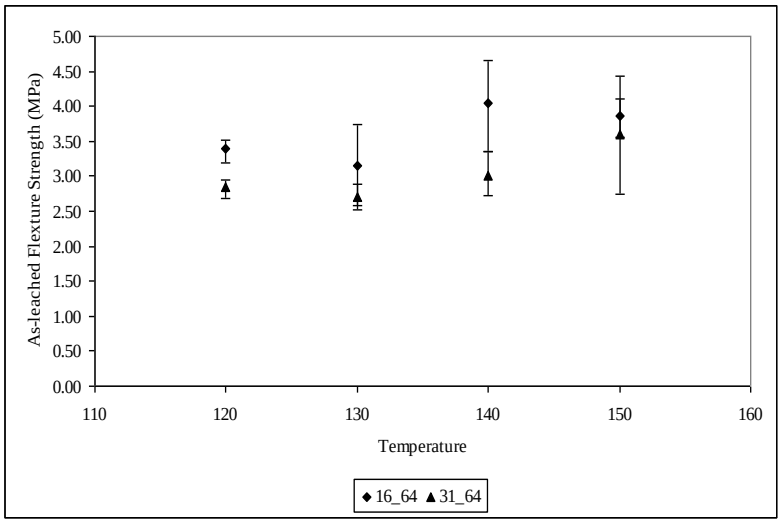

Fig. 9. - As-leached strength

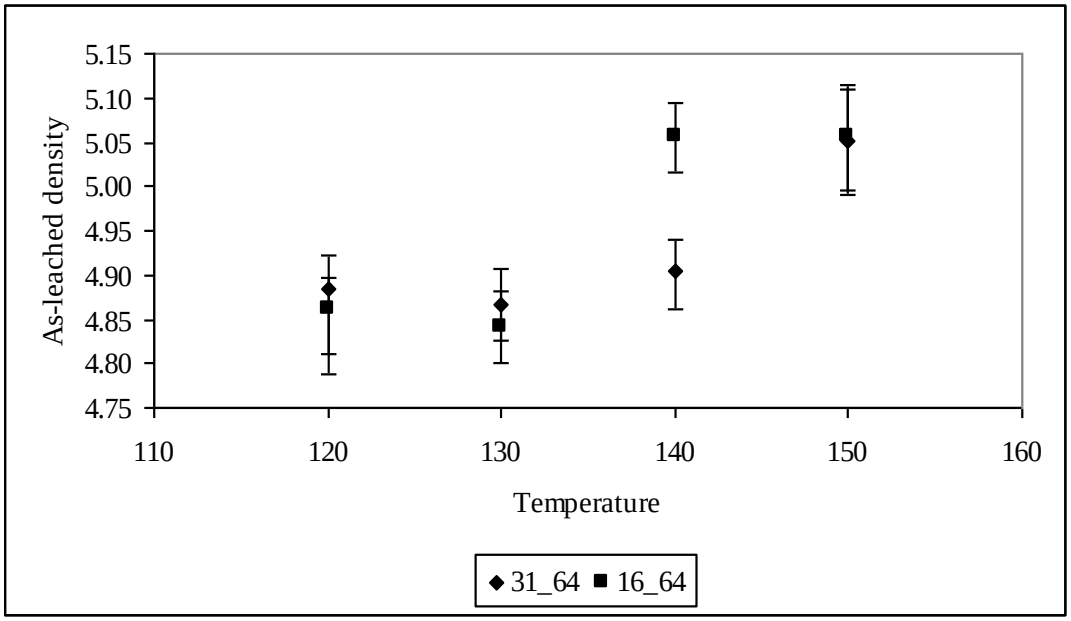

Fig. 10. - As-leached density

Since the diffusion distance for the water and PEG is short in the initial stage, the debinding rate is quite fast. As debinding proceeds, however, the pore channels extend to the inner region of the compact, and the longer diffusion length slows down the debinding rate [23-24].

The compacts that were injection molded at different temperatures were water bath at 65 ºC. Results shown in Fig. 11 (a) and 6 (b), does not indicate any significant of the injection temperature to the debinding rate.

An investigation made by Hwang et al. [13] on the solvent debinding behavior in the compact made from the 6.2 and 21.1 μm 316 L powder shows that the fine powder produced a smaller average pore size than did the coarse powders. However, their finding indicates that the critical factor that determines the debinding time is the cross-section thickness. The particle size does not affect the tortuosity for spherical powders, and thus not the debinding rate.

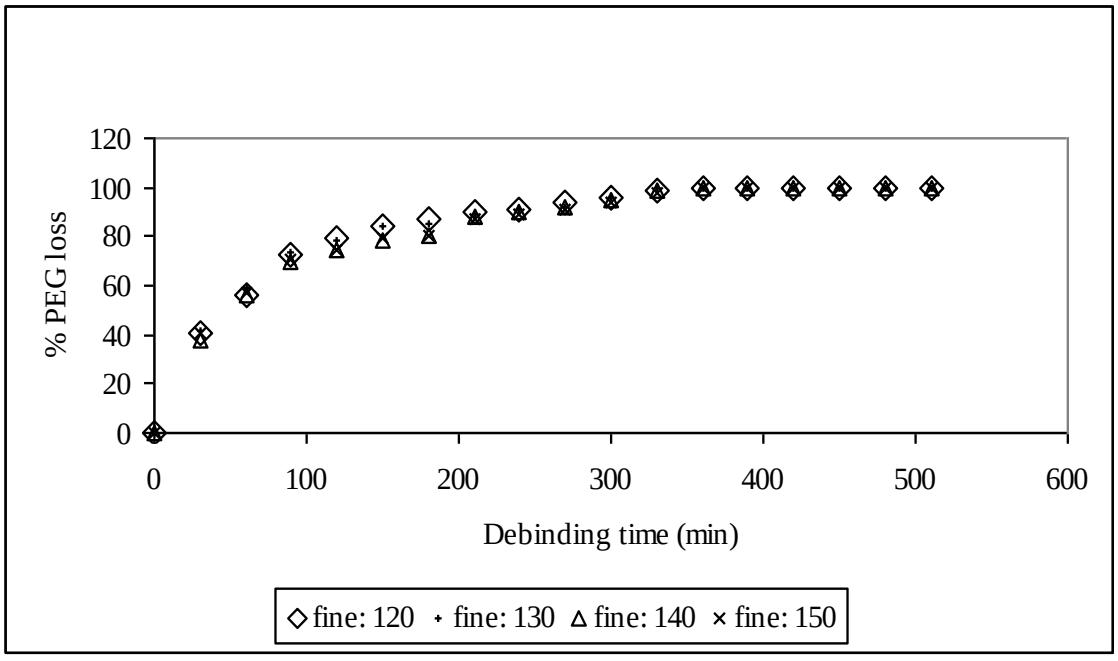

a) fine powder

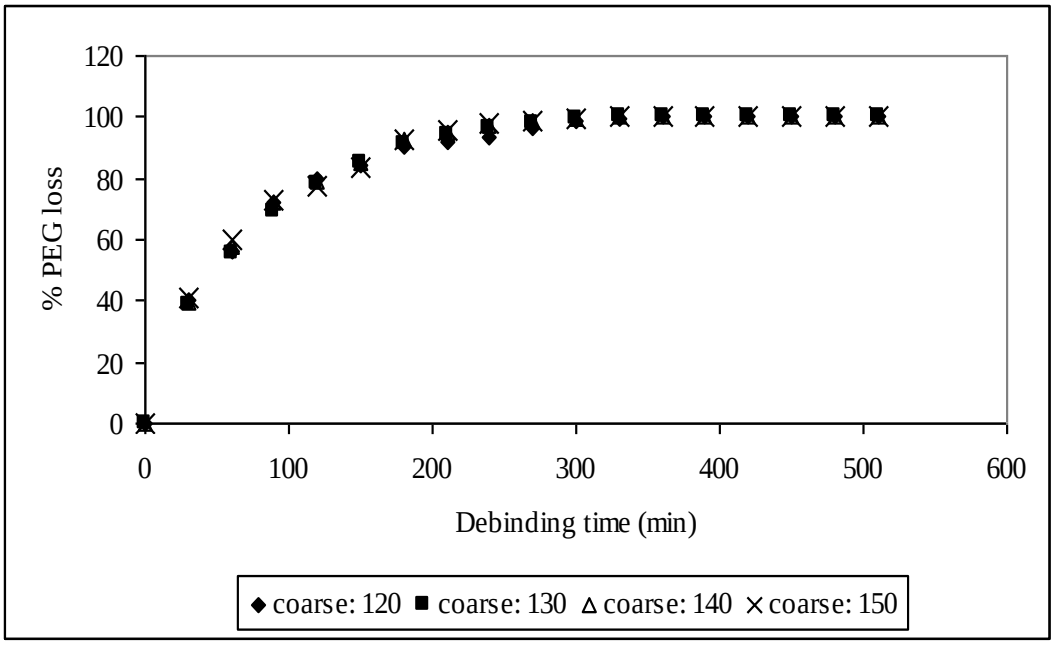

b) coarse powder

Fig. 11. - Debinding rate at 65 oC with different injection temperatures (120, 130, 140, 150 oC)

However, as shown in Fig. 12 the coarse powder feedstock debound faster when water bath at 65 and 60 °C. The same phenomena were noticed by Hwang et al. [13], but in his investigation, smaller particles debound faster. However, in different investigation presented in the same literature, indicates, though less pronounced, an opposite trend. It is possible that the differences of debinding rates could be caused by the interaction between the powder and the binder during kneading. With different particle sizes and shapes, the homogeneity of the binder matrix in the feedstock and the compact could vary. This may result in different pore characteristics within the PMMA during debinding and thus affect the debinding rate.

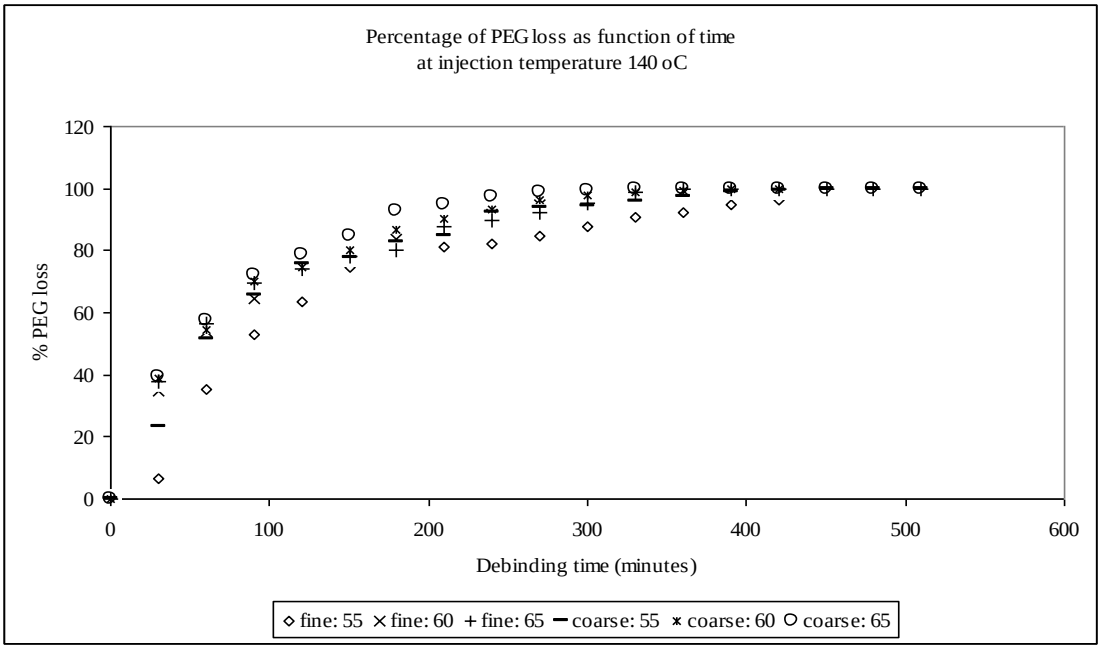

Fig. 12. - Debinding rate compact injection molded at 140 °C

Conclusions

Temperature influence on the injection of the monomodal and bimodal powder mixture has been discussed. The result discovered that the successful of the injection molding of MIM feedstock depends on the feedstock sensitivity. Fine feedstock at low powder loading has high sensitivity than the coarse powder feedstock and the sensitivity was proportional to the injection temperature.

Coarse powder feedstock at high powder loading gives better green flexure strength than the fine powder feedstock. However, fine powder gives better as-molded and as-leached density when injection molded at 140 °C while the as-leached flexure strength was also high. Finally, the investigation found that the injection temperature does not have any influence on the water-debinding rate.

References

[1] Chang S., Hao H., Bo-wen F., Jie-hua L., Tun W., Dong-yang L., Yi-min L., Hao H. Biocompatibility of vascular stents manufactured using metal injection moulding in animal experiments. Trans. Nonferrous Met. Soc. China, Vol. 32, 2022. – p. 569−580.

[2] German R. M., Bose A. Injection Molding of Metals and Ceramics. Metal Powder Industries Federation, Princeton, NJ, 1997.

[3] German R. M. A Rationalization of the Powder Injection Molding Process for Stainless Steels Based on Component Features. Advances in Powder Metallurgy and Particulate Materials, Metal Powder Industries Federation, Princeton, NJ, Vol. 5, 1998. - p. 71-83.

[4] Kulkarni K. M. Dimensional Precision of MIM Parts under Production Conditions. The International Journal of Powder Metallurgy, Vol. 33, Issue 4, 1997. - p. 29-41.

[5] Zauner R., Heaney D., Piemme J., Binet C., German R.M. The Effect of Powder Type and Powder Size on Dimensional Variability. Proceeding of PM2TEC World Congress, MPIF, 2002. - p. 191-198.

[6] Arakida Y., Miura R. Powder injection molding as a metal forming process – effects of powder morphology, size and size distribution. Key Engineering Materials, Vol. 53-55, 1991. - p. 377-382.

[7] Dihora L.V., Smith L.N., Orban R., German R.M. Experimental Study and Neural Network Modeling of the Stability of Powder Injection Molding Feedstocks. Materials and Manufacturing Processes, Vol. 15, Issue 3, 2000. -p. 419-438.

[8] Oh J.W., Lee W.S., Park S.J. Influence of nano powder on rheological behaviour of bi-modal feedstock in powder injection moulding. Powder Technol., Vol. 311, 2017. - p. 18–24.

[9] Ahn S., Park S.J., Lee S., Atre S.V., German R.M. Effect of powders and binders on material properties and moulding parameters in iron and stainless steel powder injection moulding process. Powder Technol., Vol. 193, 2009. - p. 162–169.

[10] Keshavarz Panahi A., Mianajiy H., Miandoabchi E., Hussaini Fareed M. Optimization of the powder injection moulding process parameters using the sequential simplex algorithm and sensitivity analysis. J. Manuf. Sci. Eng., Vol. 135, 2013. - p. 11006.

[11] Langlais D., Demers V., Brailovski V. Rheology of dry powders and metal injection molding feedstocks formulated on their base. Powder Technology, Vol. 396, 2022. - p. 13-26.

[12] Li Y., Li L., Khalil K.A. Effect of powder loading on metal injection molding stainless steels. Journal of Materials Processing Technology, Vol. 183, 2007. - p 432-439.

[13] Hwang K.S., Shu G.J., Lee H.J. Solvent d ebinding behavior of powder injection molded components prepared from powders with different particle sizes. Metallurgical and Materials Transactions, Vol. 36A, Issue 1, 2005. - p. 161-167.

[14] Yimin L., Baiyun H., Xuanhui Q. Improvement of rheological and shape retention properties of wax-based MIM binder by multi-polymer components. Transactions of Nonferrous Metals Society of China, Vol. 9, Issue 1.- p. 22-29.

[15] Heaney D.F., Zauner R. Variability of feedstock and its effect on component dimensional variability. Advances in Powder Metallurgy & Particulate Materials, Vol. 8, 2003. - p. 30-44.

[16] Maetzig M., Walcher H. Strategies for injection molding metals and ceramics. Advances in Powder Metallurgy & Particulate Materials, Vol. 10 2002. - p. 33-42.

[17] Rath S., Merz L., Plewa K., Ruprecht R., Hausselt J. Metal feedstocks for insolated micro parts made by PIM. Advances in Powder Metallurgy & Particulate Materials, Vol. 4, 2005. - p. 84-92.

[18] Resende L.M., Klein A.N., Prata A.T. Rheological properties of granulometric mixtures for Powder Injection Molding. Key Engineering Materials, Vol. 189-191, 2001. - p. 598-603.

[19] Dihoru L.V., Smith L.N., German R.M. Experimental analysis and neural network modeling of the rheological behavior of powder injection molding feedstocks formed with bimodal powder mixtures. Powder Metallurgy, Vol. 43, Issue 1, 2000. - p. 31-36.

[20] Khakbiz M., Simchi A., Bagheri R. Analysis of the rheological behavior and stability of 316L stainless steel-TiC powder injection molding feedstock. Materials Science and Engineering, Vol. A 407, 2005. - p. 105-113.

[21] Yang W.W., Yang K.Y., Hon M.H. Effects of PEG molecular weight on rheological behavior of alumina injection molding feedstocks. Materials Chemistry and Physics, Vol. 78, 2002. - p. 416-424.
[22] Agote I., Odriozola A., Gutierrez M., Santamaria A., Quintanilla J., Coupelle P., Soares. J. Rheological study of waste porcelain feedstocks for injection molding. Journal of the European Ceramic Society, Vol. 21, 2001. - p. 2843-2853.
[23] Hausnerova B., Sedlacek T., Slezak R., Saha P. Pressure-dependent viscosity of powder injection molding compounds. Rheological Acta, Vol. 45, 2006. - p. 290-296.
[24] Omar M.A., Ibrahim R., Sidik M.I., Mustapha M., Mohamad M. Rapid debinding of 316L stainless steel injection molded component. Journal of Materials Processing Technology, Vol. 140, 2003. - p. 397-400.
[25] Krauss V.A., Oliveira A.A.M., Klein A.N., Al-Qureshi H.A., Fredel M.C. A model for PEG removal from alumina injection molded parts by solvent debinding. Journal of Materials Processing Technology, Vol. 182, 2007. - p. 268-273.

DOI 10.52209/2706-977X_2022_3_25 **IRSTI 55.03.03** **UDC 622.267**

Manufacturing and Bench Testing a Batch of Pilot Industrial Samples of Multi-purpose Laying Systems for Supporting Mine Workings and Their Implementing in Industrial Conditions

Demin V.F., Kamarov R.K.*
Abylkas Saginov Karaganda Technical University, Karaganda, Kazakhstan
*corresponding author

Abstract. There are presented scientifically substantiated technological and technical developments on setting the parameters and implementing the technology of supporting with composite deep anchors for the development workings at junctions, supporting wide chambers (mounting and salvage ones), working crossings, broadening of the cross-sectional area for the location of technological equipment, which are essential for increasing the efficiency of mining preparation and stoping operations in the coal industry. Manufacturing and bench testing a batch of pilot industrial samples of multi-purpose laying systems for supporting mine workings were completed. The development of design documentation adjusted according to the results of bench and mine tests for manufacturing an experimental batch of a composite metal steel-polymer anchor using the capabilities of the design service of the Karaganda Machine-Building Consortium LLP was developed.

Keywords: design documentation, metal steel-polymer anchor, mine workings support, rope anchor, borehole, roof, drift, mine.

Introduction

The design documentation was developed and adjusted according to the results of bench and mine tests for manufacturing an experimental batch of a composite (accumulating, joining) metal steel-polymer anchor using the capabilities of the design service and the machine tool base of the Karaganda Machine-Building Consortium LLP and the machine shop of the Abaiskaya mine of the CD ArcelorMittal Temirtau JSC (Figure 1).

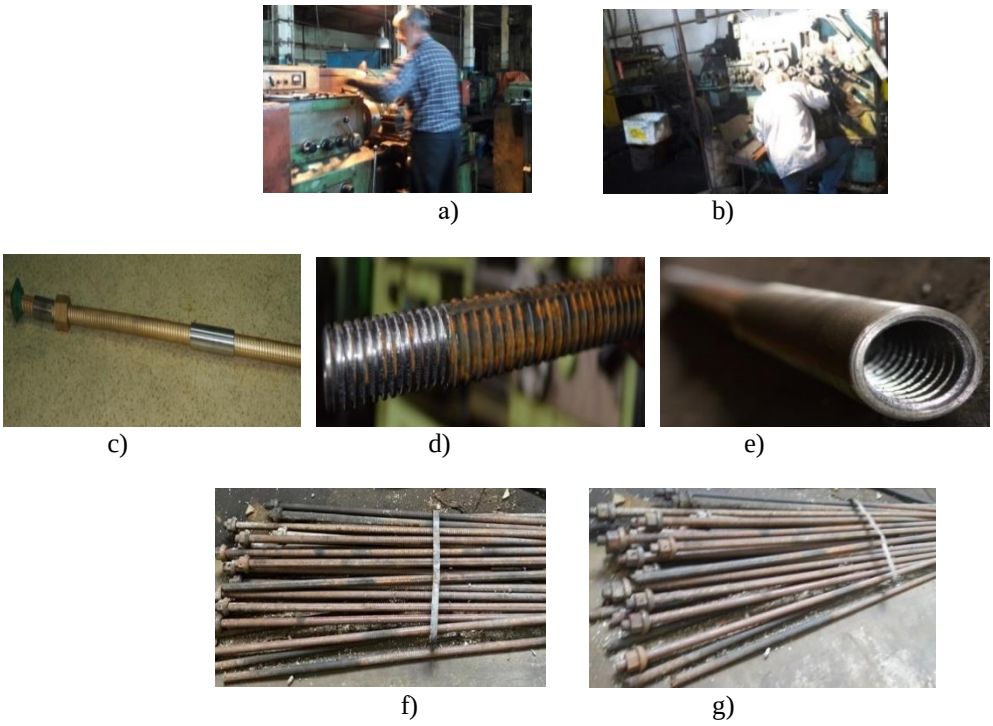

a) b) c) d) e) f) g)

a - turning operations; b - straightening and cutting the spring wire on the machine; c - assembled; d - screw part for winding the composite coupling; e - composite coupling; f, g - manufactured batch, separate and connected parts, respectively

Fig. 1. - Pilot batch of manufactured samples of combined anchors

The anchor rod is made of reinforcing steel of periodic profile A300; St5, St3ps 4.8 m long with a twisted profile with the outer diameter of 21.8 mm with tensile strength of 0.684–0.744 kN/mm^2.

Various designs of couplings were tested (Figure 2). The links of the anchor rods are interconnected by an anchor coupling with the outer diameter of 25 mm for a hole with the diameter of 28 mm made of steel grade 30HGSA, 35, 40 GSA, or KGSA with cementing.

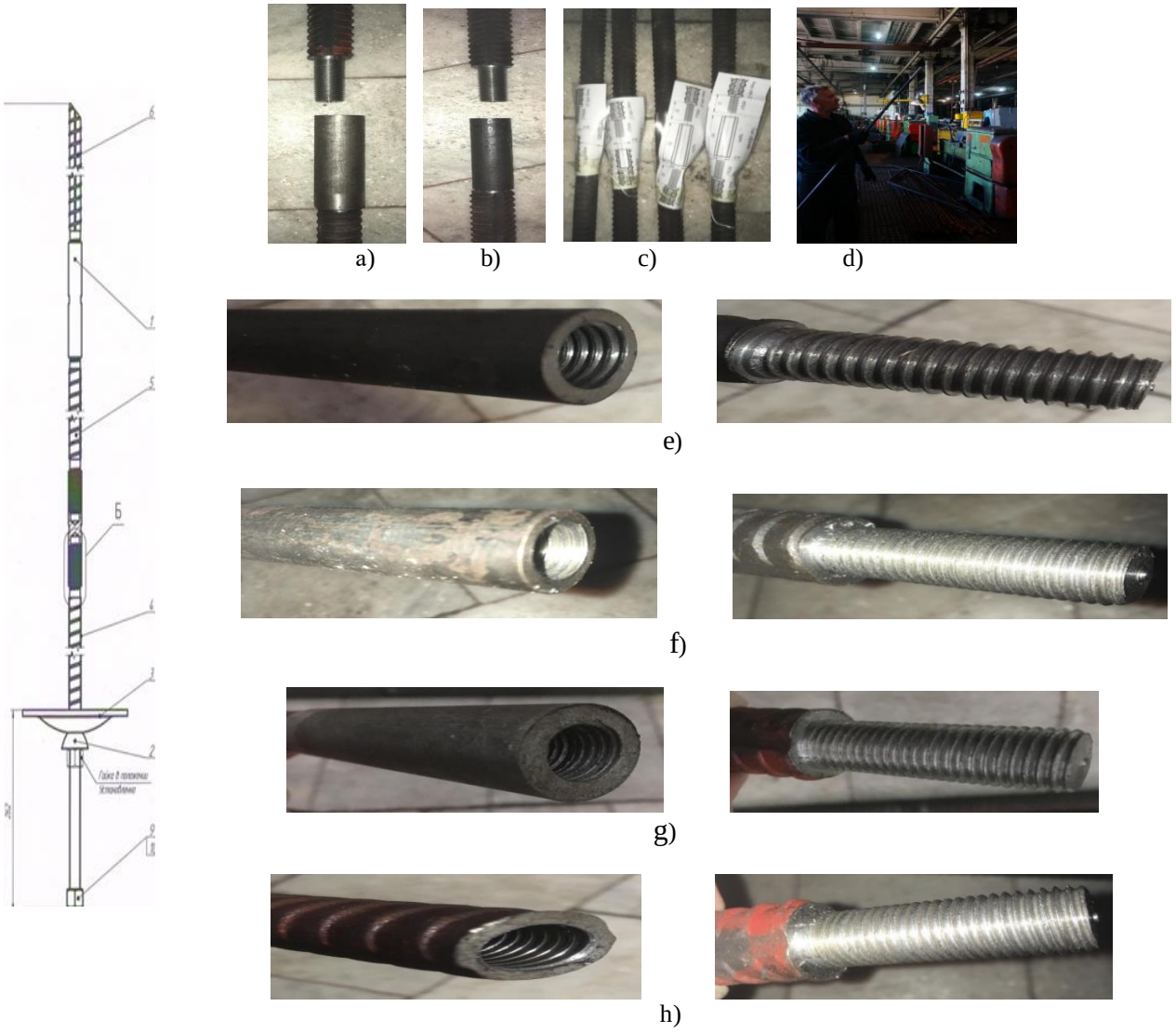

a, b – assembled structures; c - samples for testing; d - finished anchor; e, f, g, h - modifications of couplings and connecting links with different types of metric threads; and - combined anchor, assembly drawing parameters: length of the coupling (1_{co}, m); thread pitch (R_p, mm); d - l_{co} = 0.15; R_p = 1; e - 1_{co} = 0.2; R_p = 1.5; g - 1_{co} = 0.15; R_p = 1; h - 1_{co} = 0.2; R_p = 2; e - combined anchor assembly (1 - coupling; 2 - spherical washer; 3 - support-damping plate; 4 - anchor section; 5 - intermediate link; 6 - wellhead section of the anchor; 9 - nut; 10 - pin

Fig. 2. - Couplings, types of metric threads for modifications of the combined anchor

Bench tests for breaking force of pilot samples manufactured in the machine shop of the Abaiskaya mine were carried out at the cable testing station of the Ugleservice enterprise of the Energougol Production Unit of the ArcelorMittal Temirtau JSC (Figure 3).

A certified breaking machine UMM-100 (ZIM, 1972, the Artamonov plant) was used. The bench tests showed that with a combined anchor with the inner diameter of 20 mm, thread M1.5 mm, the breaking force was 12.5–13.0 tons with a gap in the cross section of the coupling with the outer diameter of 25 mm, the inner diameter of 20.5 mm with the minimum wall thickness of 2.5 mm; with an anchor with the diameter of 17.5 mm at the place of winding the coupling,

thread M1.5 mm, wall thickness of the coupling 3.7 mm, the breaking force was 15.1–15.5 tons and the break also occurred along the coupling; with an anchor with the diameter at the junction of 16 mm by the coupling, the breaking force was 14 tons with breaking the anchor rod itself.

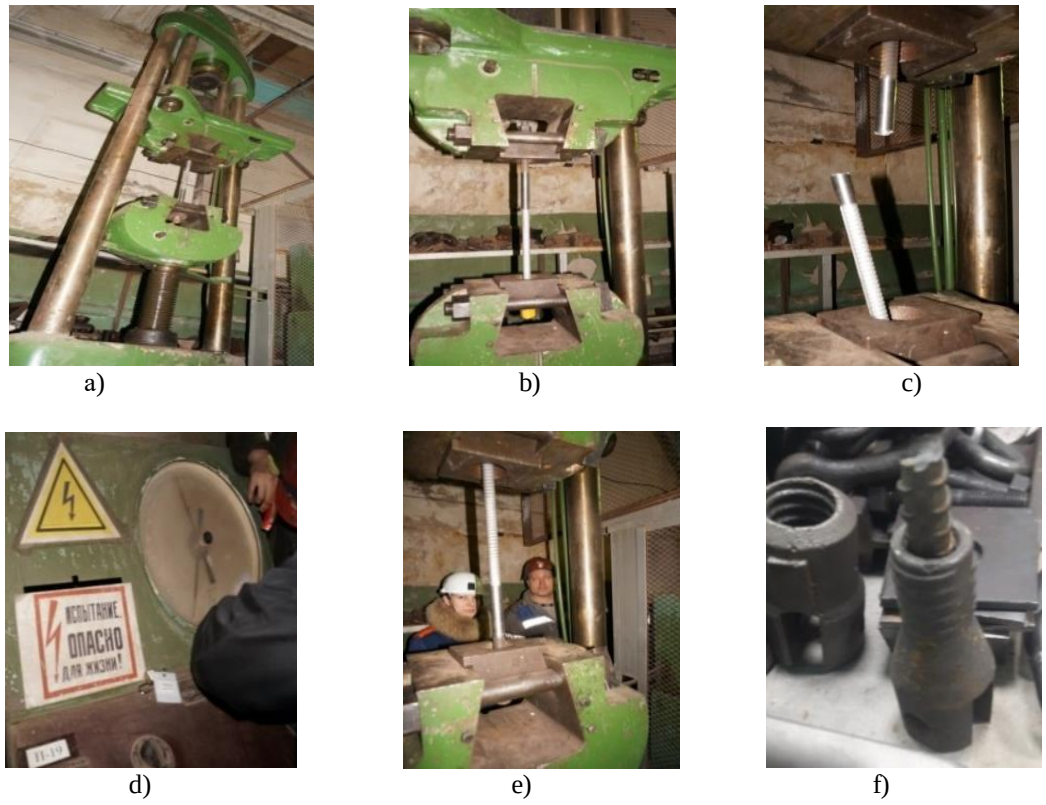

a) b) c)

d) e) f)

a – general view of the stand; b - installation of a combined anchor in clips on a full-size stand; b - the coupling of the combined anchor break under tensile loading; g - measuring console of the bench d – bench maintenance personnel; e - fixing the anchor in the cage and its break

Fig.3. - Bench tests of the combined anchors at the Ugleservice PA "Energougol" Office, CD ArcelorMittal Temirtau JSC

1. Material and methods

The dimensions and parameters of the anchor coupling and the threaded section under it for the combined anchor, justified by the test results, are shown in Figure 4.

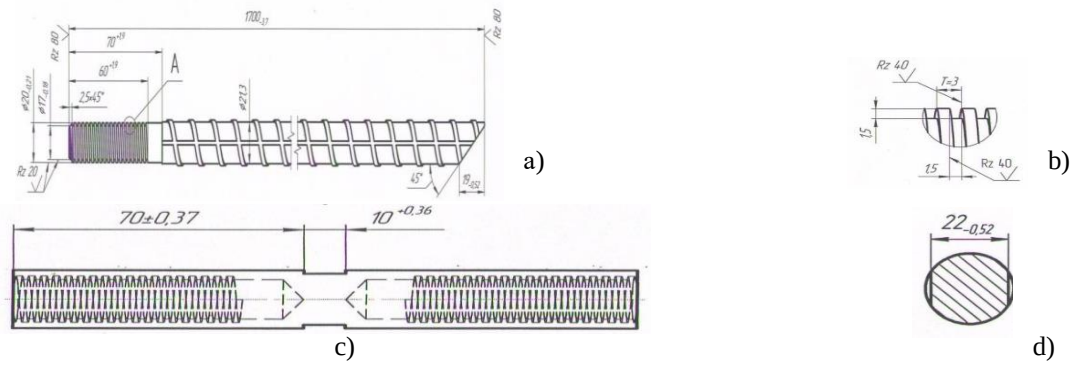

a) b)

c) d)

a - half-length of the combined anchor; b - thread for the coupling; c - thread parameters in the coupling; d - flat bevel on the sides of the rod

Fig. 4. - Dimensions and parameters of the anchor coupling for a combined anchor

Pilot industrial tests with introducing combined anchors into production when supporting the junction of conveyor drift 332к$_{12}$-yu with ventilation slope k$_{10}$ of the Abaiskaya mine of CD ArcelorMittal Temirtau JSC.

Pilot industrial tests with introducing combined anchors into production were carried out when supporting the junction of conveyor drift 332к$_{12}$-yu with ventilation slope k$_{10}$ of the Abaiskaya mine of CD of ArcelorMittal Temirtau JSC (Figure 5).

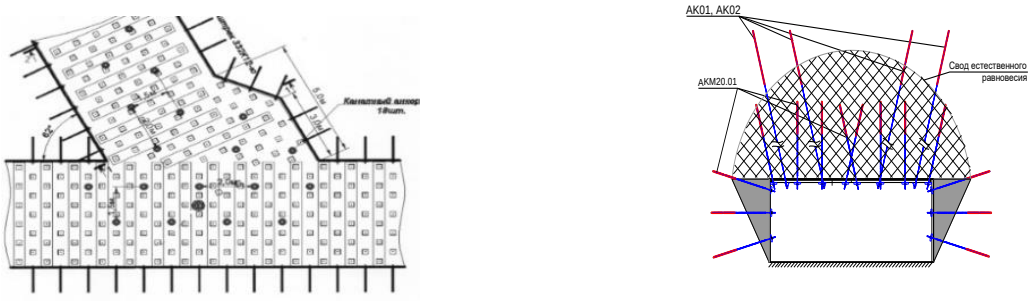

a) b)

a – plan; b – section

Fig. 5. - Pilot industrial testing of combined anchors when supporting the junction of conveyor drift 332к$_{12}$-yu with ventilation slope k$_{10}$ of the Abaiskaya mine of CD ArcelorMittal Temirtau JSC

Various types of processes and sequences of mounting combined anchors are presented during pilot testing of combined anchors when supporting the junction of conveyor drift 332к$_{12}$-yu with ventilation slope k$_{10}$ of the Abaiskaya mine of CD of ArcelorMittal Temirtau JSC (Figure 6).

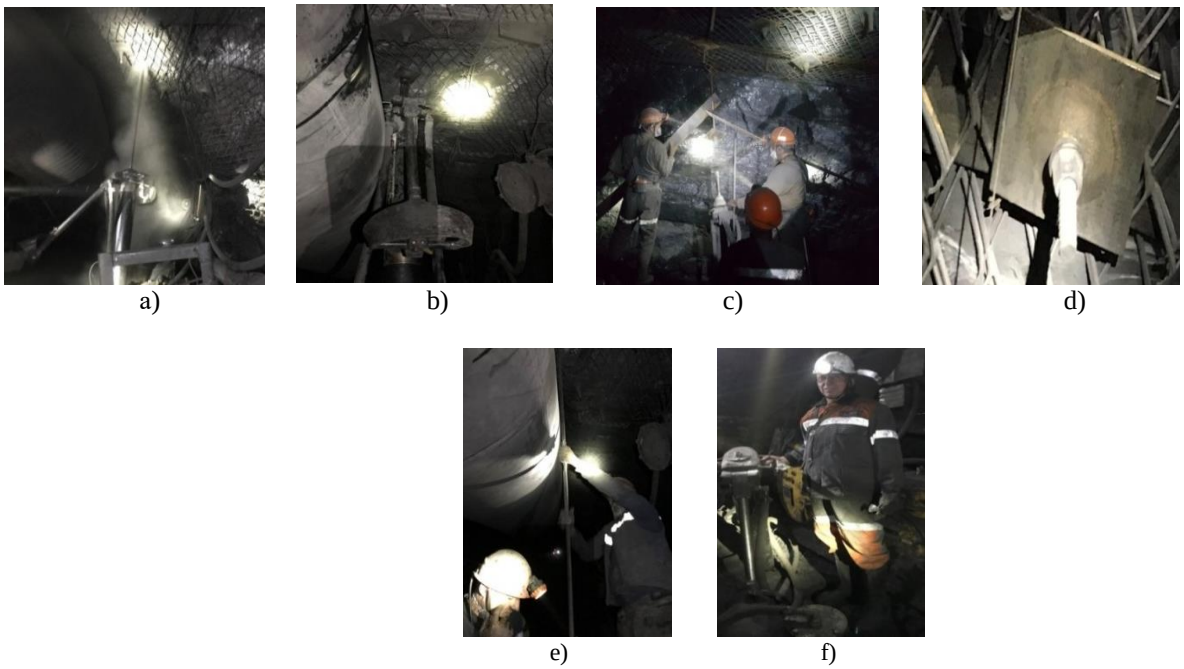

a) b) c) d)

e) f)

a - drilling holes; b - mounting anchors; c – constructing stanchions; d - mounted; anchor rod extension;
e, f - testing in the mine

Fig. 6. - The installation sequences of combined anchors are presented during pilot testing of combined anchors when supporting the junction of conveyor drift 332к$_{12}$-yu with ventilation slope k$_{10}$ of the Abaiskaya mine of CD of ArcelorMittal Temirtau JSC

Carrying out an industrial experiment at the Abaiskaya mine of the CD ArcelorMittal Temirtau JSC consisted of the following. When driving mine workings and developing the coal seams, due to the imbalance of rocks and redistribution of natural stresses in mines, geomechanical processes arise in the form of deformations, destruction, displacements of massive structures of the rock massif, while the process of rock pressure, as a result of the interaction of coal-containing rocks with mine workings is affected by geological, mining and technological factors.

An experiment was carried out for mounting combined anchors designed by KSTU when supporting the junction of conveyor drift 332к$_{12}$-yu with ventilation slope k$_{10}$ of the Abaiskaya mine of CD of ArcelorMittal Temirtau JSC fixed with 15 anchors, including 15 roofing AMB ones through 0.8 m and 4 side ones (2 metal and 2 fiberglass) after 1.0 m. The height of the junction is 3 m and the width is 6 m. An arched profile is erected along the junction fixed to the roof with anchors every 5 m at the points of their connection. As they move workings, under it there were mounted composite arched friction racks. The development was carried out at the depth of 580 m from the surface along the k$_{12}$-$_{10}$ seams. The rocks of the immediate roof are gray siltstone with the thickness of 4 m and strength of Q_{cm}=250 - 300 kg/cm^2. The rocks of the main roof are medium-grained gray sandstones with the thickness of 10 m and strength of Q_{cm}=350 - 400 kg/cm^2.

The combined anchors were made with the length of 4.8 m and the diameter of 22 mm. The upper and lower parts of the anchor are 2.4 m long. The connection was made by a compound coupling 0.2 m long, with the outer and inner diameter of 25 and 17 mm, respectively, made of high-strength steel.

The combined anchors were mounted when supporting the junction of conveyor drift 332к$_{12}$-yu with ventilation slope k$_{10}$ of the Abaiskaya mine of CD of ArcelorMittal Temirtau JSC. Holes 4.7 m long for combined anchors were drilled by the SBR drilling rig using drill rods 1.2 and 3 m long, with a drill bit 28 mm in diameter. In the first borehole there was placed fast-hardening DAK-1 ampoule (0.3 m long, hardening time 25-30 sec.) and two delayed DAK-1 ampoules (0.6 m long, hardening time 180 sec.) and 4.8 m combined anchors. There was performed partial filling of the hole (a cavity 0.4 m long remained unfilled). A 0.2 m long end piece of the short part of the anchor was left to test the bearing capacity of the anchor after it was mounted (for hanging the hydraulic jack). When testing the bearing capacity with an RH302 type anchor puller of the combined anchor, the load of 22 tons was applied that is sufficient for mounting a two-level support. There were no anchor movements.

Three delayed DAK-1 ampoules 0.6 m long were mounted in the second borehole. Complete filling of the borehole was performed (only a cavity 0.05 m long remained unfilled). There were no anchor movements.

The anchors were mounted with the frequency (density) every 1.5 m, providing the filing of the mesh tightening to the roof contour. A working drill rod was used to drill to a predetermined depth. After drilling the hole, chemical ampoules were introduced into the hole with the help of a ramming device. A stop parachute was placed behind the last ampoule. The anchor rod was inserted into the hole, an adapter mounted on the bolter was put on the rod nut, and by turning on the feed and rotation of the spindle, the anchor moved into the hole. The feeding time of the rotating anchor rod was 20–30 s, after which the anchor rod was held under thrust without rotation for at least 1 minute; turning on the rotation of the spindle again, the anchor nut was tightened. At this, the nut pin would definitely break off, the support cup was tightly pressed against the roof of the working. With the hole length equal to 4.7 m, the anchor end (4.8 m long) extends beyond the hole by no more than 0.15 m.

When testing a prototype of the anchor with the diameter at the place of winding the coupling 17.5 mm, thread M1.5 mm, wall thickness of the coupling 3.7 mm, at the laboratory of the Ugleservice PA Energougol office, CD ArcelorMittal Temirtau JSC, the breaking force amounted to 15.1–15.5 tons, and the break also occurred along the coupling.

Thus, when fixing a combined anchor in a borehole on the ampoules with a fixing composition, the breaking force increases by 1.5 times.

2. Results and discussion

Manufacturing (Figure 7) and bench testing of the combined rope-cable anchors were carried out at the Karaganda Machine-Building Consortium LLP and at the production site of the KLMZ LLP (the Karaganda Foundry and Mechanical Plant of the Kazakhmys Corporation LLP).

The technical solution consists in the development of a combined deep anchor with the possibility of its use in thin seams that meets the requirements of reliability, cost-effectiveness, mounting time and ease of execution.

The technical result consists in improving the connection of the combined anchor, improving the design that is achieved due to the reliable pressure connection between the rope and the metal anchor that is resistant to bending and breaking force.

Figure 8 shows the connection of the rope and the metal anchor, and Figure 9 shows the press for pressure connection of the combined anchor.

The advantage of this connection is high breaking shear strength. Such an anchor can be used when supporting workings, when the required length of the anchor exceeds the height of the working. Figure 8 shows the connection of the rope and the metal anchor. There are connected a metal anchor consisting of a reinforcing bar of the screw profile with the diameter of 25 mm (1), a rope consisting of 6 braided wires with the diameter of 6 mm, and a rod with the diameter of 6 mm placed in the middle with the total rope diameter of 18.3 mm (2). A hole is drilled in the metal anchor from the end, with the diameter equal to the diameter of the rope (3) and the length of 300 mm (5). The rope is inserted into the hole and the connection is compressed by a press in the round clip.

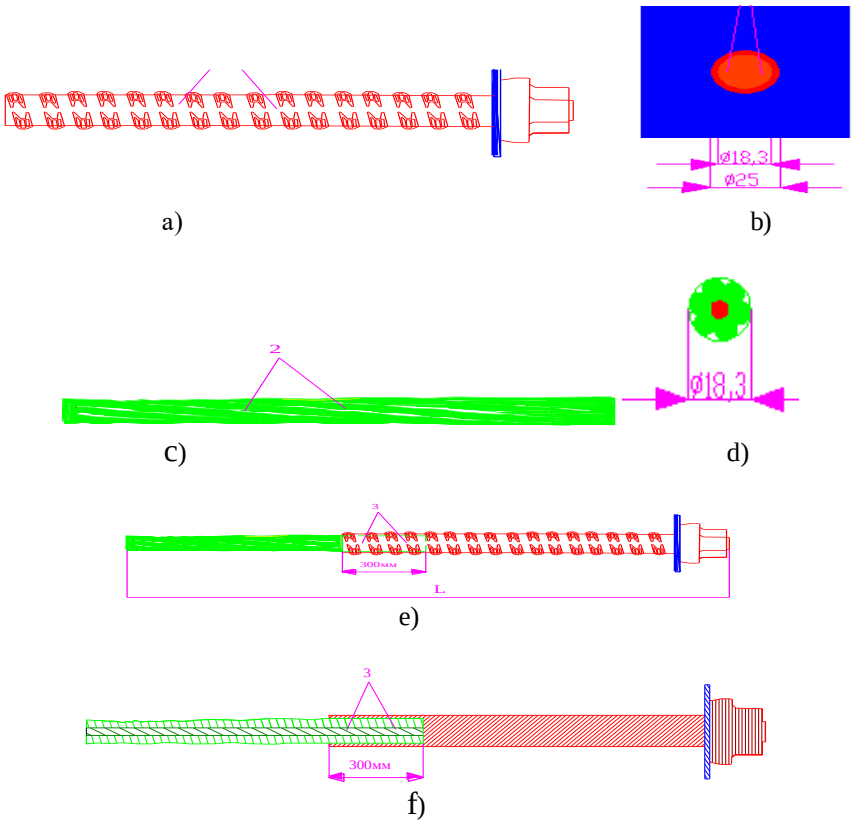

a - metal rod with the diameter of 25 mm; b - end view of the support tile; c - cable with the diameter of 18.3 mm (2 strands with the diameter of 6 mm); d – end view; e - connection of the cable and the anchor rod (3) over the length of 0.3 m; f - assembled anchor

Fig. 7. - Combined anchor assembly technology, sheet 1

g - test bench; b, c - prototypes before and after load tests

Fig. 8. - Combined anchor assembly technology, sheet 2

Bench tests of the strength and load properties of cable and cable anchors at the test site of the KLMZ plant.

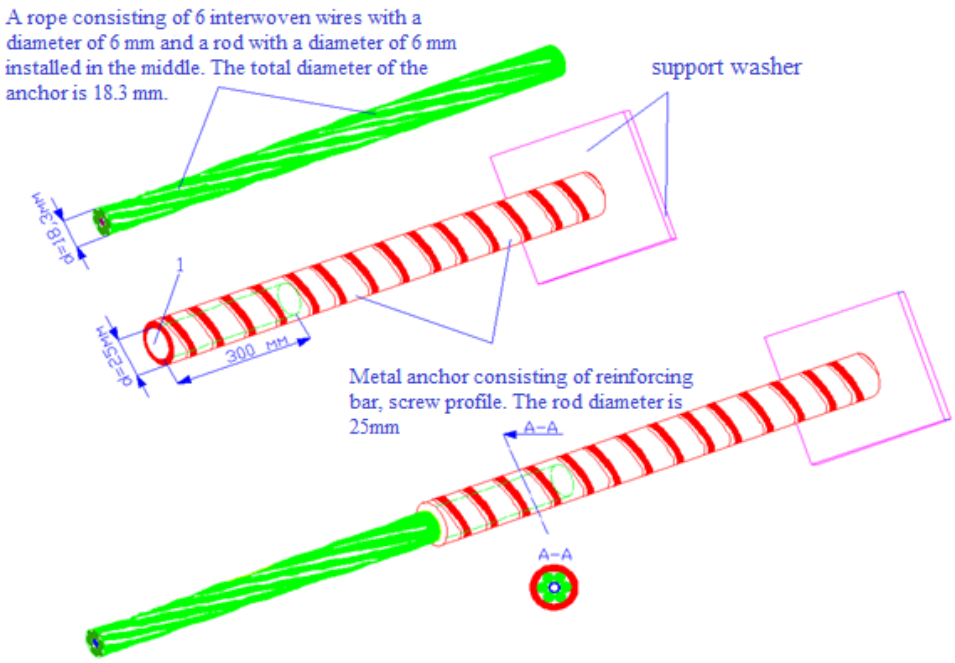

Fig. 9 – Connection of the rope and the metal anchor

The press consists of set itself 1, hydraulic tank with hydraulic oil 2, cams 3. The principle of connecting the combined anchor with a press is as follows: the combined anchor is inserted into the press so that the junction of the rope with the metal anchor is between cams 3. The pressure developed by the pump inside the press acts on piston 5 that compresses cams 3, which in turn press the connection of the combined anchor (Figure 10).

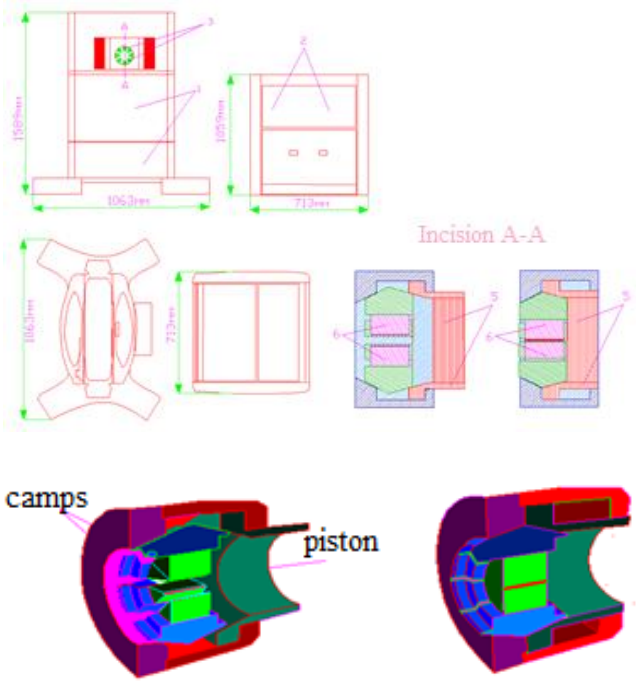

Fig. 10. – Pressing the combined anchor with a press

The connection of the cable and the metal rod is achieved as follows. The metal anchor consists of the reinforcing bar with the screw profile with the diameter of 25 mm, and the rope is made of 6 braided wires with the diameter of 6 mm and a rod with the diameter of 6 mm installed in the middle. The total rope diameter is 18.3 mm. A hole is made in the metal anchor from the end, with the diameter equal to the diameter of the rope and the length of 300 mm, into which the rope is inserted and the connection is compressed with a press.

A collet connection was also made between the steel and cable links of the combined deep cable anchor.

The technical proposal for the use of collet links consists in pulling with the tension force of 20-30 tons when supporting with contour rope anchors located opposite that are mounted in the chemical fixing composition in drilled wells at the corners of the cross section of the ongoing development working with fixing the ropes across the roof of the working. This will ensure its economic and effective anchoring. The rope anchors will be tensioned using a jack with a coupling, the fixing element in which will be collet links.

Reinforcement clamping collets are used for tight fastening of cold-drawn rebar that is used to connect the steel and cable links of the combined deep cable anchor. The clamping collet is a conical sleeve made of metal for fittings diameters from 5 to 28 mm. The elasticity of the jaws of the clamping collet provides rigid clamping of the wire with the force that would be sufficient to move it in the axial direction when the mechanism is opened. The clamping collet is designed to hold the reinforcing bar during its pre-tensioning, to provide high-quality grip and to hold the reinforcement at the moment of its tension.

The collet grip consists of a body (Figure 10, a) and a collet (petals) (Figure 10, b). There is a special thread inside the clamping collet that prevents the reinforcement from slipping along the collet; with a large tension force, the thread cuts into the reinforcing bar (Figure 10, c).

a) b) c)

Fig.11. – Collet grip for a combined anchor

The collet grip was used for tensioning reinforcement of various strength classes and steel rope. There was developed a design with filling the connection with babbit (Figures 12 and 13).

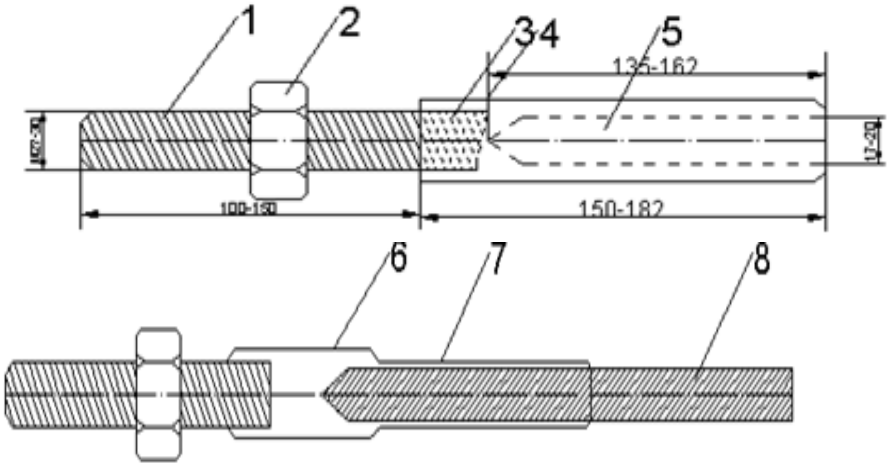

1 - wellhead link of the composite tool; 2 - support nut; 3 – crimping part of the coupling; 4 - notch on the screw profile; 5 - thinned part of the composite tool hole; 6 – coupling; 7, 8 - 2nd (hole) link of the compound tool

Fig.12. - Combined deep anchor, sheet 1

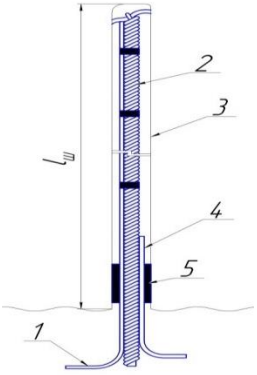

Hole with the rope anchor prepared for pumping cement mix: 1 – air pipe; 2 – steel rope; 3 – hole; 4 – cement pipe; 5 - plug

a)

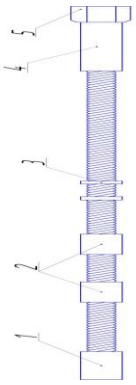

Rope anchor completion prepared for fixing in the hole with a polymer resin: 1 – Swedish filling; 2 – Swedish fittings, 3 – short fittings; 4 – sleeve; 5 – mounting head

b)

c)

d)

e)

a - design; b - appearance; c, d nb - workshop of the KLMZ LLP; f - finished design

Fig. 13. - Combined deep anchor, sheet 2

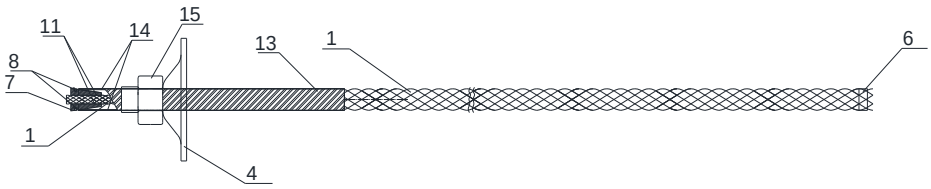

1 - rope-cable part; 2 - coupling; 3 - nut; 4 - base plate; 5 - metal tube; 6 - ring device; 7 - three-link collet; 8 - conical surfaces of the collet; 9 - rubber rim; 10 - groove for rubber rim; 11 - inner surface; 12 - three petals; 13 - hollow tube made of fittings; 14 - inner surfaces of the tube; 15 - spherical nut

Fig. 14. - Combined deep anchor: reinforcement connected to the cable

Conclusions

There are presented scientifically substantiated technological and technical developments on setting the parameters and implementing the technology of supporting with combined deep anchors for development workings at junctions, supporting wide chambers (mounting and salvage ones), working crossings, widening the cross-sectional area for the location of technological equipment (movable distribution point of longwall, pumping stations, compressor facilities), which are essential for improving the efficiency of mining and preparation and stoping operations in the coal industry.

The idea of the work consists in using scientifically substantiated parameters of the means and technology for supporting development workings with rope-cable and combined anchors to ensure stability of the environment of the system: a deep anchor, a single-level steel-polymer support that interacts with the layered thickness of enclosing rocks.

Manufacturing and bench testing a batch of pilot industrial samples of multi-purpose laying systems for supporting mine workings were performed. The development of design documentation adjusted according to the results of bench and mine tests for manufacturing an experimental batch of samples of a combined (built-up, joined) metal steel-polymer anchor using the capabilities of the design service of the Karaganda Machine-Building Consortium LLP was developed. The production of combined anchors was carried out in the machine shop of the Abayskaya mine of the CD ArcelorMittal Temirtau JSC.

References

[1] Zubov V.P. Status and directions of improving the systems of development of coal seams in promising coal mines of Kuzbass. Notes of the Mining Institute. V. 225., 2017, P. 292 - 297.
[2] Zubov V.P. Resource-saving technologies for underground mining of reservoir deposits // Mining Journal. no. [3] P. 95 - 97.
[3] Zubov V.P., Nikiforov A.V. Features of Development of Superimposed Coal Seams in Zones of Disjunctive Geological Disturbances //International Journal of Applied Engineering Research, 2017. V. 12. No. 5, P. 765.
[4] Zubov V.P., Nikiforov A.V., Kovalsky E.R. Influence of geological faults on planning mining operations in contiguous seams. Copyright@ EM International ISSN 0971–765X. Eco. Env. & Cons. 23 (2), P. 1176 – 1180.
[5] Zubov V.P., Smychnik A.D. Exploration method of potash and magnesium salts of the complex structure at great depths. Copyright@ EM International. Eco. Env. & Cons. 23 (3), 2017. - P. 1697 - 1701.
[6] Zubov V.P., Smychnik A.D. Reducing the risks of flooding potash mines during breakthroughs in underground waters. Zapiski Gornogo instituta. V. 215., 2015. - P. 29 - 37.
[7] Artemyev V.B., Korshunov G.I., Loginov A.K. Mining geomechanics. St. Petersburg: Nauka, 2011. - 102 p.
[8] Osipov A.N., Bulkin A.V., Guselnikov L.M. et al. Way to deal with heaving of the soil of mine workings. Patent of the Russian Federation No. 2438018. Publ. 12/27/2011.
[9] Zatsepin A.S., Pleskunov I.V. Method of protection of precinct development workings. Patent of the Russian Federation No. 2338066. Publ. 12/27/2011.
[10] Rozenbaum M. A., Demekhin D.N. Deformational criteria for the stability of roof rocks and rock bolts. Journal of mining science. roof bolting use in Polish coal mines. Journal of mining science. View Journal Information. V. 47. Iss. 6, 2014.
[12] Borsch-Komponiets V.I. Practical mechanics of rocks. Handbook for mining engineers. - M.: Gornaya kniga, 2013. - 322 p.
[13] Pivnyak G. Bondarenko V. Kovalevska I. Mining of Mineral Deposits - London: A Balkema Book. CRC Press is an imprint of the Taylor & Francis Group an inform business. - P. 371.

Information of the authors

Demin Vladimir Fedorovich, doctor of technical sciences, professor of the department «Development of mineral deposits» of Abylkas Saginov Karaganda Technical University, Karaganda, Kazakhstan
E-mail: vladfdemin@mail.ru

Kamarov Rymgali Kumashevich, doctor of technical sciences, professor of the department «Development of mineral deposits» of Abylkas Saginov Karaganda Technical University, Karaganda, Kazakhstan
e-mail: ipk@kstu.kz

DOI 10.52209/2706-977X_2022_3_35 **IRSTI 55.53.29** **UDC 624.132.3**

Features of the Issues of Modeling the Working Process of a Hydraulic Excavator with a Front Shovel

Shestakov V., Bezkorovainy P.*
Ural State Mining University, Russia, Yekaterinburg
*corresponding author

Abstract. At present, there are urgent tasks of improving the quality, reliability, efficiency of machinery, equipment and other machine-building products, reducing their material consumption and energy consumption, and increasing labor productivity. The modern development of the mining industry is characterized by predominant increasing the share of open-pit mining. The volume of excavated rock mass reaches 5 billion m per year. Intensifying the open method of mining mineral deposits determines the need to improve the existing and to develop new specimens of mining equipment. The world practice of developing mining equipment for open-pit mining has proved feasibility of further increasing the production of quarry hydraulic excavators. Hydraulic excavators, in comparison with rope excavators with an equal bucket capacity, have a 1.8...2.2 times smaller mass, develop 1.3...1.5 times greater digging efforts [1-3]. The working equipment has a great effect on the productivity and cost of the excavator [4-6]. Reducing the weight of the equipment reduces significantly the weight of the excavator, the moment of inertia of its rotary part [5, 7].

Keywords: hydraulic excavator, swing motion, speed, acceleration, effort, working equipment, boom, arm, bucket, hydraulic cylinder, working area, model, algorithm.

Introduction

At present, there are urgent tasks of improving the quality, reliability, efficiency of machinery, equipment and other machine-building products, reducing their material consumption and energy consumption, and increasing labor productivity.

The modern development of the mining industry is characterized by predominant increasing the share of open-pit mining. The volume of excavated rock mass reaches 5 billion m per year. Intensifying the open method of mining mineral deposits determines the need to improve the existing and to develop new specimens of mining equipment. The world practice of developing mining equipment for open-pit mining has proved feasibility of further increasing the production of quarry hydraulic excavators.

Hydraulic excavators, in comparison with rope excavators with an equal bucket capacity, have a 1.8...2.2 times smaller mass, develop 1.3...1.5 times greater digging efforts [1-3]. The working equipment has a great effect on the productivity and cost of the excavator [4-6]. Reducing the weight of the equipment reduces significantly the weight of the excavator, the moment of inertia of its rotary part [5, 7].

1 Materials and methods

The working process of a hydraulic excavator includes the operations of scooping, transporting a loaded bucket to the point of unloading, unloading, transferring the empty bucket to the face.

To determine the kinematic and power parameters, a mathematical description of these operations is needed. It will allow, according to the given initial data, determining the possible working area of the excavator, the forces acting on the elements of the working equipment, and solving some special problems, including subsequent strength calculations when substantiating the rational parameters of the excavator.

Digging by turning the bucket has widely been used now. When filling the bucket in this way, there are the least energy costs, but the face after mining will have a rather uneven surface.

After mining a quarry, they often perform reclamation and form zones for further exploitation. During reclamation, the surface must be leveled. When working out the face with hydraulic excavators, the teeth of the excavator bucket must move along a straight path for leveling. Using software control units and the corresponding elements for hydraulic control of the extension speeds of the boom, the arm and the bucket hydraulic cylinder rods, any required trajectory can be obtained in the developed mathematical model [8].

.

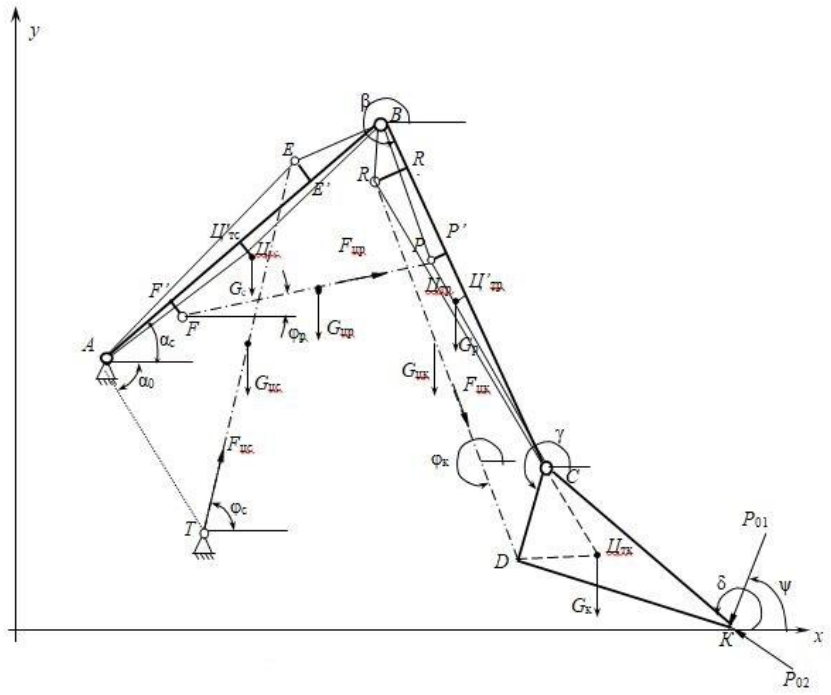

A, T, E, F, P, R, B, C, D - hinges; *K* - the top of the bucket tooth; *KSD* - bucket profile diagram; *CB* - arm; *AB* - boom; *TE*, *FP*, *R*D - hydraulic cylinders for turning the boom, arm and bucket; G_c, $G_р$, $G_к$, $G_{цс}$, $G_{цр}$, $G_{цк}$ - the gravity of the boom, the arm, the bucket, hydraulic cylinders of the boom, the arm, the bucket; $Ц_{тс}$ $Ц_{тр}$ $Ц_{тк}$ – center of gravity of the boom, the arm and the bucket; α_c, β, γ - angles of inclination to the horizontal of the boom, the arm, the bucket

Fig. 1. – Scheme for calculating the parameters of a mathematical model

The initial data for building the model are the dimensions of the working equipment; the distances between the axes of the elements are used for the calculation (Fig. 1).

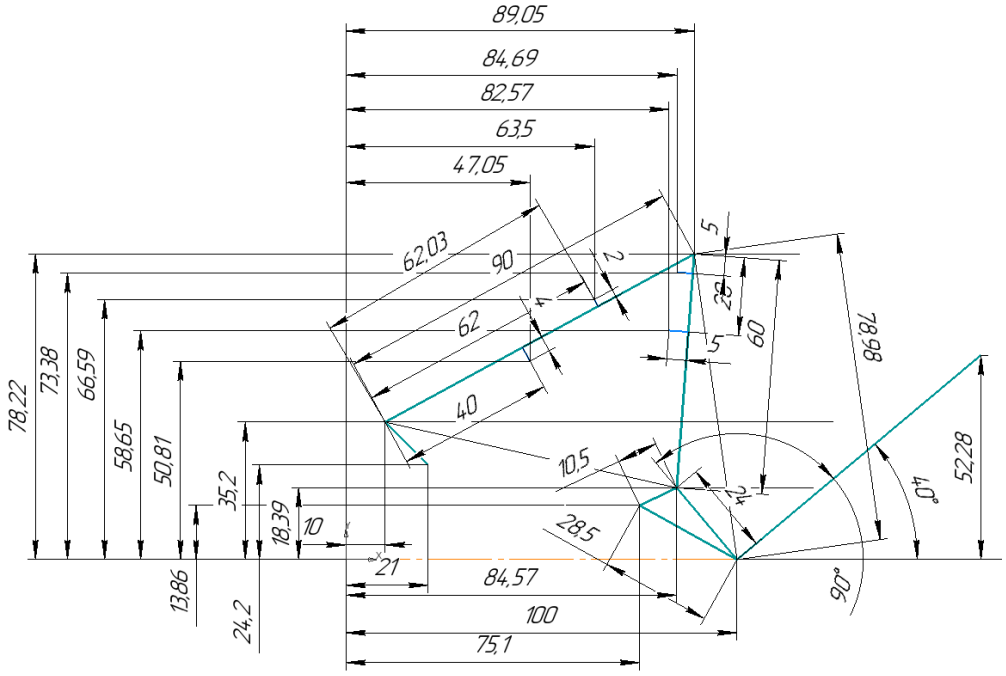

Fig. 2. – A fragment of the working equipment scheme for proving the mathematical model adequacy

Fig. 2 shows the designations of the elements used to compile the expression for calculating the parameters of the working area and the values of the parameters of a hydraulic excavator with a 6 m^3 bucket.

The movement of the bucket within the working area is performed by changing the lengths of the boom, the arm and the bucket cylinders from the minimum value to the maximum one.

The model for calculating the coordinates of points includes a large number of fairly complex expressions. To prove the adequacy of the model, the model scheme was built in the Compass 2D design package on a scale. The proof is the coincidence of the values obtained by the formulas of the model and the values of measurements according to the drawing.

Fig. 2 shows a fragment of the scheme of working equipment to prove the adequacy of the mathematical model. The measurements carried out on the fragment proved the adequacy: the deviations are within the accuracy of the measurements.

The hydraulic excavator process of digging is determined by the operation of the hydraulic cylinders for turning the bucket, arm and boom. The lowest energy consumption is achieved when digging by turning the bucket relative to the "bucket-arm" hinges (point C, Fig. 1), while the hydraulic cylinders for turning the boom and the arm work in the brake mode keeping the boom and the arm from moving. When pressure in the hydraulic cylinders exceeds the setting pressure of the safety valves, the movement of the rods of the corresponding hydraulic cylinders and the rotation of the boom or the arm begin [10].

The greatest digging force that can be realized on the bucket teeth is determined not only by the force of the bucket hydraulic cylinder but by operation of the boom and arm hydraulic cylinders. This feature makes it difficult to determine the digging effort.

2 Results and discussion

To calculate the maximum digging force, there is used an algorithm for finding a possible solution. At the beginning of search, a very large value of the tangential component of the digging resistance force P_{01} is set on the bucket teeth, which is obviously greater than the digging force of the excavator under consideration. According to the given P_{01}, the forces on the rods of the hydraulic cylinders of the boom $F_{\text{цс}}$, the arm $F_{\text{цр}}$ and the bucket $F_{\text{цк}}$ are determined. The forces on the rods are compared with the values of the forces when the safety valves are actuated. Moreover, with positive calculated values, the comparison is performed with the forces determined by pressure in the piston cavity, and with negative ones, in the rod cavity of the hydraulic cylinder. If the safety valve is actuated, P_{01} is reduced and the calculations are repeated until the forces on the rods are lower than the forces when the safety valves are actuated.

The force on the rods of the boom hydraulic cylinders is determined by the equilibrium condition relative to the hinge A:

$$\sum M_A = 0$$

$$G_{\text{с}}\left(x_{\text{цтс}} - x_A\right) + G_{\text{р}}\left(x_{\text{цтр}} - x_A\right) + G_{\text{к}}\left(x_{\text{цтк}} - x_A\right) + G_{\text{цс}}\left(\frac{x_{\text{T}} + x_{\text{E}}}{2} - x_A\right) + G_{\text{цр}}\left(\frac{x_{\text{F}} + x_{\text{P}}}{2} - x_A\right) + \\ + G_{\text{цк}}\left(\frac{x_{\text{R}} + x_{\text{D}}}{2} - x_A\right) + P_{\text{y}}\left(x_{\text{к}} - x_A\right) + P_{\text{x}}\left(y_{\text{к}} - y_A\right) - F_{\text{цс}} \cdot L_{AT} \sin(\pi - \alpha_0 - \varphi_c) = 0 \quad (1)$$

where

$P_x = -P_{01}\cos\psi - P_{02}\sin\psi$ is projection on the x-axis of the digging resistance force;

$P_y = -P_{01}\sin\psi + P_{02}\cos\psi$ is projection on the y-axis of the digging resistance force.

$$F_{\text{цс}} = \frac{G_{\text{с}}\left(x_{\text{цтс}} - x_A\right) + G_{\text{р}}\left(x_{\text{цтр}} - x_A\right) + G_{\text{к}}\left(x_{\text{цтк}} - x_A\right) + G_{\text{цс}}\left(\frac{x_{\text{T}} + x_{\text{E}}}{2} - x_A\right) + G_{\text{цр}}\left(\frac{x_{\text{F}} + x_{\text{P}}}{2} - x_A\right) + }{} \\ \frac{+ G_{\text{цк}}\left(\frac{x_{\text{R}} + x_{\text{D}}}{2} - x_A\right) + P_{\text{y}}\left(x_{\text{к}} - x_A\right) + P_{\text{x}}\left(y_{\text{к}} - y_A\right)}{L_{AT}\sin(\pi - \alpha_0 - \varphi_c)} \quad (2)$$

The force on the rods of the hydraulic cylinders of the arm is determined by the condition of equilibrium with respect to the hinge B. In addition to the force in the rod, to the hinge B, there will also be applied half the gravity of the hydraulic cylinder of the arm:

$$G_{\text{р}}\left(x_{\text{цтр}}-x_B\right)+G_{\text{к}}\left(x_{\text{цтк}}-x_B\right)+G_{\text{цк}}\left(\frac{x_{\text{R}}+x_{\text{D}}}{2}-x_B\right)+P_{\text{у}}\left(x_{\text{к}}-x_B\right)+P_{\text{х}}\left(y_{\text{к}}-y_B\right)+$$
$$+0{,}5G_{\text{цр}}\left(x_P-x_B\right)-F_{\text{цр}}\cdot L_{BP}\sin\angle FPB=0 \quad (3)$$

$$F_{\text{цр}}=\frac{G_{\text{р}}\left(x_{\text{цтр}}-x_B\right)+G_{\text{к}}\left(x_{\text{цтк}}-x_B\right)+G_{\text{цк}}\left(\frac{x_{\text{R}}+x_{\text{D}}}{2}-x_B\right)+P_{\text{у}}\left(x_{\text{к}}-x_B\right)+P_{\text{х}}\left(y_{\text{к}}-y_B\right)+0{,}5G_{\text{цр}}\left(x_P-x_B\right)}{L_{BP}\sin\angle FPB} \quad (4)$$

The force on the rods of the bucket hydraulic cylinders is determined by the equilibrium condition relative to the hinge C. In addition to the force in the rod to the hinge C, there will also be applied half the gravity of the bucket hydraulic cylinder:

$$G_{\text{к}}\left(x_{\text{цтк}}-x_B\right)+P_{\text{у}}\left(x_{\text{к}}-x_C\right)+P_{\text{х}}\left(y_{\text{к}}-y_C\right)-0{,}5G_{\text{цк}}\left(x_D-x_C\right)-F_{\text{цк}}\cdot L_{CD}\sin\angle RDC=0 \quad (5)$$

$$F_{\text{цк}}=\frac{G_{\text{к}}\left(x_{\text{цтк}}-x_C\right)+P_{\text{у}}\left(x_{\text{к}}-x_C\right)+P_{\text{х}}\left(y_{\text{к}}-y_C\right)-0{,}5G_{\text{цк}}\left(x_D-x_C\right)}{L_{CD}\sin\angle RDC} \quad (6)$$

The above expressions are used to determine the possible forces on the bucket teeth when digging by turning the bucket, and it is shown that the algorithm for finding a possible value takes into account the restrictions on the maximum forces in the boom and arm hydraulic cylinders. Alongside with such restrictions, when digging, it is necessary to take into account the excavator stability.

When digging, situations are possible in which a part of the caterpillars will separate from the soil of the face: the turn of the caterpillar bogie together with the platform relative to the track rollers closest to the face. This movement limits the force on the bucket teeth when digging: the forces of the hydraulic cylinder rods could provide more force but the displacement of the working equipment when the platform rotates does not allow this.

The overturning moment when digging relative to the track rollers of the undercarriage is caused by the gravity forces from the working equipment and the digging forces, and the holding moment is the result of the gravity forces of the turntable (without working equipment) and the undercarriage.

After determining the force on the bucket teeth according to the conditions, so that the forces on the rods of the hydraulic cylinders do not exceed the allowable values (forces when the safety valves are actuated), the condition $M_{\text{уд}}\geq M_{\text{опр}}$ is additionally checked. If the condition is not met, then the force on the bucket teeth is reduced until the condition is met.

The algorithm for calculating the boundaries of the working area and forces at points inside the area includes three cycles and is organized as follows:

- in the external first cycle, the distance between the points *TE* changes (Fig. 1) by extending the rods of the boom rotation hydraulic cylinders from the minimum (the rods of the boom hydraulic cylinders are fully retracted) to the maximum values (the rods of the boom hydraulic cylinders are fully extended);
- in the second cycle, for each value of the distances *TE*, the value of the segment *FP* changes from the minimum possible value (the rods of the arm hydraulic cylinders are fully retracted) to the maximum possible value (the rods of the arm hydraulic cylinders are fully extended);
- in the third cycle, for each value of the distances *TE* and *FP*, the value of the segment *RD* changes from the minimum possible value (the bucket hydraulic cylinder rods are fully retracted) to the maximum possible value (the bucket hydraulic cylinder rods are fully extended).

The algorithm includes the fourth cycle of searching for an acceptable solution when calculating the possible digging force inside the working area. Before the cycle, the tangential component of the digging resistance force P_{01} is set, which is obviously greater than the possible digging force of the excavator under consideration. According to P_{01}, the forces on the rods of the hydraulic cylinders of the boom $F_{цс}$, the arm $F_{цр}$ and the bucket $F_{цк}$ are determined. The forces on the rods are compared with the values of the maximum forces of the hydraulic cylinders of the boom, the arm and the bucket when the safety valves are actuated. If the maximum forces of the hydraulic cylinders of any of the calculated values $F_{цс}$, $F_{цр}$ or $F_{цк}$ are exceeded, the force P_{01} decreases, and the calculations are repeated until the specified forces on the rods of all hydraulic cylinders are greater than or equal to the calculated forces [10].

The mathematical model and the algorithm are implemented by a computer program in the algorithmic language *Visual Basic for Application*.

The program implements the output of the results in tabular form and in the form of a figure, which shows the scheme of the excavator and the working area with possible digging forces on a scale (Fig. 3, 4).

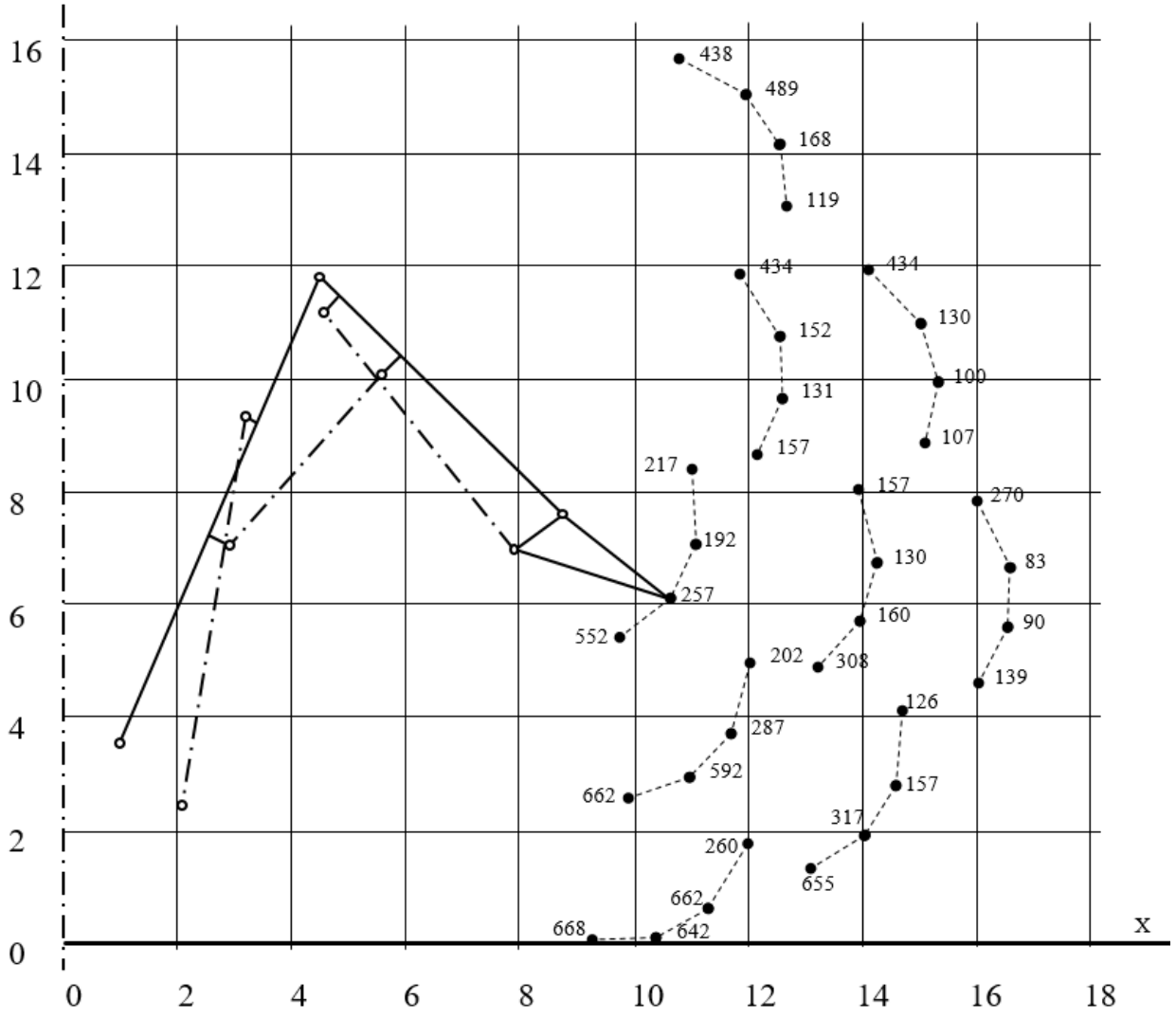

Fig. 3 – The results of calculating forces on the bucket teeth within the working area

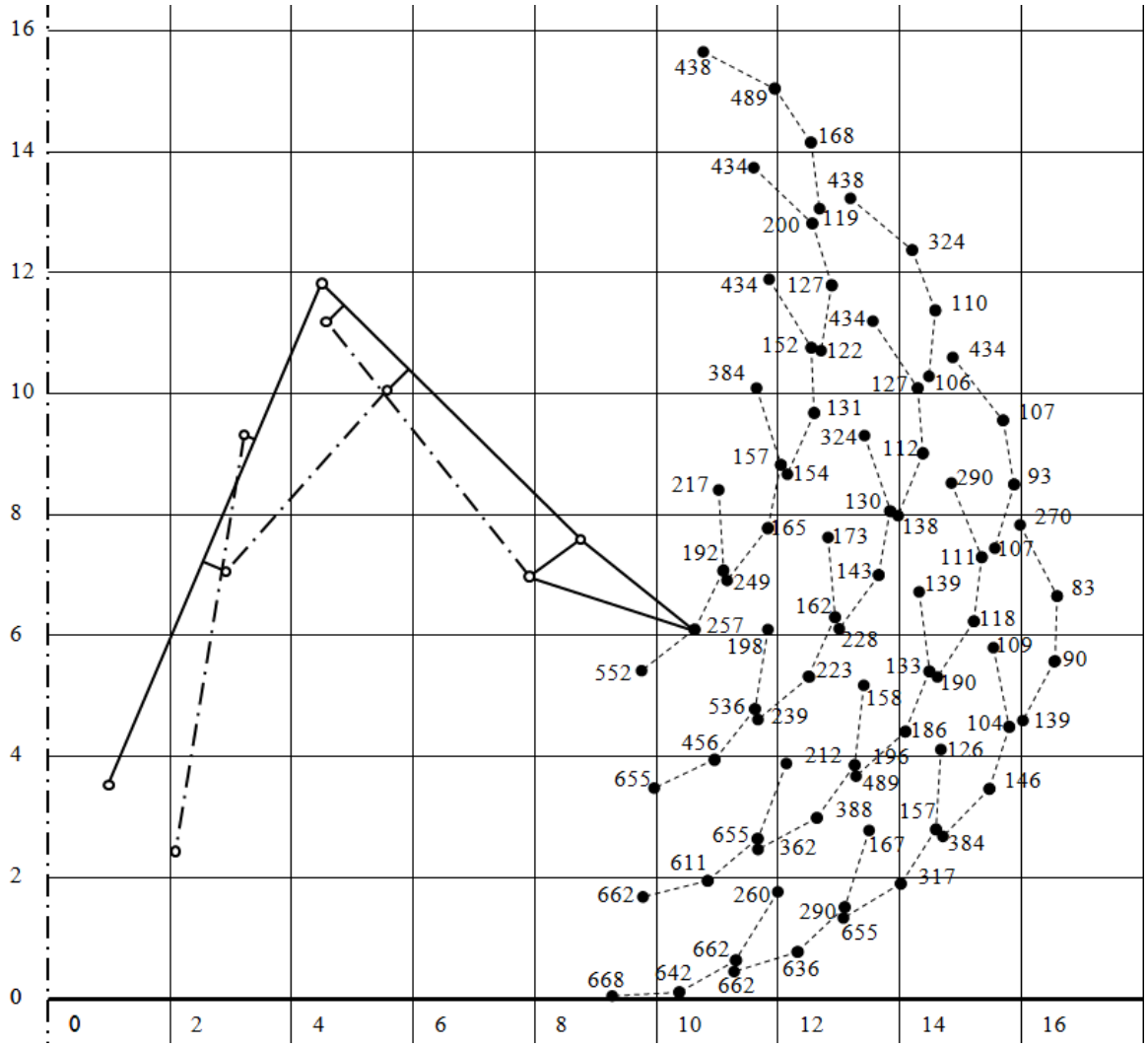

Fig. 4 – The results of calculating forces on the bucket teeth within the working area

Conclusions

The considered feature of the mechanisms interaction when digging leads to difficulties in the calculations: it is impossible to set the maximum efforts to all the hydraulic cylinders and to determine the acting forces in the all elements of the working equipment. The forces were calculated according to the above algorithm for finding feasible solutions.

The developed mathematical model and computer program make it possible to determine the working area of the excavator, and the boundary of the area is specified according to the conditions for ensuring digging at the calculated values of force.

The developed mathematical model, the algorithm and the program make it possible to analyze the design parameters of the excavator. So, the diagrams show that at 4 points the limiting digging force is the maximum force of the bucket hydraulic cylinder $F_{\text{цр.max}}$, at 3 points it is the maximum force of the handle hydraulic cylinder $F_{\text{цс.max}}$, at the remaining points it is the maximum force of the boom hydraulic cylinder $F_{\text{цс.max}}$. If the values of the calculated forces are insufficient to fill the bucket, then it is necessary to increase pressure of the limiting hydraulic cylinder. In the considered option, if it is necessary to increase the digging force, it is needed to increase pressure in the boom hydraulic cylinder, since the force depends to a greater extent on it.

References

[1] Pobegailo P.A. Heavy Duty Single Bucket Hydraulic Excavators: Selecting basic geometries for work equipment in the early stages of design. - M.: LENAND, 2013. - 296 p.

[2] Lagunova Yu. A., Komissarov A.P., Shestakov V.S. (2017). Designing of mining excavators. - M.: Innovative mechanical engineering. - 228 p.

[3] Poderny R.Yu., Peter B. Efficiency of the use of powerful hydraulic excavators as the result of increasing their reliability //*Mining industry*, No. 1 (119), 2015, P. 46.
[4] Ivanov I.Yu., Komissarov A.P., Teliman I.V., Lukashuk O.A. Analysis of lever-hydraulic mechanisms of working equipment of hydraulic excavators. Technological equipment for mining and oil and gas industry //Proceedings of the XV International Scientific and Technical Conference, 2017, P. 51-54.
[5] Zykov P.A. The method of optimal choice of the model of a single-bucket hydraulic excavator for the given mining-geological and technical conditions //*Mining equipment and electromechanics*. No. 1., 2014, P. 37-42.
[6] Babenkov P.Yu., Shestakov V.S. (2018). Modeling the working process of a hydraulic excavator //Mining equipment and electromechanics, No. 1., P. 10-14.
[7] Lukashuk O.A., Komissarov A.P., Lagunova Yu.A. Development of a digital control system for the main drives of a mining excavator as the most important direction for increasing the efficiency of the excavator //IOP Conference Series: Materials Science and Engineering, 709 (2), 2020,. https: // www.scopus.com DOI: 10.1088 / 1757-899X / 709/2/022117
[8] Komissarov A.P., Shestakov V.S. Simulation model of the functioning of the working equipment of a hydraulic excavator //Mining equipment and electromechanics, No. 8, 2013, P. 20-24.
[9] Pobegailo P.A. Mathematical model for determining the loading of a single-bucket hydraulic excavator of reverse digging // Interstroymekh - 2002. P. 179-181
[10] Victor Shestakov, Pavel Bezkorovainyy and Tatyana Franz. Determination of the working area of a hydraulic excavator // E3S Web of Conferences, Volume 177, April 2-11, 2020, P. 100-104.

Information of the authors

Shestakov Viktor Stepanovich, candidate of technical sciences, professor of the department “Mining Machines and Complexes” of Ural State Mining University
E-mail: shestakov.v.s@mail.ru

Bezkorovainy Pavel Genadievich, PhD student of the department “Mining Machines and Complexes” of Ural State Mining University
E-mail: bpg82_karlion@mail.ru

DOI 10.52209/2706-977X_2022_3_42 **IRSTI 55.03.12** **UDC 621.9.048**

Studying the Processes that Take Place in Vibroabrasive Machining of Complex-Shaped Parts

Zhanibekov T.[1], Nikonova T.[1*], Imasheva K.I.[1], Zhukova A.V.[1], Kozhanov M.G.[1], Rakhutin M.G.[2]
[1]Abylkas Saginov Karaganda Technical University, Kazakhstan, Karaganda
[2]Moscow Institute of Steel and Alloys, Moscow, Russia
*corresponding author

Abstract. There are presented the main technological possibilities of vibroabrasive machining. The classification of the main processes occurring during vibration processing is given. The scheme of the elements of the abrasive tool and its characteristics that affect the operational properties of the workpieces are considered.

Keywords: *burrs, cleaning, finishing, vibroabrasive machining, abrasive granules.*

Introduction

One of the areas of using vibration machining methods in mechanical engineering is vibroabrasive machining. In mechanical engineering vibroabrasive machining (VAM) is mainly used in machining complex-shaped large parts.

One of the important features of vibroabrasive machining is that the surfaces of parts in the working environment are cleaned of various contaminants, oxides and acquire increased activity. This property is used for applying thin films of metals and other materials with special properties (anticorrosion, antifriction, etc.) to the surface of products.

The scope of vibroabrasive machining is very wide, for example, cleaning the surface of complex-shaped parts from scale, molding sand residues, traces of corrosion, removing burrs and rounding sharp edges on profiled and small parts, polishing and grinding the surface of complex-shaped parts. In addition, vibroabrasive machining makes it possible to harden the surface of parts increasing their microhardness; to apply coatings with running-in materials, such as molybdenum disulfide; to clean parts from grease, etc.

The technological scheme of VAM is shown in Figure 1. The parts to be processed are placed in a working chamber that is filled with a working medium of the required characteristics. The working chamber, mounted on elastic elements, has the ability to oscillate in different directions. Oscillations are communicated from the vibrator in the form of a rotating shaft with unbalanced weights with the amplitude of 1–8 mm and frequency of 20–45 Hz. In the process of oscillation, the part and the working medium are constantly subjected to accelerations of variable sign, come into intense relative movement, oscillating and circulating. From the side walls of the working chamber, vibrations are transmitted to the adjacent layers of the working medium, which transmit it to the next layers, etc.

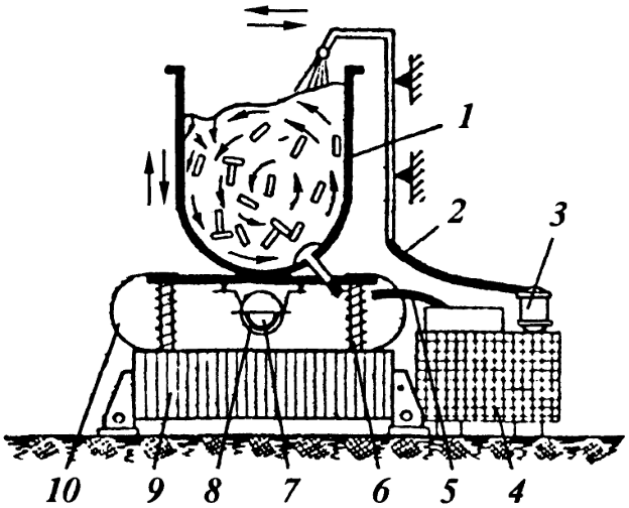

Fig. 1. – Scheme of vibroabrasive machining

In the course of analyzing the existing scientific papers and articles on the topic under consideration, one should notice a low number of works, or consideration of the topic in a general topic. In this paper, the authors consider studying the processes occurring in the vibroabrasive machining complex-shaped parts.

After analyzing the early existing scientific papers and articles on the topic under consideration, it was revealed that the productivity of machining depends on the duration and the mode of machining, the grain size of the abrasive medium, abrasive granules, the properties of the coolant and its volume.

Vibration machining of parts depends largely on the characteristics of abrasive granules. The steady growth and expansion of the possibilities of this machining method urgently requires expanding the range of abrasive granules, improving their technological characteristics, and studying the effect of the latter on the parameters of the vibration machining process.

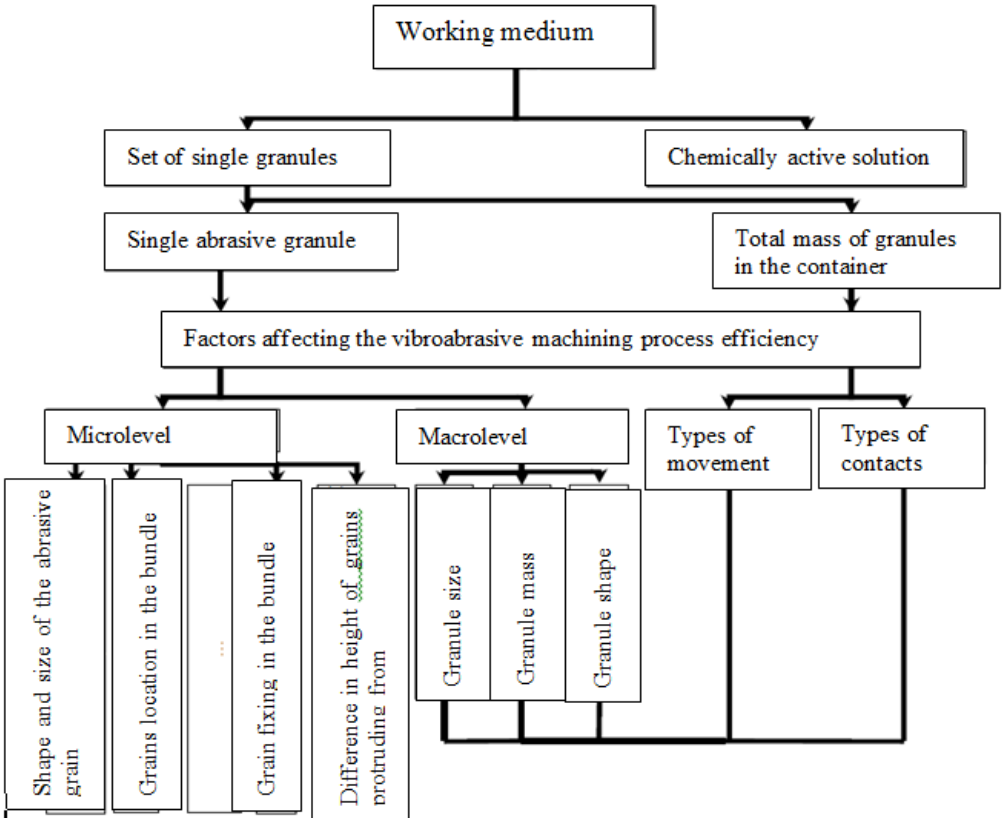

Fig. 2. - Structural diagram of the abrasive tool elements and its characteristics that affect the performance properties of the parts

The evidence of the shape, grain size, structure uniformity, cutting properties of abrasive granules effect on the efficiency, there was the analysis carried out.

For this study, the analysis was carried out that revealed that there is a sense in changing the shape of abrasive granules, as well as its effect on processing parameters.

The research method was revealed by the fact that the variable characteristic would be the shape of the granules, while all the other parameters would remain the same, namely:

1. In the theoretical study, granules are made on a polymer bond of polymethyl methacrylate powder (PMA) and monomer (MMA). This choice is explained by the fact that polymer-bonded granules have high wear resistance, cutting qualities, and an abrasive granule of any shape can be made using a polymer [2].

2. The abrasive concentration is 50-60 %, because previous studies have shown that this range of grain concentration is optimal.

These abrasive granules have the following composition of the components [3]:

- abrasive: up to 53 %; the recommended value (grain size can vary from 6 to 100 microns);
- polymer: beaded polymethyl methacrylate PMA; 23 %
- monomer: liquid methyl methacrylate MMA; 23 %;
- hardener: dimethylaniline; up to 1 %.

There were abrasive granules in the form of cones, pyramids having a square at the base (P4), pyramids having a non-convex hexagon at the base (P6), and two-sided pyramids, in the cross section of which there lied a non-convex hexagon (P12) (Table 1).

Table 1. The results of experimental studies of the machines samples roughness

Sample type, dimensions and material	Surface roughness Ra, μm		Technological operation time, min.			
	Before machining	After machining	Granule type			
			Cone	Pyramid (P4)	Pyramid (P6)	Pyramid (P12)
Solid cylinders Ø 25×10 mm, brass LS 59-1L	3.4…3.5	1.15…1.3	60	55	50	35
Parallelepipeds 20×10×10 mm, brass LS59-1L	3.5…4.1	1.18…1.3	60	50	45	35

As a result, it can be concluded that under the same modes of machining the part, the best result is in a short time obtained by abrasive granules in the form of a two-sided pyramid, in the cross section of which there is a non-convex hexagon.

Mathematical modeling of the process of vibration machining is a rather difficult task. First of all, this is conditioned by the fact that the working medium is a granular medium, the characteristics of which vary significantly depending not only on the properties of its elements but also on the operating modes and design parameters of the vibration machine. At the same time, there change such properties as the ability of the medium to transmit a force impulse to the machining zone, transportation of the working medium, the appearance of zones with different processing intensity in the container.

As a result, one or another calculation method is justified within the framework of a certain particular case, and in the future it cannot be applied sometimes even with a slight change in the parameters of the technological process. An example would be methods of calculating metal removal or roughness that are tied to empirical parameters.

It is obvious that experimental studies are even more laborious, since they require continuous readjustment of equipment that is quite difficult to implement.

These are, for example studies of a wide range of oscillation frequencies of the vibration exciter, as well as its location relative to the container, studying the effect of the container shape, tracking the movement of a part inside the working environment, studying the trajectory of movement and collision of the walls of the container and elements of the working environment. The latter is one of the most important factors, since it is at this stage that the power pulse is transferred to the machining zone.

To date, computing equipment allows implementing numerically most of these studies, so the main task is to select an approach on which base an adequate mathematical model will be implemented.

In [4, 5] the classification of mathematical models is given depending on various theoretical approaches and hypotheses applied.

Thus, the following groups were identified:

– models based on representing the working medium as an elastic viscous plastic fluid,

– probabilistic-kinematic models,

– models that consider direct contact between the granule and the fragment of the part surface,

– rheological models, in which the working medium is presented as a system of elastic and damping elements.

Each of these methods is relevant within the framework of the task set by the researcher and was reasonably used to solve it.

When studying the process under consideration, it must be taken into account that the main input parameters are the operating modes, as well as the design parameters of the machine and tool. The end result should be a model that will allow studying the dependence of the result of the operation on the listed parameters. In this case, the main difficulty, as already noted, is that the tool has a reverse effect on the vibration machine container movement, and its parameters change depending on the specified parameters.

Vibration machining consists of several interrelated processes and their relationship can be illustrated by the diagram shown in Fig. 1.

The first element of the diagram considers the movement of the device: the vibration machine container depending on the parameters of its design and operation, such as:

- the weight and size of the container,
- the location and stiffness of the suspension,
- the location and parameters of the vibration exciter, the unbalance rotation speed.

Fig. 2 lists the works in which the main attention was paid to this particular issue. Studies that take into account the mutual influence of the movements of the working environment and the container are in the minority, since it is quite difficult not only to evaluate but also to select a method of describing the characteristic behavior of the working

environment as a single mass interacting with the container upon impact (taking into account, as already mentioned, the dependences of these characteristics on the trajectory and frequency of the container movement).

It should be noted that in these studies, one of the most significant parameters will be the shape of the container.

In works that study such issues as the occurrence of passive zones in the container [4, 6], the efficiency of transferring a force pulse from the container walls to the machining zone, or circulation movement, there is, as a rule, used a hypothesis following which, the working environment is simplified in some way. It can be represented in the form of a pseudo-liquid, which has the properties of elasticity and energy dissipation, during the transfer of momentum or in the form of a system of bodies interconnected by rheological bonds.

Such approaches are complicated by the fact that the dependences between the parameters of the rheological elements, the applied model, and the parameters of the operation and design of the vibration machine are established only empirically, in relation to certain conditions and working environments.

In addition, in many works the principle of interaction between the working medium and the walls of the container is simplified.

There are a number of works [5] in which attempts were made to apply probabilistic-kinematic or gas-dynamic approaches. However, such solutions are not sufficiently substantiated theoretically, they contain a large number of assumptions and have all the disadvantages listed above.

On the other hand, they are promising, since they allow going directly to the final parameter: metal removal or hardening.

The third point has been deeply explored, since despite the conflicting conclusions regarding the possibility of considering this process as deterministic or stochastic one, the parameters vary to a much lesser extent that allows concluding that there is currently a reasonable methodology of determining the parameters of interaction between the elements of the working environment and the part.

Thus, in order to select the optimal design parameters of a vibration machine and its operating modes, it is necessary to provide the most accurate assessment of all the factors effect on the machining process.

Modeling the movement of a container is a necessary link between the parameters of operation and design of a vibration machine and the end result: energy, a force pulse transmitted from the walls of the container to the working medium and further into the machining zone, removal or hardening depth depending on the goal.

The description of the container movement, taking into account its loading, is also an urgent task for the reason that only on this basis it is possible to carry out further analysis of the working environment movement.

Taking into account the requirements formulated above and the analysis of the developments available in this area, the following design scheme for the model of the movement of the container of the vibration machine is proposed (Fig. 3).

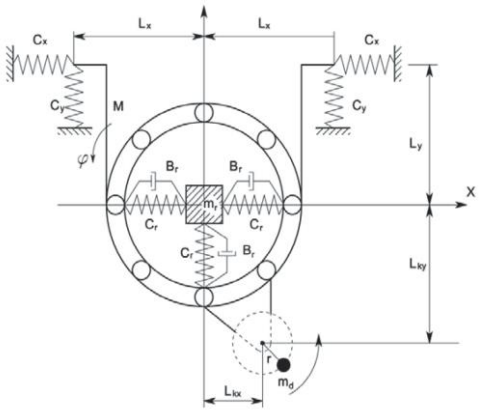

C_x ,Cy is the coefficient of elasticity of suspensions; Lx ,Ly is the distance along the X,Y axis from the center of mass to the fixing points of the left and right suspensions; Cr is the coefficient of elasticity of the working medium; Br is the damping coefficient of the working medium; Lkx ,Lky is the distance along the X,Y axis from the center of mass to the point of application of the perturbing force; M is the mass of the container and the attached part of the load; m_r is the mass of the load, according to the scheme located in the center of the container and moving under the influence of a layer in contact with its walls; m_d is the unbalanced mass of unbalanced weights, r is the eccentricity of the mass of the unbalance relative to its axis of rotation; coordinate axes X, Y are drawn through the center of mass of the container, ϕ is the angle of rotation of the container relative to the center of mass of the system counterclockwise.

Fig. 3. – Design scheme for the mathematical model of the vibration machine operation

1. Materials and methods

The development of new technological processes that improve the quality of parts is one of the most important tasks for increasing the production efficiency. A technological process is a complex dynamic system in which equipment, means of control and management, a machining tool or environment, as well as people carrying out this process, are combined into a single complex. To perform the tasks set in production, the technological process must have be highly reliable. Reliability of the technological process must be ensured in terms of both qualitative and quantitative indicators. Based on the above, there can be formulated the following definition: reliability of a process is its ability to function within the required period of time under given operating conditions providing the required product quality and productivity. Difficulties in ensuring reliability of the technological process are associated with the great complexity of technological systems, the presence of numerous and diverse relationships, etc.

The practice of industrial production shows that probabilistic methods of calculating reliability and the quality of technological processes make it possible to assess both qualitatively and quantitatively the factors that affect the technological system, to develop effective technological and design measures to improve technologies.

Quite a lot of research are dealing with improving reliability of technological equipment [8, 9] and reliability of technological processes of blade machining [10], but there are no works to improve reliability of technological processes of machining in abrasive media, with the exception of the work by Korolkov Yu. “Rotational machining in an abrasive medium” written on the basis of Don State Technical University.

The main property of the object under study is its complexity, which is determined by the number of distinct states in which the object can be. An important characteristic of the object under consideration is its controllability. The task of studying the object is facilitated by its formalization or the successful choice of its model (Fig. 5). Due to the fact that mathematical methods of impact planning are based on the cybernetic approach to the controlled object, the most appropriate model of the latter is the "black box" [11].

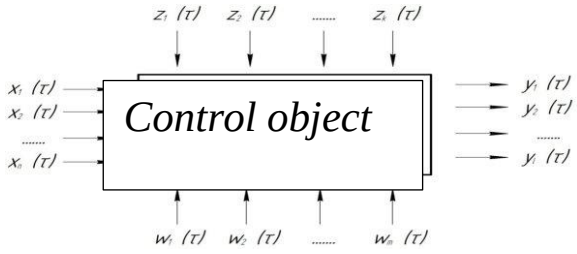

Fig. 4. – The black box model

The $y_1(\tau),\ldots,y_l(\tau)$ are subject to optimization and provision in the process of object control. The arrows included in the object correspond to the possible ways of influence. The group of factors designated $x_1(\tau),\ldots,x_n(\tau)$ correspond to the controlled factors, with purposeful change of which the object is directly studied and the required parameter values are provided. The factors $z_1(\tau),\ldots,z_k(\tau)$ and $w_1(\tau),\ldots,w_m(\tau)$ represent a group of uncontrolled impacts that significantly increase the noise field against which the useful signal stands out. The factors $z_1(\tau),\ldots,z_k(\tau)$ can be controlled in the production process, and the factors $w_1(\tau),\ldots,w_m(\tau)$ are perturbing uncontrolled impacts on the control object.

The meaning of the cybernetic approach lies in the fact that by changing the inputs of the "black box", the outputs are registered, i.e., the optimization parameters, while paying little attention to the mechanism of phenomena occurring with the object. This approach makes it possible to establish a connection between the input and output of the object under consideration and describe such a connection by some mathematical model without considering the nature of the ongoing processes.

Each control system consists of a control object and a control device. The object of control can be an optimized process, a technological system, etc. The control device can be a technical device (for example, an auto-adjuster), and in cases where the object of control is the process itself, a system of technological preparation of production, in which control decisions are developed.

In the general case, the technological process is represented as a multidimensional object with specific features (Fig. 2), at the input of which the vector of input variables $x(\tau)$ acts:

$$x(\tau)=[\, x_1(\tau),\ldots, x_l(\tau)]. \qquad (1)$$

The components of the vector characterize the complete set of workpiece properties (dimensions and their deviations, structural parameters, etc.) used in the object. The output variables are described by the vector $y(\tau)$:

$$y(\tau)=[\, y_1(\tau),\ldots,y_l(\tau)]. \quad (2)$$

The components of this vector characterize, for example, the properties of the finished part (dimensional accuracy, surface roughness, etc.). The components of both the input and output vectors can be not only the structural and technological properties of the workpieces, but also values that reflect the technical and economic indicators of the process.

The parameters characterizing the conditions for implementing the technology are described in the general case by the vector $z_1(\tau),\ldots,z_k(\tau)$:

$$z(\tau)=[\, z_1(\tau),\ldots,z_k(\tau)] \quad (3)$$

The components of this vector are the amplitude and frequency of oscillations, coolant, as well as the factors that have a destabilizing effect on the course of the technological process.

The dimension of the s $x(\tau)$, $y(\tau)$, $z(\tau)$ vector for real processes is quite large, and it is impossible to take into account all their components. The components of these vectors are often considered as random functions.

The $x(\tau)$ vector includes measured and non-measured input variables. Some variables can be controllable. It is impossible to take into account all the input variables that affect the course of the process and the output variables. In the current production, they are limited to a small part of the main input variables that determine the output variables, and the rest are attributed to uncontrollable factors.

2. Results and discussion

Due to the fact that vibroabrasive machining (VAM) is a dynamic multifactorial system, its reliability is affected by a fairly large number of various factors. Significant dominant factors that affect the output variables of the control object are as follows.

A great impact on reliability of the VAM technological process is exerted by the characteristics of the workpiece to be machined. These characteristics of the workpiece include its shape, weight, dimensions, roughness, mechanical characteristics of the material of the part, the presence of burrs, flash, etc.

VAM allows you to process surfaces of complex shape, however, the uniformity of machining can be different for different surfaces. A higher efficiency of VAM is observed when removing metal from the outer surfaces of the workpiece and rounding off sharp edges.

With sufficiently large overall dimensions of the part, a violation of the stable circulation of the entire mass of the load is possible, which reduces the intensity of machining and as a result the quality of machining can be worsened.

A great impact on reliability of the technological process is exerted by the mass of the workpiece to be machined. With a sufficiently large mass of the workpiece, it will not circulate with the total mass of the load but rather interfere with its proper circulation. In this regard, it is necessary to select correctly the machining medium, the machining modes, the volume of the working chamber, etc.

Machining modes include the following elements: the frequency and amplitude of oscillations of the working chamber, the loading volume of the working chamber, the presence and composition of coolant, the amount of coolant supplied, type, characteristics of the working medium.

The frequency and amplitude of oscillations of the bottom of the working chamber is the most important factor determining the intensity and quality of processing. Reliability of the obtained machining results depends on the value and stability of this parameter. With too intense machining, on the surface of the part, there can be high roughness and bottomholes.

The loading volume of the working chamber also has a great impact on the intensity and quality of machining. For each abrasive medium, there is some optimal value of the working chamber loading volume, at which the highest machining performance is achieved. If the load volume deviates from this optimal value, there is possible a violation of the formation of a stable circulation flow, decreasing the machining productivity, and a deterioration in the quality of the treated surface are possible.

The presence, the type, the chemical composition and the rate of coolant flushing have a great impact on reliability of the VAM process. During machining, the coolant provides cleaning of the mass of the load, removes the wear products of the working environment and the material removed from the workpiece. Depending on the chemical composition of the coolant used, the working medium can perform mechanical or chemical-mechanical treatment. The washing speed is also an important factor. With excessive flushing of the coolant, the dynamic properties of the medium can deteriorate, and the machining intensity can decrease. With insufficient flushing, wear products are poorly removed from the working chamber, which can lead to decreasing the machining efficiency, charging the surfaces of the parts made of soft materials.

The quality and stability of machining are largely determined by the choice of equipment, including the shape and dimensions of the working chamber, lining material, etc.

The shape of the working chamber affects the intensity of machining and the shape of the flow of the medium, stability of circulation at various volumes of loading the working chamber, which largely determines the quality of the treated surfaces and the productivity of machining.

The lining material of the inner surface of the working chamber has a great impact on the entire machining process. The working chamber can be lined with rubber, polyurethane and depending on the material used, can provide different machining intensity. Lining materials and thickness have different physical properties that affect the quality and stability of machining. In particular, different lining materials have different coefficients of friction, different wear resistance, different damping properties, etc. The coefficient of friction largely determines the circulation rate of the load mass, and determines the interval of the loading volume, at which a stable circulation flow is formed.

Any element of technological equipment has its own resource of work. Although the machining equipment is simple in design, it has elements in its composition that have their own specific resource of work.

The characteristics and dimensions of the working medium have a great impact on the VAM reliability.

With increasing the grain size of the abrasive medium, metal removal increases due to the greater depth of grain penetration into the metal, which causes more intense destruction of the treated surface.

One of the main factors leading to deterioration of the quality and productivity of machining is the working environment wear. To maintain the quality of machining over time, it is necessary either to add the medium to replace the worn one, or to replace it completely. In this regard, it is necessary to determine the time intervals needed to restore the working environment. In order to reduce the impact of the working medium wear on machining performance, it is necessary to select the right washing speed for the working medium. If the washing speed of the working medium is not high enough, the machining productivity can decrease, the surface quality of the parts will deteriorate, etc.

The hardness and type of abrasive bond has a lesser effect on the VAM reliability.

Conclusions

As a result, it can be concluded that under the same modes of machining the part, abrasive granules in the form of a two-sided pyramid, in the cross section of which there is a non-convex hexagon, have the best result in a short time.

The dynamic model is based on the method of calculating the motion of systems with a centrifugal vibration exciter. The assumptions adopted in the model are based on classical theoretical mechanics, and are widely used in the design methods of vibration equipment, including VAM machines:

– the mass of the elastic elements is negligible compared to the mass of the container and the load;

- the rigidity of the system is concentrated in the suspension and is directly proportional to the displacement (the Hooke law);

– the perturbing force acting on the system is harmonic with a constant frequency ω and is applied at one point;

– the position of the center of mass of the container does not depend on the rotation of the unbalance.

This approach will allow:

- studying the trajectory of the vibration machine movement container movement dependence on the location of the vibration exciter with the subsequent possibility of using these results to evaluate the circulation movement;

- studying the intensity of the vibration treatment process dependence on the location of the vibration exciter.

In view of the fact that solutions to the issues of ensuring and improving reliability in many industries are of great importance, the purpose of the work is to ensure and to improve reliability of the technological process of VAM parts, which requires a deeper study of the most significant parameters that affect reliability of the VAM process. At the same time, it is possible to obtain such indicators as the accuracy factor for the controlled parameter, the instantaneous dispersion coefficient for the controlled parameter, the bias factor for the controlled parameter, the accuracy margin factor for the controlled parameter. The results of these studies will allow designing reliable technological processes and wide disseminating VAO in various industries.

References

[1] Mechanical engineering. Encyclopedia: in 40 volumes / [Ed. advice: K.V. Frolov (prev.) and others]. - M.: Mashinostroenie, 2000. V. 3: Technology for the manufacture of machine parts / A.M. Dalsky, A.G. Suslov, Yu.F. Nazarov and others; total ed. A.G. Suslov. 2002. - 840 p.

[2] Studying the properties of abrasive granules on polymer bonds/ Kozhukhova A.V., Tolmacheva L.V., Novoselova T.V. In the collection: Status and prospects for the development of the agro-industrial complex. Collection of scientific papers of the XII International Scientific and Practical Conference within the framework of the XXII Agro-Industrial Forum of the South of Russia and the Interagromash exhibition. Don State Technical University, Agrarian Research Center "Donskoy". Rostov-on-Don, 2019, P. 417-420.

[3] Kozhukhova A.V., Ponomarenko A.S., Timofeev V.A., et al. Studying the impact of the shape of abrasive granules on the parameters of vibroabrasive processing of parts //Collection of selected articles based on materials of scientific conferences of the National Research Institute "National Development", St. Petersburg, October 27–31, 2019, P. 42-45.

[4] Kalmykov M.A. Improving the efficiency of the process of vibration processing of large-sized products: Dis... Cand. Tech. Sciences. Lugansk, 2005. - 223 p.

[5] Brunspice E.V. Improving the efficiency of vibroabrasive processing by rational choice of its main parameters: Dis... Cand. Tech.Sciences. Lugansk, 2001. - 265 p.
[6] Yasunik S.N. Improving the efficiency of the process of processing parts in vibrating containers: Dis... Cand. Tech. Sciences: 05.03.01. Lugansk, 2003. - 215 p.
[7] Goncharevich I.F., Frolov K.V. Theory of vibration technique and technology. - M.: Nauka, 1981. - 320 p.
[8] Pronikov A. S., Parametric reliability of machines. M.: Publishing house of MSTU im. N. E. Bauman, 2002. - 560 p.
[9] Grigoryan G.D. Elements of the reliability of technological processes: Proc. allowance. Kyiv; Odessa: Vishcha school, 1984. 214 p.
[10] Ryzhkin A. A., Slyusar B. N., Shuchev K. G. Fundamentals of the theory of reliability: Proc. allowance. Rostov n/a: DSTU Publishing Cente, 2002. - 182 p.
[11] Gvozdikov, O. Yu. Investigation of the reliability of technological processes of vibration treatment in an abrasive environment / O. Yu. Gvozdikov. Text: direct // Young scientist, 2016, No. 4 (108), P. 29-33.

Information of the authors

Zhanibekov Timur Zhanibekuly, master student of the department "Technological equipment, mechanical engineering and standardization"of Abylkas Saginov Karaganda Technical University
E-mail:

Nikonova Tatyana Yurievna, candidate of technical sciences, acting associate professor of the department "Technological equipment, mechanical engineering and standardization"of Abylkas Saginov Karaganda Technical University
E-mail: nitka82@list.ru

Imasheva Kulzhan Imashevna, senior lecturer of the department "Technological equipment, mechanical engineering and standardization"of Abylkas Saginov Karaganda Technical University
E-mail: imasheva-gulzhan@mail.ru

Zhukova Alla Valentinovna, senior lecturer of the department "Technological equipment, mechanical engineering and standardization" of Abylkas Saginov Karaganda Technical University
E-mail: aluny@mail.ru

Rakhutin Maxim Grigorievich, doctor of technical sciences, professor of department “Mining Equipment, Transport and Mechanical Engineering” of Moscow Institute of Steel and Alloys
E-mail: rahutin.mg@misis.ru

DOI 10.52209/2706-977X_2022_3_50 **IRSTI 55.29.33** **UDC 62-756.8**

Using the Vibration Recorder Mobile Diagnostic Complex for Studying Vibration Processes

Moyzes B.*, Gavrilin A., Kuvshinov K., Smyshlyaev A., Koksharova I.
National Research Tomsk Polytechnic University, Tomsk, Russia
*corresponding author

Abstract. The relevance of studying vibration processes be means of registering its parameters is obvious. In some cases, vibration is a source of premature failure of technical systems, in other cases vibration is the basis for implementing technological processes. This work is dealing with a brief review of the tasks solved by using the Vibration recorder mobile diagnostic complex with special software and mathematical software developed by scientists from the National Research Tomsk Polytechnic University, employees of the ViTek LLC and the ViTek Siberia LLC. This complex allows registering vibration displacements, vibration velocities or vibration accelerations of the object under study, generating reports in text format with the output of time and spectral diagrams. Vibration registration was performed during vibration diagnostics of metalworking equipment elements and hydraulic drive power units, in the development of vibration damping systems based on high-pressure hoses, in physical modeling the operation of finishing machines and seismic signal sources. The paper presents schemes of test benches with examples of experimental plans, time and spectral diagrams. Studies of vibration parameters in modeling the operation of seismic signal sources are considered in detail.

Keywords: technical systems, registration of vibration parameters, mobile diagnostic complex.

Introduction

Studying vibration processes is relevant in the modern world, both in terms of generating useful vibration for implementing technological processes, and in terms of its damping during the operation of technological machines. An example of vibrational processes that affect the quality of work of the entire technological system can be metalworking, in which the resulting vibration leads not only to deterioration in accuracy and roughness but also to intense tool wear [1–4]. The sources of seismic signals [6], benches for testing vibration activity [7-8] can act as devices generating useful vibration. The issues of studying vibration processes are considered in the development of vibration dampers of various designs [10, 11].

When studying the parameters of vibration processes, it is necessary to register such vibration parameters, as vibration displacements, vibration velocities and vibration accelerations. Selecting the type of parameter is determined by the frequency range of the studied vibration process.

To solve this problem, various devices, complexes and systems are used, which can be divided into:

- built-in for the continuous monitoring of vibration parameters;
- stationary for deep research;
- mobile devices for periodic monitoring the level of the operating equipment elements vibration without dismantling it.

Therefore, selecting the measuring instrument is based on the list of tasks in a certain area of professional activity in the development, production or operation of various technical systems.

The team of authors of this work faces various tasks, some of which are as follows:

- determining the technological modes of operation of technological equipment without a significant level of vibration [12-14];
- detecting the elements that are a source of increased vibration [15, 16];
- developing the damping systems based on high pressure hoses (HPH) as elastic elements;
- developing the finishing machines for grinding products;
- developing the seismic signal sources [6, 17].

In this regard, the task was to determine the measuring instrument for registering vibration parameters.

Scientists of the Tomsk Polytechnic University, employees of the ViTek LLC (St. Petersburg) and the ViTek Siberia LLC (Tomsk) have developed and are actively using a mobile complex for online diagnostics of a technological system [18, 19] with special software [20].

The use of this complex for diagnostics of metalworking equipment confirmed its efficiency [12, 13]. Therefore, it was decided to use it to solve the other problems considered in this paper.

1. Methods

The diagnostic complex consists of four elements: piezoelectric sensors, an analog-to-digital converter, a laptop with special software and information channels. The main method of studying the use of the Vibration recorder mobile diagnostic complex is the development of test benches for the physical modeling of the operation processes of various technical systems.

Let's consider examples of the developed benches.

An information and measuring system for simulating the grinding process in a finishing machine with registration of vibration parameters is shown in Figure 1.

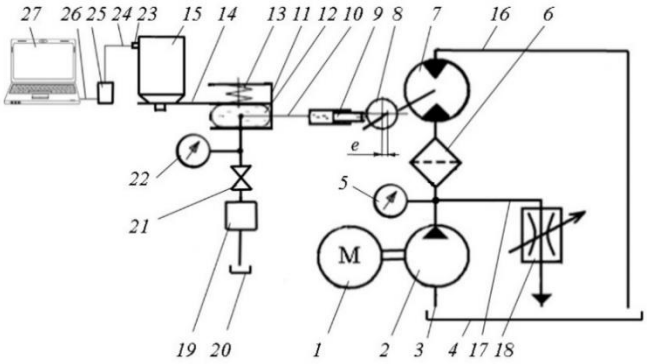

1 - electric motor; 2 - axial piston pump; 3 - pressure line; 4, 20 - main and auxiliary tank; 5, 22 - manometer; 6 - filter; 7 - axial piston hydraulic motor; 8 - eccentric mechanism; 9 - plunger; 10, 12 - HPH; 11 - frame; 13 - spring; 14 - platform; 15 - working chamber; 16, 17 - drain line; 18 - throttle; 19 - hand pump; 21 - crane; 23 - vibration transducer; 24, 26 - information channel; 25 – vibration measuring module; 27 – laptop

Fig. 1. – Information and measuring system for studying the grinding process in the finishing machine

The hydraulic drive consists of electric motor 1 that gives rotational motion to the shaft of axial piston pump 2. Pump 2 supplies the working fluid (oil) from tank 3 through filter 6 to hydraulic motor 7. Hydraulic motor 7 rotates the shaft with eccentric 8, which pushes the plunger 9, which delivers a certain volume of liquid to the HPH 12. The HPH located in frame 12 is preloaded by spring 13. The vibrations caused by the compression-straightening of shell 12 are transmitted to the platform on which the chamber with working solids is placed. To supply oil to the HPH (developing medium pressure), hand pump 19, tank 20 and valve 21 are used. The pressure in the system is controlled using pressure gauges 5 and 22.

Small workpieces are placed in the working chamber, which, when moving relative to the solid bodies, are subjected to grinding.

The technological parameters that affect the surface roughness at the constant time or the time it takes to reach a certain roughness are as follows:

• pressure in HPH 12, which forms the rigidity of the hydraulic spring;

• frequency of rotation of the shaft of hydraulic motor 8, which forms the speed of the relative movement of the workpiece and working bodies.

In this regard, an experiment plan form has been developed (Table 1).

Table 1. Experiment plan form for studying the grinding process

No.	Pressure, MPa	Speed of rotation, rpm	Grinding time, min	Roughness, Ra	No.	Pressure, MPa	Speed of rotation, rpm	Grinding time, min	Roughness, Ra
1					6				
2					7				
3					8				
4					9				
5					10				

The purpose of developing the second bench (Figure 2) was to study the process of vibration damping in the physical simulation of the impact processing equipment operation, for example, forging and pressing.

In this system, the volume of liquid supplied by plunger 9 forms the shock-vibration load developed by the hydraulic cylinder in impact mechanism 15.

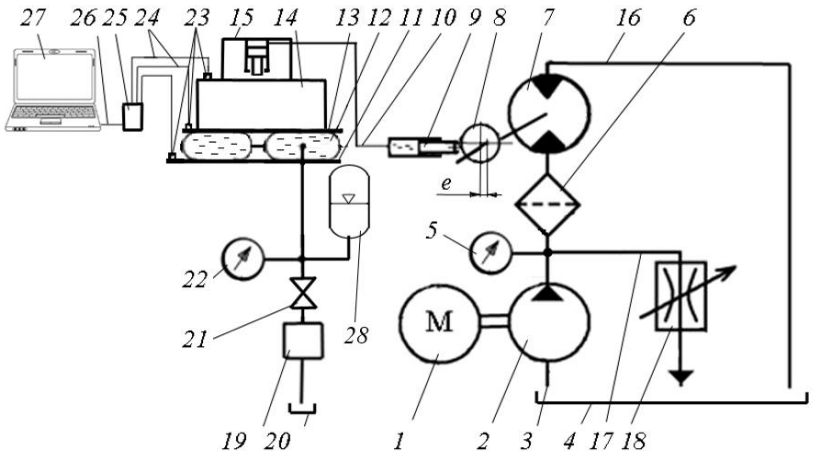

1 - electric motor; 2 - axial piston pump; 3 - pressure line; 4, 20 - main and auxiliary tank; 5, 22 - manometer; 6 - filter; 7 - hydraulic motor; 8 - eccentric mechanism; 9 - plunger; 10, 12 - HPH; 11 - base; 13 - platform; 14 - platform; 15 - percussion mechanism; 16, 17 - drain line; 18 - throttle; 19 - hand pump; - crane; 23 - sensors; 24, 26 - information channels; 25 – vibration measuring module; 27 - laptop; 28 – pneumatic hydro-accumulator

Fig. 2. – Information and measuring system for damping process studies

The impact energy is not transferred from the load (a simulator of the technological machine element) to the foundation and the operator but is dissipated due to the presence of high pressure hoses 12 and accumulator 28, into which liquid is supplied during the impact.

The parameters affecting the level of quenching are as follows:

• pressure in high pressure hose 12;

• frequency of rotation of the hydraulic motor shaft, which creates the impact frequency of the working element, for example, a hammer;

• pressure in the hydraulic cylinder of percussion mechanism 15, which forms the impact force.

The form of the experiment plan is given below (Table 2).

Table 2. Experiment plan form for studying the damping process

No	Pressure, MPa		Speed of rotation, rpm	Vibration displacement, μm		No	Pressure, MPa		Speed of rotation, rpm	Vibration displacement, μm	
	HPH	Hydro-cylinder		Platform	Foundation		HPH	Hydro-cylinder		Platform	Foundation
1						1					
2						2					
3						3					
4						4					
5						5					

The idea of developing the third bench is to continue studying the development of seismic signal sources (Figure 3) based on the inventions.

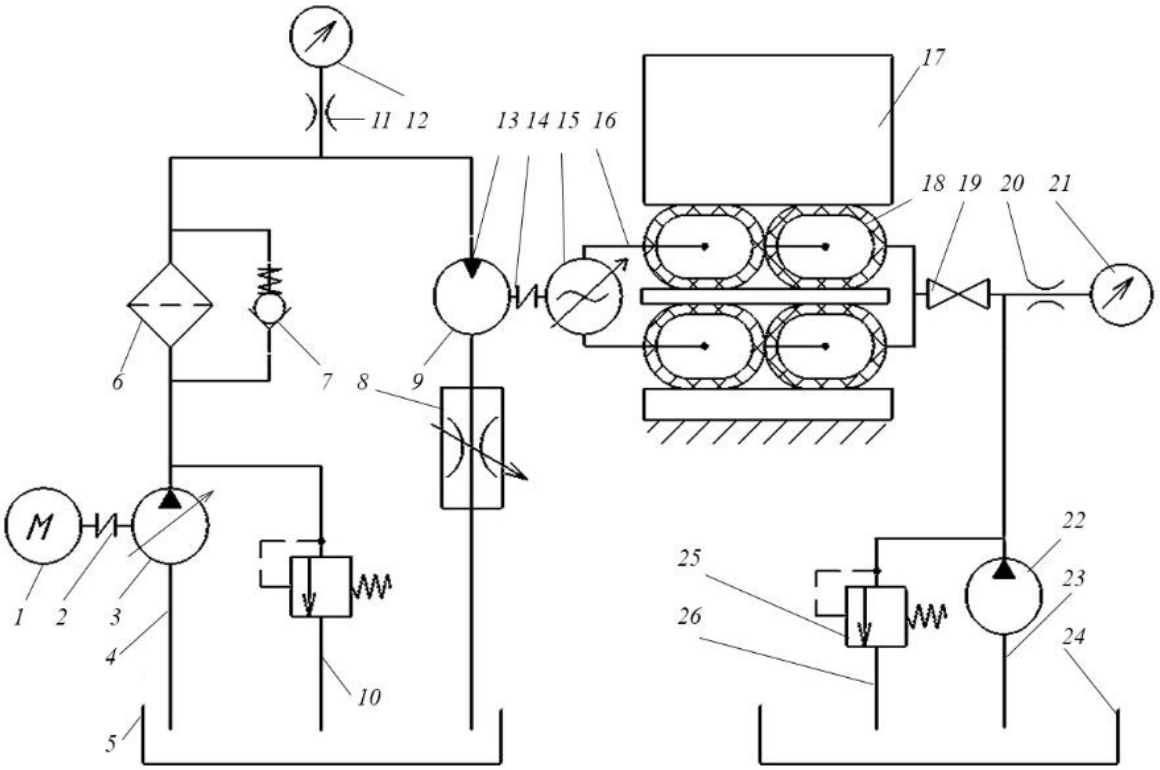

1 - asynchronous electric motor; 2, 14 - coupling; 3 - axial piston pump; 4, 13, 23 - pressure line; 5 – hydraulic tank; 6 - filter; 7 - check valve; 8 - throttle; 9 - axial piston hydraulic motor; 10, 26 - drain line; 11, 20 - throttle; 12, 21 - manometer; 15 – oscillation generator; 16, 18 - HPH; 17 - weight; 19 - valve; 25 - safety valve

Fig. 3. – Hydraulic scheme of the bench

The bench has two hydraulic systems interconnected by oscillation generator 15. The hydraulic drive for generating the excitation frequency and the system for creating an average pressure in HPH 18 have similar structures as in the above-described benches.

When the bench is operating, oscillation generator 15 supplies a certain volume of liquid to HPH 18, thereby generating a vibration load. Due to a relatively large weight of the load (309 kg), this load is transferred to the foundation, which imitates the surface of the Earth.

Let us consider the studies carried out on this bench in more detail.

2. Results and discussion

Four piezoelectric sensors (Figure 4, a) are based on the elements of the executive mechanism of the bench (a weight and its platform, the foundation of the bench, the frame) using a magnet (Figure 4, a) connected through information channels with the analog-to-digital converter that transmits information to the laptop (Figure 4, b).

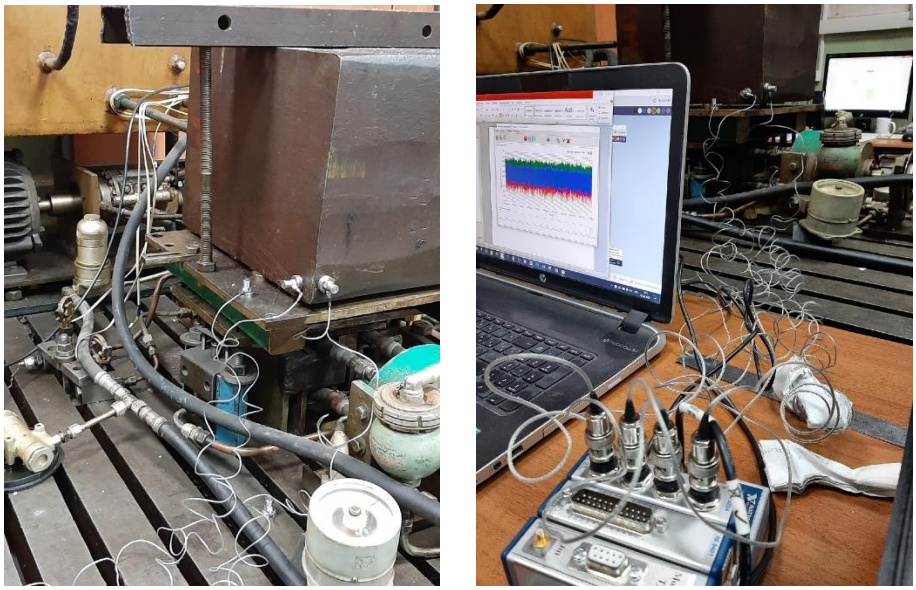

a *b*

Fig. 4 – Elements of the information and measuring system:
a - actuator; b – mobile diagnostic complex

In the system there is formed an average pressure and the hydraulic drive is started. The vibration load recorded by the complex is transferred to the bench frame (Figure 5, 6).

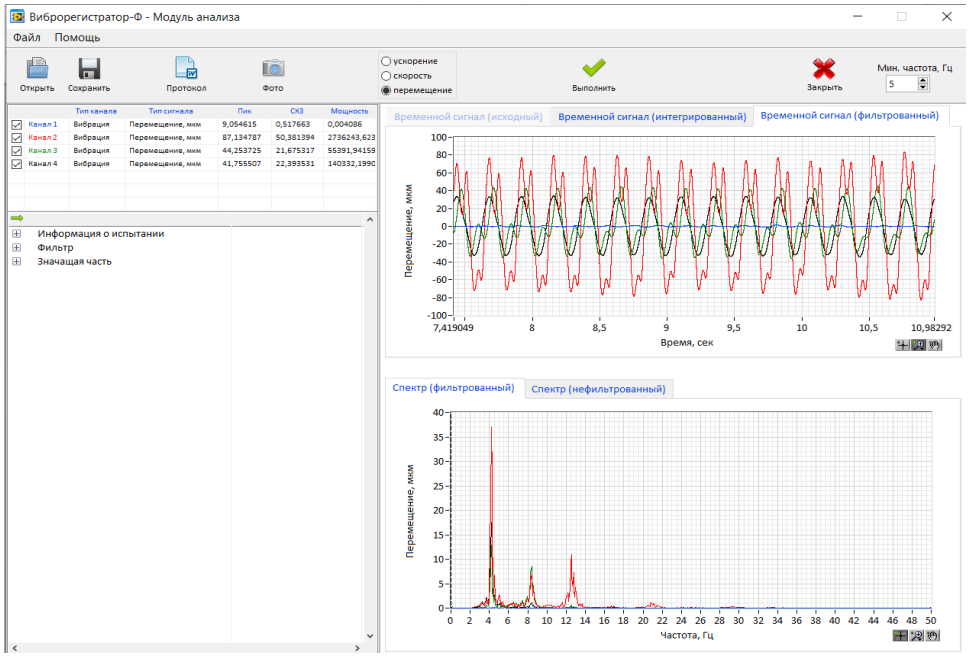

Fig. 5 – Software window at 6.5 Hz excitation frequency with vibration information of filter settings, timing and spectral diagram

As a result of the work there has been developed an experiment plan in the form of a table supplemented with the results of testing (Table 3).

Table 3. Experiment plan form

No	Frequency, Hz	Pressure, MPa	Plate displacement, μm	Vibration level on the foundation, μm
1	10	0.8	237.2	2.1
2		1.6	360.6	9.1
3		2.4	399.8	4.8
4		3.2	407.7	3.1
5		4	411.2	3.8
6	15	0.8	372.2	8.8
7		1.6	481.7	12.2
8		2.4	521.0	6.6
9		3.2	577.4	9.2
10		4	550.4	5.0
11	20	0.8	996.0	12.2
12		1.6	933.7	15.5
13		2.4	935.0	14.9
14		3.2	921.1	13.6
15		4	821.7	10.7

The preliminary analysis showed that the best results in terms of the level of force transferred to the ground were in experience No. 12 (Table 3). Based on the measurement results, a graph was built (Fig. 6).

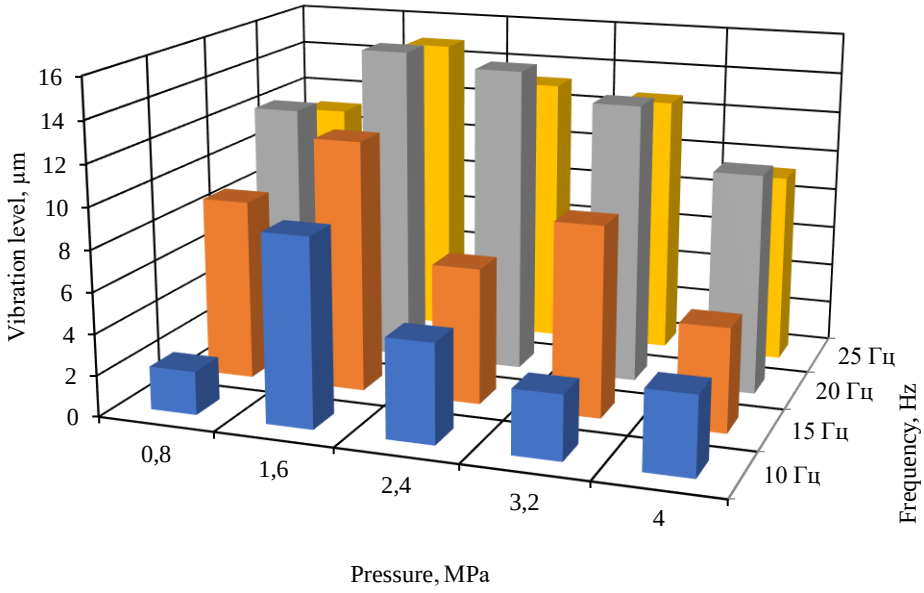

Fig. 6 – Graph of the foundation vibration level dependence on the operating modes of the bench

Thus, the experiments carried out made it possible to establish preliminary dependences of the vibration level on the platform on frequency and pressure. There is observed increasing and decreasing the vibration level before and after 1.6 MPa, which is firstly explained by the insufficient rigidity of the hydraulic springs, then by its increase. The dependence of the level of forced vibration on the frequency of external action is of a typical nature: increasing, achieving the maximum value and decreasing.

According to this experiment, the region of 20 Hz, 1.6 MPa is promising for further research.

Conclusions

Work at studying vibration parameters on test benches using the Vibration recorder mobile diagnostic complex demonstrated the prospects for its use for a wide range of tasks.

This complex allows subsequent analyzing the vibration parameters, based on it drawing a conclusion about the needed technological modes of the equipment. As a result, it is possible to increase reliability of technical systems and make their operation more efficient.

References

[1] Andreнev V.N., Borovsky G.V., Borovsky V.G., Grigorнev S.N. The tool for high-performance and environmentally friendly cutting. – M.: Mashinostroenie, 2010. - 479 p.

[2] Bolsunovsky S.A., Vermel V.D., Gubanov G.A. Kazan A.V. Experience in manufacturing turbocharger model blades with increased accuracy in pilot production conditions//CAD and graphics. No. 3, 2009, P. 80-82.

[3] Bolsunovsky S.A., Vermel V.D., Gubanov G.A., Kacharava I.N., Leontyev A.E. (2012). Computational and experimental assessment of rational technological parameters of high-performance milling as part of an automated system for technological preparation for the production of aerodynamic models of aircraft//Proceedings of the Samara Scientific Center of the Russian Academy of Sciences. V. 14, No. 4 (2)., 2012, P. 374-379.

[4] Gavrilin A.N., Moyzes B.B., Cherkasov A.I. Constructive methods for increasing the vibration resistance of metal-cutting equipment//Control. Diagnostics. No. 13., 2013, P. 82-87.

[5] Gavrilin A.N., Moyzes B.B., Zharkevich O.M. Constructive and processing methods of reducing vibration level of the metalworking machinery elements. // Journal of Vibroengineering, Vol. 17, Issue 7., 2015, P. 3495-3504.

[6] Kuvshinov K.A., Moyzes B.B., Krauinsh P.Ya. Pulse-vibration source of seismic signals // News of the Tomsk Polytechnic University. V. 317. No. 1. P., 2010, P. 77-81.

[7] Nizhegorodov A., Gavrilin A., Moyzes B., Ditenberg I., Zharkevich O., Zhetessova G., Muravyov O., Bets M. Bench for dynamic testing technical products in the mode of amplitude-frequency modulation with hydrostatic vibratory drive. Journal of Vibroengineering. V. 18 (6)., 2016, P. 3734-3742.

[8] Nizhegorodov A.I., Gavrilin A.N., Moyzes B.B. Hydraulic power of vibration test bench with vibration generator based on switching device. Key Engineering Materials. V. 685., 2016, P. 320-324.

[9] Nizhegorodov A.I., Gavrilin A.N., Moyzes B.B., Cherkasov A.I., Zharkevich O.M., Zhetessova G.S., Savelyeva N.A. Radial–piston pump for drive of test machines. IOP Conference Series: Materials Science and Engineering. V. 289 (1) – 012014, 2018

[10] Gavrilin A.N., Rozhkov P.S., Angatkina O.O., Moyzes B.B. Dynamic vibration damper with an automatic tuning system for vibration frequency. Izvestiya of the Tomsk Polytechnic University. V. 318, No. 2, 2011, P. 26-29.

[11] Pat. 2298122 Russian Federation, MPK7 F 16 F 15/023. Hydropneumatic shock absorber / Krauinsh P.Ya., Smailov S.A., Moyzes B.B., Voronko I.V., Suprunov A.Yu., Kuvshinov K.A.; applicant and patent holder SO VPO Tomsk Polytechnic University. No. 2005137254/11; appl. 30.11.05; publ. 27.04.2007. Bull. No. 12. 5 p.

[12] Gavrilin A., Moyzes B., Kuvshinov K., Vedyashkin M., Surzhikova O. Determining optimal milling modes by means of shock–vibration load reduction on tool and peak–factor equipment. Materials Science Forum. V. 942., 2019, P. 87-96.

[13] Gavrilin A.N., Moyzes B.B. Method of operational diagnostics of a metal-cutting machine for processing workpieces such as bodies of revolution//Control. Diagnostics. No. 9., 2013, P. 81-84.

[14] Ivanov S.E., Gavrilin A.N., Kozyrev A.N., Moyzes B.B. Improving the efficiency of milling by reducing shock-vibration loads // Polzunovskiy Vestnik. No. 1., 2018, P. 77-81.

[15] Song Shichen, Zhang Xiaoliang, Moises B.B., Gavrilin A.N. Development of information technologies in the diagnostics of hydraulic drive units // Proceedings of the XV International Scientific and Practical Conference of Students, Postgraduates and Young Scientists "Youth and Modern Information Technologies". - Tomsk: TPU Publishing House, 2018. - P. 197-198.

[16] Kirillova V.I., Moyzes B.B., Gavrilin A.N., Sun Sh., Alimbaev S.T. Development of information-measuring systems in the aspect of vibration diagnostics of hydraulic drives // Proceedings of the International Scientific and Practical Conference "Integration of Science, Education and Production as the Basis for the Implementation of the Plan of the Nation" (Saginov's Readings No. 10), in 7 parts. Karaganda: Publishing house of A. Saginov KTU., 2018. - P. 230-232.

[17] Smyshlyaev A.S., Averkiev A.E., Koksharova I.B. Development of vibro-impulse energy sources based on high-pressure hoses // Proceedings of the International Scientific and Practical Conference "Integration of Science, Education and Production as the Basis for the Implementation of the Nation's Plan" (Saginov's Readings No. 14), June 16-17, 2022. In 2 parts. Part 2. Ministry of Education and Science of the Republic of Kazakhstan, A. Saginov Karaganda Technical University. Karaganda: Publishing House of KTU. P. 258-260.

[18] Gavrilin A., Moyzes B., Cherkasov A., Mel′nov K., Zhang X. Mobile complex for rapid diagnosis of the technological system elements // MATEC Web of Conferences. 01078, 2016

[19] Certificate of state reg. of the computer program No. 2009613214 RF. Software package for collection, processing and analysis of vibration signals nkRecorder/N.A. Kochinev, F.S. Sabirov, M.P. Kozochkin. OBPBT. No. 4 (69), 2009, 6 p.
[20] Certificate of state reg. of the computer program No. 2017614049 RF. Vibration recorder-M2 / Gavrilin A.N., Seryabryakov K.V., Melnov K.V., Khairullin A.R., Moyzes B.B.; applicant and patent holder Tomsk Polytechnic University. No. 2017611112; appl. 02/13/2017; publ. 04/05/2017. 1 p.
[21] Pat. No. 2324954 RF, MPK7 G01V 1/155 (2008). Vibropulse source / Krauinsh P.Ya., Smailov S.A., Moyzes B.B., Suprunov A.Yu., Kuvshinov K.A.; applicant and patent holder GOU VPO Tomsk Polytechnic University. - No. 2006137548/28; appl. 23.10.06; publ. May 20, 2008, Bull. No. 14. - 5 p.: ill.
[22] Pat. No. 2240582 RF, MPK7 G 01 V 1/155 (2004). Vibropulse energy source / Krauinsh P.Ya., Ioppa A.V., Smailov S.A., Moyzes B.B., Voronko I.V.; applicant and patent holder Tomsk Polytechnic University. No. 2003108773/28; appl. 03/28/03; publ. November 20, 2004. Bull. No. 32., 2004, 5 p.

Information of the authors

Moyzes Boris, candidate technical sciences, associate professor, department of control and diagnostics of Tomsk Polytechnic University
E-mail: mbb@tpu.ru

Gavrilin Alexey, doctor of technical sciences, professor of mechanical engineering department of Tomsk Polytechnic University
E-mail: gawral@tpu.ru

Kuvshinov Kirill, senior lecturer of the division for mechanical engineering of National Research Tomsk Polytechnic University
E-mail: kuvshinov_k@mail.ru

Smyshlyaev Aleksandr, master's student of the division for testing and diagnostics of National Research Tomsk Polytechnic University
E-mail: smyshlyaev_a@mail.ru

Koksharova Inna, master's student of the division for testing and diagnostics of National Research Tomsk Polytechnic University
E-mail: koksharova_i@mail.ru